Organisms Diversity & Evolution (2023) 23:631–681
https://doi.org/10.1007/s13127-023-00623-w

ORIGINAL ARTICLE

Taxonomy and phylogeny of Dalytyphloplanida Willems et al., 2006 (Platyhelminthes: Rhabdocoela), with the description of a new family, a new genus, and sixteen new species from Cuba and Panama

Yander L. Diez[1,2] · Marlies Monnens[2] · Arlien Wuyts[3] · Luc Brendonck[3] · Patrick Reygel[2] · Andreas Schmidt-Rhaesa[1] · Tom Artois[2]

Received: 18 March 2023 / Accepted: 24 August 2023 / Published online: 23 October 2023

Abstract

Twenty-two marine species of Dalytyphloplanida from Cuba, Panama, and Lanzarote are presented, sixteen of which are new to science. Five known species are recorded from Cuba: *Kytorhynchus microstylus*, *Ceratopera paragracilis*, *Trigonostomum armatum*, *T. franki*, and *T. vanmecheleni*. *Neokytorhynchus pacificus* is recorded for the first time in the Atlantic (Lanzarote). For one species, a new genus is erected to be included in a new family. A new genus and thirteen new species from Cuba and three new species from Panama are described. The new species are mainly distinguished from their congeners by the specific morphology of the copulatory structures. The new taxa are discussed in the context of a new phylogenetic analysis of Dalytyphloplanida. This analysis includes sequences of 238 species, 14 of which were sequenced for the first time. The phylogenetic analysis and the detailed morphology suggest that *K. microstylus* may constitute a complex of cryptic species. The internal phylogenetic relationships of *Trigonostomum* and *Promesostoma* were separately analysed to include new sequence data of the mitochondrial *cox1* gene. These genera are shown to consist of several diagnosable clades, concurring with the results of early morphological studies of these taxa. Morphological and molecular data support the notion that *Trigonostomum sinensis* is a junior synonym of *T. vanmecheleni*, and we therefore propose their synonymisation. A new family is erected, Schockaertiidae **fam. n.**, to include a monophyletic clade of neodalyellids with a pharynx rosulatus and a copulatory bulb devoid of hard structures (*Schockaertia aprostatica* **gen. n. sp. n.** and *Einarella argillophyla*). We propose a new classification into families of Thalassotyphloplanida, which envolves elevating the status of Adenorhynchinae to family level (Adenorhynchidae **status novus**). All previously recognised thalassotyphloplanid families are recovered as monophyletic (Kytorhynchidae, Byrsophlebidae, Promesostomidae, and Trigonostomidae). No support was found for the previously described subfamilies, except Paramesostominae, and we, therefore, propose to suppress these taxa.

Keywords Neodalyellida · Thalassotyphloplanida · Systematics · Free-living flatworms · Biodiversity · Meiofauna

Zoobank article registration: http://zoobank.org/urn:lsid:zoobank.org:pub:A32516F6-CD56-40C0-BA44-B49E615E0C42

✉ Yander L. Diez
yanderluis87@gmail.com

Marlies Monnens
marlies.monnens@uhasselt.be

Arlien Wuyts
arlien.wuyts@hotmail.com

Luc Brendonck
luc.brendonck@kuleuven.be

Patrick Reygel
patrick.reygel@uhasselt.be

Andreas Schmidt-Rhaesa
a.schmidt-rhaesa@leibniz-lib.de

Tom Artois
tom.artois@uhasselt.be

[1] Museum of Nature Hamburg - Zoology, Leibniz Institute for the Analysis of Biodiversity Change (LIB), Martin-Luther-King-Platz 3, 20146 Hamburg, Germany

[2] Hasselt University, Centre for Environmental Sciences, Research Group Zoology: Biodiversity and Toxicology, Universitaire Campus Gebouw D, B-3590 Diepenbeek, Belgium

[3] Animal Ecology, Global Change and Sustainable Development, KU Leuven, Charles Deberiotstraat 32 - Box 2439, 3000 Leuven, Belgium

Introduction

Rhabdocoel microturbellarians are traditionally subdivided into two monophyletic subtaxa: Kalyptorhynchia Graff, 1905 (rhabdocoels with a proboscis), and Dalytyphloplanida Willems et al., 2006 (rhabdocoels without proboscis) (Willems et al., 2006). Van Steenkiste and Leander (2022) recently recognised a third clade: Mariplanellida Ax & Heller, 1970. Within Dalytyphloplanida, two clades are recognised: Neodalyellida Willems et al., 2006, and Neotyphloplanida Willems et al., 2006. Neotyphloplanida comprises Thalassotyphloplanida Willems et al., 2006, and Limnotyphloplanida Van Steenkiste et al., 2013. However, no apomorphies for these clades have been found to date; therefore, they were established based on the results of molecular phylogenetic analyses.

In the Western Atlantic, species of Thalassotyphloplanida have mostly been studied in the United States of America (USA) (Ax, 1995; Graff, 1911, 1913; Rieger, 1974), Canada (Ax & Armonies, 1987; Ax, 2008), Brazil (Marcus, 1948, 1951, 1952), Bermuda (Karling, 1978), and Uruguay (Van Steenkiste et al., 2008). At the start of the twentieth century, Graff (1911, 1913) for the first time recorded several byrsophlebids, promesostomids, and trigonostomids from North America. Later, Rieger (1974) described several taxa belonging to the newly described family Kytorhynchidae and Ax (1995) described two new species of *Promesostoma* Graff, 1882. Ax and Armonies (1987) included in their work several records from Canada and also described two species of *Promesostoma*. From Brazil, Marcus (1948) described *Trigonostomum divae* Marcus, 1948, a species later synonymised with *T. lilliei* (Graff, 1911) Meixner, 1924 (Artois et al., 2013). Later, Marcus (1951) described *Brinkmanniella augusti* Marcus, 1951, and Marcus (1952) described *Memyla phocanella* Marcus, 1952, and *Promesostoma scylax* Marcus, 1952. More than two decades later, Karling (1978) found three known species in Bermuda: *Trigonostomum setigerum* Schmidt, 1852; *Microvahine corallicola* Karling et al., 1972; and *Ceratopera paragracilis* Ehlers & Ax, 1974, and described two new ones from the same locality: *T. denhartogi* (Karling, 1978) Willems et al., 2004b and *Parapharyngiella mackfirae* (Karling, 1978) Diez et al., 2018. Van Steenkiste et al. (2008) described two thalassotyphloplanids from Uruguay (*Vauclusia multistriata* Van Steenkiste et al., 2008 and *Coronhelmis mimosa* Van Steenkiste et al., 2008) and recorded for this area *Byrsophlebs caligulachaena* (Ehlers & Ehlers, 1981) Karling, 1985 and *Ceratopera axi* (Riedl, 1954) Den Hartog, 1964. Apart from these, two thalassotyphloplanid species have been recorded from the Caribbean: *T. armatum* Schmidt, 1852, is known from Curaçao (Willems et al., 2004b) and recently Diez et al. (2018) described *P. caribbaea* Diez et al., 2018, from Cuba.

A few species of Neodalyellida are also known from the Western Atlantic. Firstly, species of the endosymbionts *Paravortex* were recorded from the USA by Graff (1882, 1911), Powers (1936) recorded *Syndesmis antillarum*, and Jones (1938) reported on several species of Solenopharyngidae. Marcus (1948) described the first neodalyellid from Brazil: *Artinga evelinae* Marcus, 1948. In the following years, Marcus (1951, 1952, 1954) described seven additional species from Brazil: *Daelja secuta* Marcus, 1951; *Kalyla gabriellae* Marcus, 1951; *Lenopharynx triops* Marcus, 1951; *Pogaina suslica* (Marcus, 1951) Marcus, 1954; *Trisaccopharynx pusa* (Marcus, 1952) Ehlers, 1972; *Pogaina tifa* Marcus, 1954; and *Nygulgus evelinae* Marcus, 1954. Later, Marcus (1968) described *Syndesmis evelinae* Marcus, 1968, from Saint-Barthélemy (Lesser Antilles) and from this country and Jamaica Hertel et al. (1990) described *S. collongistyla* (Hertel et al., 1990; Jondelius, 1996). Another endosymbiotic neodalyellid was described from Argentina; *Collastoma wahlli* Ponce de León & Mañé-Garzón, 1979. Ax and Armonies (1987) and Ax (2008) also recorded several neodalyellids from the Canadian Atlantic coast. More recently, Brusa et al. (2006) and Van Steenkiste et al. (2008) respectively described *Paravortex mesodesma* Brusa et al., 2006, and *Baicalellia forcipifera* Van Steenkiste et al., 2008, from Uruguay.

The interrelationships of Dalytyphloplanida remain poorly understood. The first molecular phylogenetic analysis including thalassotyphloplanids confirmed the monophyly of the genera *Ceratopera* den Hartog, 1964; *Trigonostomum* Schmidt, 1852; *Promesostoma*; and *Proxenetes* Jensen, 1878, and the subfamilies Promesostominae Luther, 1948; Paramesostominae Luther, 1948; and Trigonostominae Luther, 1948 (Van Steenkiste et al., 2013). Conversely, the two largest families, Trigonostomidae Graff, 1905, and Promesostomidae den Hartog, 1964, were demonstrated to be polyphyletic, leading Van Steenkiste et al. (2013) to call for a revision of Thalassotyphloplanida. However, more exhaustive taxon sampling and the use of additional molecular markers are needed to fully resolve the internal phylogeny of this group.

In this contribution, we present the results of an extensive collecting effort in Cuba during the last six years, and of several campaigns to Panama (2011 and 2016) and the Canary Islands (2011). A taxonomic account of dalytyphloplanid taxa collected during these sampling campaigns is provided. A new phylogeny for Dalytyphloplanida is inferred from ribosomal (18S and 28S rDNA) and, for the first time, mitochondrial DNA (mtDNA) sequences (*cox1*). Systematic implications are discussed in this molecular framework.

Material and methods

Sampling and morphological study

Dalytyphloplanids were collected in several localities in Cuba (January 2016 to March 2022) and processed in the Laboratory of Zoology of the Department of Biology and Geography, Universidad de Oriente (Cuba). Morphological analyses of the material from Cuba, the species collected in Lanzarote (2011), and Panama (December 2011 and February 2016) were conducted in the laboratory of the Research Group 'Zoology: Biodiversity and Toxicology' of Hasselt University (Belgium). The geographic coordinates of the localities are provided in Table 1. The holotype specimens of the new species were deposited in the Museum of Nature Hamburg - Zoology (ZMH) and the paratypes and reference material in the collection of Hasselt University (HU). The authors variously contributed to the descriptions of the taxa, and this is reflected by the respective authority designations.

Live specimens were extracted from the sediment and algae using the $MgCl_2$ decantation method (Schockaert, 1996) and studied alive. Specimens selected for the morphological study were whole mounted with lactophenol. Drawings of sclerotised structures were made using a camera lucida on a Nikon Eclipse 80i or Leica DM 2500 LED microscope, using Nomarski interference contrast. Measurements were taken along the central axis of the measured object. The position of structures is expressed in percentages of the total body length (distance from the anterior tip of the body). Drawings without a scale are freehand. A number of specimens were fixed in hot (50 °C) Bouin's fixative for histological observation: These specimens were subsequently embedded in paraffin and serially sectioned (4 µm). After sectioning, they were stained with Heidenhain's haematoxylin, using erythrosin as counterstain. Specimens selected for molecular work were fixed in 99% EtOH and stored at −20 °C until processing.

DNA extraction, PCR amplification, and sequencing

DNA was extracted from complete specimens using the QIAampH DNA Micro Kit with QIAamp MinEluteH columns (QIAGEN), following the manufacturer's protocol. Extracts were stored in duplicate (40 and 20 µl). Partial 18S rDNA, 28S rDNA, and *cox1* mtDNA gene fragments were amplified using the primers and PCR protocols listed in Table 2.

Reactions were prepared using PuReTaq Ready-To-Go PCR beads (GE Healthcare). For amplification of 18S and 28S rDNA, each reaction included 2.5 µl of each primer (5 µM), 1 µl DNA extract, and 19 µl molecular grade water

Table 1 Coordinates of the sampling localities

Country/region	Area	Localities	Latitude N	Longitude W
Panama	Taboga Island	Taboga	08°48′05″	79°33′17″
	Portobelo	Bahía Can Can	09°32′23″	79°40′31″
	Archipelago Las Perlas	Las Perlas	08°23′16″	79°07′31″
Cuba	La Habana province, Playa municipality	Playa	23°05′32″	82°28′17″
	Matanzas province, Ciénaga de Zapata municipality	Playa Caletón	22°16′31″	81°13′01″
	Holguín province, Banes municipality	Playa Morales	20°54′17″	75°37′53″
		Guardalavaca	21°07′32″	75°49′39″
	Santiago de Cuba province, Guamá municipality	Las Sardinas	19°56′24″	76°46′41″
		Chivirico	19°58′13″	76°23′55″
		Hotel Guamá	19°57′60″	76°22′18″
		Bahía Larga	19°58′57″	76°18′15″
	Santiago de Cuba province, Santiago de Cuba municipality	Bueycabón	19°57′38″	75°57′28″
		Belmares, Bahía de Santiago de Cuba	19°58′55″	75°51′57″
		Embarcadero de Cayo Granma, Bahía de Santiago de Cuba	19°58′34″	75°52′12″
		Aguadores	19°58′56″	76°49′56″
		Sardinero	19°57′42″	75°47′00″
		Siboney	19°57′34″	75°42′07″
		Juraguá	19°56′21″	75°40′20″
Canary Islands	Lanzarote	Orzola	29°13′20″	13°26′58″
		Mala	29°05′01″	13°26′59″

Table 2 Primer sequences and PCR regimes used for PCR amplification

Primer	Direction	Primer sequence (5′-3′)	Reference
Subunit 18S			
TimA	Forward	AMCTGGTTGATCCTGCCAG	Tessens et al. (2014)
Poly18SR2	Reverse	GCMRGKTCACCTACRGAAACCTTGTT	Tessens et al. (2014)
95 °C * 5 min 10 s, 30X (94 °C * 30 s, 55 °C * 30 s, 72 °C * 90 s), 72 °C * 5 min			
Subunit 28S			
LSU5	Forward	TAGGTCGACCCGCTGAAYTTA	Van Steenkiste et al. (2013)
LSU6-3B	Reverse	GAGAAGGGTTCCATGTGAACAGC	Van Steenkiste et al. (2013)
95 °C * 5 min 10 s, 30X (94 °C * 60 s, 50 °C * 60 s, 72 °C * 90 s), 72 °C * 5 min			
Subunit *cox1*			
RhCo1F	Forward	CHACTAAHCATAAGGATATAGG	Van Steenkiste et al. (2018)
RhCo1R	Reverse	TCWGGRTGHCCAAAAAAYCA	Van Steenkiste et al. (2018)
95 °C * 3 min, 9X (94 °C * 30 s, 53 °C * 30 s (-0.5 °C/cycle), 72 °C * 60 s), 34X (94 °C * 30 s, 49 °C * 30 s, 72 °C por 60 s), 72 °C * 7 min			

for a final volume of 25 µl. For amplification of *cox1*, 4.4 µl of each primer (10 µM), 1 µl DNA extract, and 15.2 µl water were combined for a final volume of 25 µl. PCRs were carried out on a Bio-Rad PCR C-1000 or T-100 Touch thermal cycler and products were verified on a 1.4% agarose gel, stained with GelRed™. DNA quantities were measured on a Qubit Fluorometer using the Qubit™ dsDNA HS Assay Kit (ThermoFisher Scientific). PCR products were commercially purified and sequenced by Macrogen Europe B.V. (Amsterdam, The Netherlands) under BigDye™ terminator cycling conditions on an ABI3730XL DNA Sequencer.

Phylogenetic molecular analysis

Obtained contigs were quality-trimmed (error probability = 0.05) and assembled in Geneious v11.1.5 (Kearse et al., 2012). Consensus sequences were subjected to a BLAST search (Altschul et al., 1990) on the NCBI website (ncbi.nlm.nih.gov) to check for signs of contamination. To detect potential pseudogenes, newly obtained *cox1* mDNA sequences were translated in Geneious (translation table 9) and visually screened for the presence of stop codons (see discussion). All available dalytyphloplanid sequences were mined from GenBank (Benson et al., 2012), and a separate dataset was compiled for 18S (228 sequences) and 28S rDNA (191 sequences). Based on the studies of Van Steenkiste et al. (2013), we selected *Acrorhynchides robustus* (Karling, 1931) Strand, 1928 and *Placorhynchus octaculeatus* Karling, 1931 as outgroups. Separate datasets were compiled to resolve intrageneric relationships within *Promesostoma* and *Trigonostomum*. In addition to the ribosomal markers mentioned above, 11 sequences of the *cox1* mtDNA were used to elucidate the internal relationships of *Trigonostomum* and *Promesostoma*. *Astrotorhynchus intermedius* Van Steenkiste et al., 2018; *Promesostoma meixneri* Ax, 1951; and *Ceratopera pilifera* Karling, 1986 were selected as outgroups for these analyses of *Trigonostomum*. *Astrotorhynchus intermedius*; *C. pilifera* Karling, 1986; and *Trigonostomum vanmecheleni* Artois et al., 2013, were selected as outgroups for these analyses of *Promesostoma*. An overview of all used sequences and corresponding accession numbers is presented in Table 3.

Ribosomal datasets were aligned using the online version of MAFFT v7 (Katoh & Standley, 2013; Katoh et al., 2017). The Q-INS-i algorithm was specified to account for secondary structures. *Cox1* datasets were translationally aligned using the MUSCLE v3.8.425 (Edgar, 2004) executable implemented in Geneious. Ambiguously aligned regions were identified and eliminated on the Gblocks v0.91b server (Castresana, 2000), employing options for a less stringent selection. The resulting alignments were concatenated in Geneious. An initial partitioning scheme defining gene boundaries was manually constructed. Separate partitions were specified for the three codon positions in the *cox1* alignment. The concatenated alignment and partition files were used as input for the ModelFinder tool (Kalyaanamoorthy et al., 2017) on the IQ-TREE webserver (Trifinopoulos et al., 2016). Model fit was evaluated using the Akaike Selection Criterion and partition merging was enabled (Lanfear et al., 2012). The latter feature determines the best-fit partitioning scheme for a particular dataset, while also calculating the best-fitting evolutionary models for each selected subset.

Maximum likelihood (ML) analyses were conducted using the 'Tree Inference' tool on the IQ-TREE server (Nguyen et al., 2015), using edge-linked partitions. Branch support was assessed by ultrafast bootstrapping (UFboot) (Hoang et al., 2017) and the nonparametric approximate likelihood-ratio test (SH-aLRT) (Guindon et al., 2010), both with 1000 replicates. Bayesian inference (BI) was carried out using the Metropolis-coupled Markov Chain Monte Carlo (MC^3) algorithm, implemented in MrBayes v3.2.6 (Ronquist

Table 3 GenBank accession numbers used in the study (* new sequences)

Species	18S rDNA	28S rDNA	*cox*1
Neodalyellida			
Schockaertia aprostatica **gen. n. sp. n.***	OR608003	OR616257	-
Adenopharynx mitrabursalis	KC529520.1	KC529641.1	-
Austradenopharynx sp.	KC529521.1	KC529642.1	-
Solenopharyngidae sp.	KC529519.1	KC529640.1	-
Trisaccopharynx westbladi	AY775774.1	-	-
Einarella argillophyla	AY775756.1	-	-
Anoplodium hymanae	MH327508.1	-	-
Anoplodium stichopi	AF167424.1	-	-
Syndesmis aethopharynx	MF125897.1	MF460995.1	-
Syndesmis echinorum	MF460997.1	MF460996.1	-
Syndesmis kurakaikina	MT622644.1	-	-
Umagillidae sp.	MH337260.1	MH337261.1	-
Seritia elegans	KC529517.1	KC529638.1	-
Wahlia macrostylifera	KC529518.1	KC529639.1	-
Tamanawas kalipis	MH337259.1	MH337262.1	-
Provortex balticus	AJ312268.1	AJ315648.1	-
Provortex karlingi	KC529510.1	-	-
Provortex tubiferus	AJ312269.1	AF100195.1	-
Vejdovskya ignava	KC529513.1	KC529635.1	-
Vejdovskya pellucida	KC529512.1	-	-
Baicalellia brevituba	KC529505.1	KC529630.1	-
Baicalellia beauchampi	KC529504.1	KC529629.1	-
Baicalellia canadensis	KC869833.1	KC869886.1	-
Baicalellia daftpunka	MH337253.1	MH337257.1	-
Baicalellia pusilla	MH337252.1	-	-
Baicalellia solaris	MH337256.1	MH337255.1	-
Pterastericola astropectinis	AF100196.1	-	-
Pterastericola australis	AJ012518.1	AY157161.1	-
Pterastericola psilastericola	KC529516.1	KC529637.1	-
Dalyellioida sp. 'houdini'	KC529522.1	-	-
Pseudograffilla arenicola	KC529514.1	-	-
Graffilla buccinicola	AJ012521.1	AJ313232.1	-
Pogaina paranygulgus	MH337254.1	H337258.1	-
Pogaina shenzhenensis	MK509004.1	MK509009.1	-
Pogaina sinensis	MK509001.1	MK509007.1	-
Pogaina sp. 1	KC529507.1	KC529632.1	-
Pogaina sp. 2	KC529508.1	KC529633.1	-
Pogaina sp. 3	KC529506.1	KC529631.1	-
Provorticidae sp.	KC529509.1	KC529634.1	-
Balgetia semicirculifera	KC529503.1	KC529628.1	-
Dalyellioida sp.	KC529523.1	KC529643.1	-
Dalyellioida sp. NVS 2013	KC529523.1	KC529643.1	-
Bresslauilla relicta	KC869832.1	KC529636.1	-
Eldenia reducta	KC529502.1	KC529627.1	-
Orostylis dohae	KC529525.1	KC529645.1	-
Orostylis donanae	KC529524.1	KC529644.1	-
Thalassotyphloplanida			
Kytorhynchidae sp. 1	KC529401.1	KC529527.1	-
Kytorhynchidae sp. 2	KC529402.1	KC529528.1	-
Kytorhynchidae sp. 3	KC529403.1	KC529529.1	-

Table 3 (continued)

Species	18S rDNA	28S rDNA	*cox*1
Kytorhynchidae sp. 4	KC529404.1	KC529530.1	-
Kytorhynchus sp. n	KC869777.1	KC869882.1	-
Kytorhynchus sp.	KC529400.1	KC529526.1	-
*Neokytorhynchus pacificus**	OR607997	OR616254	-
Kytorhynchus microstylus A*	OR607995	OR616252	-
Kytorhynchus microstylus B*	OR607996	OR616253	-
Kytorhynchus yusdieli **sp. n.***	OR607998	-	-
Gaziella sp.	AY775776.1	-	-
Gaziella cochleata **sp. n.** A*	OR607992	OR616249	-
Gaziella cochleata **sp. n.** B*	OR607993	OR616250	-
Gaziella glandulosa **sp. n.***	OR607993	OR616251	-
Beklemischeviella angustior	KC529412.1	KC529538.1	-
Beklemischeviella contorta	KC529413.1	KC529539.1	-
Trigonostomum armatum Cuba*	OR608004	OR616258	OR643857
Trigonostomum armatum France	KC529419.1	KC529545.1	-
Trigonostomum denhartogi	AY775773.1	-	-
Trigonostomum franki	KC529416.1	KC529542.1	***OR643860**
Trigonostomum penicillatum	KC529414.1	KC529540.1	***OR643859**
Trigonostomum setigerum	KC529418.1	KC529544.1	**-**
Trigonostomum sinensis isolated 3	MN316548.1	MN316544.1	-
Trigonostomum sinensis isolated 4	MN316549.1	MN316545.1	-
Trigonostomum tillicum	MF321753.1	MF321762.1	-
Trigonostomum tori	MF321754.1	MF321763.1	MG266163.1
*Trigonostomum vanmecheleni**	OR608005	OR616259	OR643856
Trigonostomum venenosum	KC529417.1	KC529543.1	***OR643861**
Trigonostomum watsoni	KC529415.1	KC529541.1	***OR643858**
Proxenetes bilioi	KC529407.1	KC529533.1	-
Proxenetes fasciger	KC529408.1	KC529534.1	-
Proxenetes flabellifer	AY775764.1	-	-
Proxenetes karlingi	KC529409.1	KC529535.1	-
Proxenetes puccinellicola	AY775765.1	-	-
Proxenetes quadrispinosus	AY775766.1	-	-
Proxenetes quinquespinosus	KC529406.1	KC529532.1	-
Proxenetes simplex	KC529410.1	KC529536.1	-
Proxenetes trigonus	AY775768.1	-	-
Ptychopera japonica	MF321751.1	MF321760.1	-
Ptychopera plebeia	AY775769.1	-	-
Ptychopera unicornis	MF321752.1	MF321761.1	-
Ptychopera westbladi	AY775770.1	KC529546.1	-
Ptychopera sp. 1	KC529420.1	-	-
Ptychopera sp. 2	KC529420.1	KC529547.1	-
Ceratopera axi	MF321746.1	MF321756.1	-
Ceratopera gracilis	KC529422.1	KC529549.1	-
Ceratopera complicata	MF321747.1	MF321757.1	-
Ceratopera pilifera	MF321749.1	MF321759.1	MG266160.1
Ceratopera pacifica	MF321748.1	MF321758.1	-
*Ceratopera paragracilis**	OR607991	-	-
Ceratopera sp.	KC529421.1	KC529548.1	-
Parapharyngiella caribbaea A*	OR607999	-	-
Parapharyngiella caribbaea B*	OR608000	-	-
Parapharyngiella caribbaea C*	OR608001	-	-

Table 3 (continued)

Species	18S rDNA	28S rDNA	*cox*1
Parapharyngiella sp. 1	KC529405.1	KC529531.1	**-**
Parapharyngiella sp. 2	MF321750.1	-	-
Cilionema hawaiensis	KC529428.1	KC529556.1	-
Coronhelmis lutheri	KC529426.1	KC529554.1	-
Coronhelmis multispinosus	KC529427.1	KC529555.1	-
Tvaerminnea karlingi	MF321755.1	MF321764.1	-
Litucivis serpens	AY775758.1	KC529552.1	-
Promesostoma caligulatum	KC529432.1	KC529560.1	-
Promesostoma cochleare A	KC869831.1	KC869884.1	KC869891.1
Promesostoma cochleare B	KC529429.1	KC529557.1	***OR643862**
Promesostoma cubanum **sp. n.***	-	OR616246	-
Promesostoma dipterostylum	MG256039.1	MG256083.1	MG256140.1
Promesostoma maculosum	KC529434.1	KC529562.1	**-**
Promesostoma marmoratum	KC529430.1	KC529558.1	***OR643864**
Promesostoma meixneri	KC529433.1	KC529561.1	***OR643863**
Promesostoma neglectum	-	KC529564.1	-
Promesostoma roseapharynx **sp. n.***	OR608002	OR616256	-
Promesostoma rostratum	-	KC529563.1	-
Promesostoma sp. 1	MN165841.1	-	-
Promesostoma sp. 2	MG256040.1	MG256084.1	MG256141.1
Promesostoma sp. 3	AY775763.1	-	-
Promesostoma sp. 4	KC529431.1	KC529559.1	-
Astrotorhynchus bifidus	-	MG256098.1	-
Astrotorhynchus hakaiensis	MG256032.1	MG256076.1	-
Astrotorhynchus intermedius	MG256063.1	MG256107.1	MG256165.1
Astrotorhynchus regulatus	MG256048.1	-	-
Microvahine corallicola	KC529423.1	KC529550.1	-
Kymocarens sp.	KC529425.1	-	-
Brinkmanniella palmata	KC529424.1	KC529553.1	-
Brinkmanniella tenebrosa **sp. n.***	OR607988	OR616247	-
Kaitalugia sp.	KC529482.1	KC529613.1	-
Maehrenthalia agilis	AF100190.1	AJ315645.1	-
Styloplanella strongylostomoides	AY775772.1	-	-
Thalassoplanella collaris	KC529483.1	KC529614.1	-
Byrsophlebs delamarei	KC529435.1	KC529565.1	-
Byrsophebs thalassicola **sp. n.***	OR607990	OR616255	-
Byrsophlebs sp.*	OR607989	OR616248	-
Byrsophlebidae sp.	KC529436.1	KC529566.1	-
Limnotyphloplanida			
Opistomum arsenii	KC529491.1	KC529620.1	-
Carcharodopharynx sp.	KC529481.1	KC529612.1	-
Krumbachia sp.	KC529488.1	KC529618.1	-
Castrada lanceola	AY775751.1	-	-
Rhynchomesostoma rostratum	KC529500.1	KC529625.1	-
Mesocastrada sp.	U70081.1	-	-
Typhloplana viridata	KC529484.1	KC529615.1	-
Castrada hofmanni	KC529496.1	-	-
Castrada intermedia	KC529497.1	-	-
Castrada luteola	AY775752.1	-	-
Castrada neocomensis	KC529498.1	-	-
Castrada viridis	AY775753.1	-	-

Table 3 (continued)

Species	18S rDNA	28S rDNA	*cox*1
Gieysztoria acariaia	KC529470.1	KC529601.1	-
Gieysztoria ashokae	KC529466.1	KC529597.1	-
Gieysztoria beltrani	KC529475.1	KC529606.1	-
Gieysztoria cf. *billabongensis*	KC529442.1	KC529573.1	-
Gieysztoria choctaw	KC529476.1	KC529607.1	-
Gieysztoria complicata	KC529473.1	KC529604.1	-
Gieysztoria cuspidata	KC529458.1	KC529589.1	-
Gieysztoria cf. *cuspidata*	KC529457.1	KC529588.1	-
Gieysztoria dodgei	KC529479.1	KC529610.1	-
Gieysztoria garudae	KC529467.1	KC529598.1	-
Gieysztoria iberica	KC529461.1	KC529592.1	-
Gieysztoria infundibuliformis	KC529468.1	KC529599.1	-
Gieysztoria knipovici	KC529463.1	-	-
Gieysztoria ornata	KC529460.1	KC529591.1	-
Gieysztoria pavimentata	KC529472.1	KC529603.1	-
Gieysztoria rubra	KC529480.1	KC529611.1	-
Gieysztoria triquetra	KC529478.1	KC529609.1	-
Gieysztoria zuluensis	KC529465.1	KC529596.1	-
Gieysztoria sp. n. 1 scissors	KC529454.1	KC529585.1	-
Gieysztoria sp. n. 2 spine	KC529455.1	KC529586.1	-
Gieysztoria sp. n. 3 aberrant	KC529456.1	KC529587.1	-
Gieysztoria sp. n. 4 indian	KC529464.1	KC529595.1	-
Gieysztoria sp. n. 5 red	KC529469.1	KC529600.1	-
Gieysztoria sp. n. 6 'brown'	KC529474.1	KC529605.1	-
Gieysztoria sp. n. 7 hooklet	KC529477.1	KC529608.1	-
Gieysztoria sp. n. 8 sardinia	KC529462.1	KC529593.1	-
Gieysztoria sp. ZXY 2011	HQ993097.1	-	-
Gieysztoria sp. ZCX 2012_1	JQ999991.1	-	-
Gieysztoria sp. ZCX 2012_2	JQ999992.1	-	-
Gieysztoria sp. par YG 2018	MG820105.2	MG820107.2	-
Gieysztoria sp. pel YG 2018	MG820112.1	MG820115.1	-
Olisthanella truncula	KC529494.1	KC529623.1	-
Protoplanella simplex	KC529490.1	-	-
Phaenocora foliacea	KC529492.1	KC529621.1	-
Phaenocora unipunctata	AY775762.1	-	-
Phaenocora sp. n	KC529493.1	KC529622.1	-
Phaenocora sp. apu gw18	MW367557.1	-	-
Dochmiotrema limicola	KC529495.1	KC529624.1	-
Dochmiotrema sp. Kopanang A	KP702198.1	-	-
Dochmiotrema sp. BL 2017	MF542309.1	-	-
Bryoplana xerophila	KC529489.1	KC529619.1	-
Bothromesostoma personatum	KC529501.1	-	-
Mesostoma lingua	AY775759.1	KC529626.1	-
Mesostoma thamagae	AY775760.1	-	-
Strongylostoma devleeschouweri	KC529486.1	-	-
Strongylostoma elongatum	AY775771.1	-	-
Strongylostoma radiatum	KC529485.1	KC529616.1	-
Strongylostoma sp. c YC 2021	MW916326.1	MW930399.1	-
Strongylostoma sp. h YC 2021	MW916329.1	MW930401.1	-
Acrochordonoposthia conica	KC529487.1	KC529617.1	-
Dalyelliidae sp.	KC529441.1	KC529572.1	-

Table 3 (continued)

Species	18S rDNA	28S rDNA	*cox*1
Dalyelliidae n. gen. n. sp.	KC529441.1	-	-
Microdalyellia armigera	KC529451.1	KC529582.1	-
Microdalyellia brevispina	KC529450.1	KC529581.1	-
Microdalyellia fairchildi	KC529447.1	KC529578.1	-
Microdalyellia fusca	KC529453.1	KC529584.1	-
Microdalyellia kupelwieseri	KC529445.1	KC529576.1	-
Microdalyellia nanella	KC529449.1	KC529580.1	-
Microdalyellia picta	KC529446.1	KC529577.1	-
Microdalyellia rossi	KC529448.1	KC529579.1	-
Microdalyellia sinensis	JF429837.1	-	-
Microdalyellia sp. ZXY 2011	HQ993095.1	-	-
Pseudodalyellia alabamensis	KC529440.1	KC529571.1	-
Dalyellia tatrica	KC529443.1	KC529574.1	-
Dalyellia viridis	KC529444.1	KC529575.1	-
Castrella pinguis	KC529438.1	KC529569.1	-
Castrella truncata	AY775777.1	KC529570.1	-
Jensenia angulata	-	KC529568.1	-
Halammovortex sp.	KC529437.1	KC529567.1	-
Grappleria corona	MW052803.1	MW052802.1	-
Scutariella sinensis	MF773690.1	MF773687.1	-
Didymorchis sp.	AY157182.1	AY157163.1	-
Diceratocephala boschmai Ngamiyom	KC517073.1	-	-
Diceratocephala boschmai Tavakol	-	MW443040.1	-
Decadidymus gulosus	MW443041.1	-	-
Decadidymus sp. n. GWB-2018	MG345101.1	-	-
Temnocephala fasciata	KC869834.1	KC869888.1	-
Temnocephala sp. 1 DTL	AJ012520.1	-	-
Temnocephala sp. 2 Carranza	AF051332.1	-	-
Temnocephala sp. Rohde	L41137.1	-	-
Temnosewellia acicularis	-	KX095259.1	-
Temnosewellia albata	-	KX095262.1	-
Temnosewellia aphyodes	-	KX095263.1	-
Temnosewellia belone	-	KX095272.1	-
Temnohaswellia capricornia	-	KX095296.1	-
Temnohaswellia comes	-	KX095305.1	-
Temnosewellia minor	AY157183.1	AY157164.1	-
Temnohaswellia simulator	-	KX095312.1	-
Temnohaswellia verruca	-	KX095322.1	-
Gelasinella powellorum	-	MW443044.1	-
Craspedella pedum	MN073837	-	-
Craspedella spenceri	-	MW443042.1	-
Craspedella sp.	-	MW443043.1	-
Outgroup			
Acrorhynchides robustus	KC602396.1	KC602398.1	-
Placorhynchus octaculeatus	KC602395.1	KC602397.1	-

et al., 2012) on the CIPRES Science Gateway (Miller et al., 2010). Best-fitting partitions and substitution models were specified where possible (see Table 4); otherwise, the second most complex model implemented in MrBayes was chosen. Two independent runs were conducted simultaneously for 10,000,000 generations, each including one cold and three heated chains. Trees were sampled every 1000th generation, the first 25% being discarded as burn-in. Chain

Table 4 Best-fitting partitions and substitution models used in the phylogenetic analyses of Dalytyphloplanida, as calculated in ModelFinder (Kalyaanamoorthy et al., 2017) according to AICc

Dataset	Partition scheme	Substitution model	MrBayes friendly model
Dalytyphloplanida	18S rDNA; 28S rDNA	GTR+G+I	GTR+G+I
Promesostoma	18S rDNA; 28S rDNA	GTR+G+I	GTR+G+I
	1st codon positions of *cox1*	TN+I	GTR+I
	2nd codon positions of *cox1*	TVM+G	GTR+G
	3rd codon positions of *cox1*	TIM+G	GTR+G
Trigonostomum	18S rDNA; 28S rDNA	GTR+G+I	GTR+G+I
	1st codon positions of *cox1*	TIM2+I	GTR+I
	2nd codon positions of *cox1*	TPM3+G	GTR+G
	3rd codon positions of *cox1*	TIM2+G	GTR+G

convergence was confirmed by the average standard deviation of split frequencies dropping below 0.01, the potential scale reduction factor approaching 1.0, and the log probability reaching a stationary distribution. Obtained topologies were summarised in a majority-rule consensus tree. Inferred posterior probabilities (pp) were employed as support values. ML and BI trees were visualised and rooted in FigTree v1.4.3 (Rambaut, 2006–2019). Weakly supported clades (UFboot < 95, SH-aLRT < 80, and pp < 0.95) were collapsed.

Upon collecting and studying the morphological characteristics of *Trigonostomum vanmecheleni*, we observed a high degree of similarity to what has been described for *T. sinensis* Wang & Hu in Hu et al., 2019, prompting us to consider the possibility that these species might be synonyms (see results and discussion for further details). To investigate the genetic variations within and between these two species, we calculated the inter- and intraspecific genetic distances (ML distances) within *Trigonostomum* using a model-based approach in PAUP* v4.0 (Swofford, 2003). The model parameters were determined based on the output of IQ-TREE for the *Trigonostomum* dataset, using the same parameters mentioned earlier.

Abbreviations used in the figures

Ar, adenal rhabdites; **b**, bursa; **ba**, bursal appendage; **bg**, basophilic gland; **br**, brain; **bsr**, bursal seminal reservoir; **ca**, common genital atrium; **cb**, copulatory bulb; **cg**, common gonopore; **ci**, cilia; **cig**, cirrus glands; **cm**, circular muscles; **cir**, cirrus; **e**, eyes; **ed**, ejaculatory duct; **eg**, eosinophilic gland; **ep**, epithelium; **fd**, female duct; **fg**, female gonopore; **fgl**, female glands; **gl**, anterior glands; **ilm**, internal longitudinal muscles; **in**, anterior invagination; **lm**, longitudinal muscles; **m**, mouth; **ma**, mantle; **mb**, male copulatory bursa; **md**, male duct; **mg**, male gonopore; **od**, oviduct; **oe**, oesophagus; **ov**, ovary; **pa**, parenchyma sheath; **pg**, prostatic glands; **ph**, pharynx; **phg**, pharyngeal gland; **pl**, mantle plate; **pp**, penis papilla; **ppc**, prepharyngeal cavity; **pv**, prostate vesicle; **rm**, radial muscles; **sbc**, sclerotised bursal channel; **sc**, sclerotised cap; **sm**, sperm; **sph**, sphincter; **sr**, seminal receptacle; **st**, stylet; **sv**, seminal vesicle; **t**, testis; **tp**, tail plate; **va**, vagina; **vc**, vacuoles; **vi**, vitellaria; **x**, see in the text.

Results

Twenty-two species of marine Dalytyphloplanida from Cuba, Panama and Lanzarote are presented, sixteen of which are new to science and for one species a new genus is erected. One species belongs to Neodalyellida and the others to Neotyphloplanida (Thalassotyphloplanida).

Taxonomical account

Neodalyellida Willems et al., 2006
Schockaertiidae fam. n. Diez, Monnens, Reygel & Artois
urn:lsid:zoobank.org:act: D4A0F96C-611A-43EA-A79D-03D1164B4960

Diagnosis. Small neodalyellids with pharynx rosulatus. Testes, ovaries and vitellaria paired. Atrial organs devoid of sclerotised structures. Female system with one or two apertures to the outside.
Type genus. *Schockaertia* **gen. n.** Diez, Monnens, Reygel & Artois, here designated.
Contained taxa. *Einarella argillophyla* Luther, 1948 and *Schockaertia aprostatica* **sp. n.** Diez, Reygel & Artois.

***Schockaertia* gen. n. Diez, Reygel & Artois**
urn:lsid:zoobank.org:act: F150B284-F9DB-49C5-93DF-0DBABFA9BF6D

Diagnosis. Representative of Schockaertiidae **fam. n.** with a simple, unarmed and sac-shaped copulatory bulb. Genital system without prostate vesicle, bursa or uterus. Apart from its connection to the common genital atrium, a vagina connects the female system to the outside.

Type species. *Schockaertia aprostatica* **sp. n.**, by monotypy.
Etymology. The new name of the family and its type genus are dedicated to Prof. Dr. Ernest Schockaert (Hasselt University, Belgium) for his extraordinary contribution to the knowledge of microturbellarian taxonomy, Rhabdocoela in particular.

***Schockaertia aprostatica* sp. n. Diez, Reygel & Artois**
(Figs. 1 and 2)
urn:lsid:zoobank.org:act: C8BB595A-E09B-4A05-8DA9-1FE94B5B25ED
Typhlo sp. 8 in Diez et al. (2023)

Material and distribution. Cuba: Observations on live animals, two serially sectioned afterwards, one of which is designated holotype (ZMH, No. V13677) and the other paratype (HU, No. 854), collected in Las Sardinas (type locality) (22 June 2017); silty and very fine-grained sand, 0.5 m deep, salinity 31‰. One specimen used for molecular analyses, collected near the Hotel Guamá (October 21, 2020); silty and very fine-grained sand, 0.8 m deep, salinity 32‰.

Etymology. The epithet refers to the absence of a prostate vesicle.
Diagnosis. Provisionally with the same diagnosis of the genus.
Description. The animals are 0.2 mm long ($n=2$), measured on sections, unpigmented, with a pair of eyes (Figs. 1a, c and 2a: e). The syncytial and fully ciliated epidermis is 2–3 µm thick. The epidermis contains a single type of vacuole, filled with a fine-grained eosinophilic secretion (Fig. 1c: vc). The rhabdites are globular, 0.5–1 µm in diameter, located at the apical side of the epidermis. The cilia are 4–5 µm long. Three kinds of sac-shaped glands open at the anterior body end: coarse-grained basophilic ones (stained dark blue-black) (Fig. 1c: gl1), fine-grained basophilic ones (stained purplish) (Fig. 1c: gl2), and fine-grained eosinophilic ones (stained brownish) (Fig. 1c: gl3).

The pharynx (Figs. 1a–c and 2a–d: ph) is 62–77 µm in diameter ($\bar{x}=70$ µm; $n=2$), measured on sections, located at 50%. The prepharyngeal cavity (Fig. 1c: ppc) is lined with a nucleated epithelium and opens to the outside through the

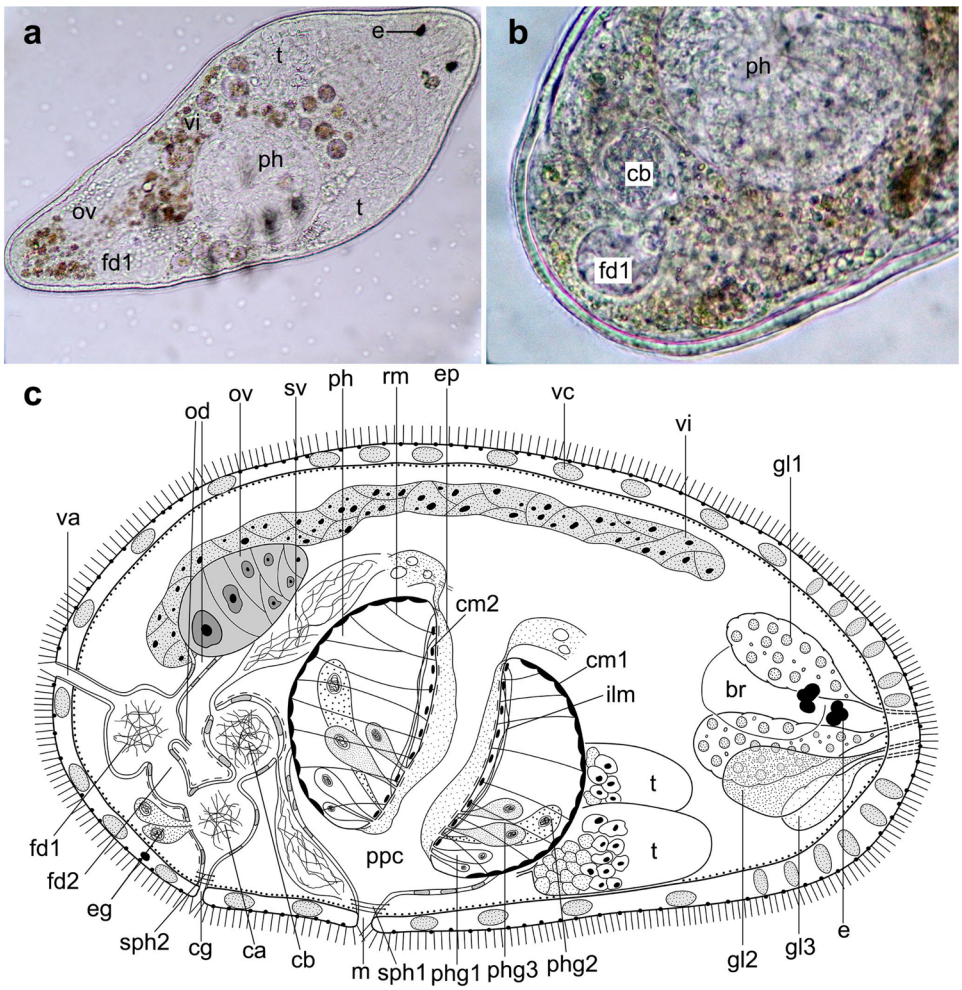

Fig. 1 *Schockaertia aprostatica* **gen. n. sp. n**. **a**, **b** A live animal. **c** Schematic reconstruction from sagittal sections of the body from the right side. The left ovary and vitellarium are not drawn. Structures oriented with the anterior end toward the right side of the plate

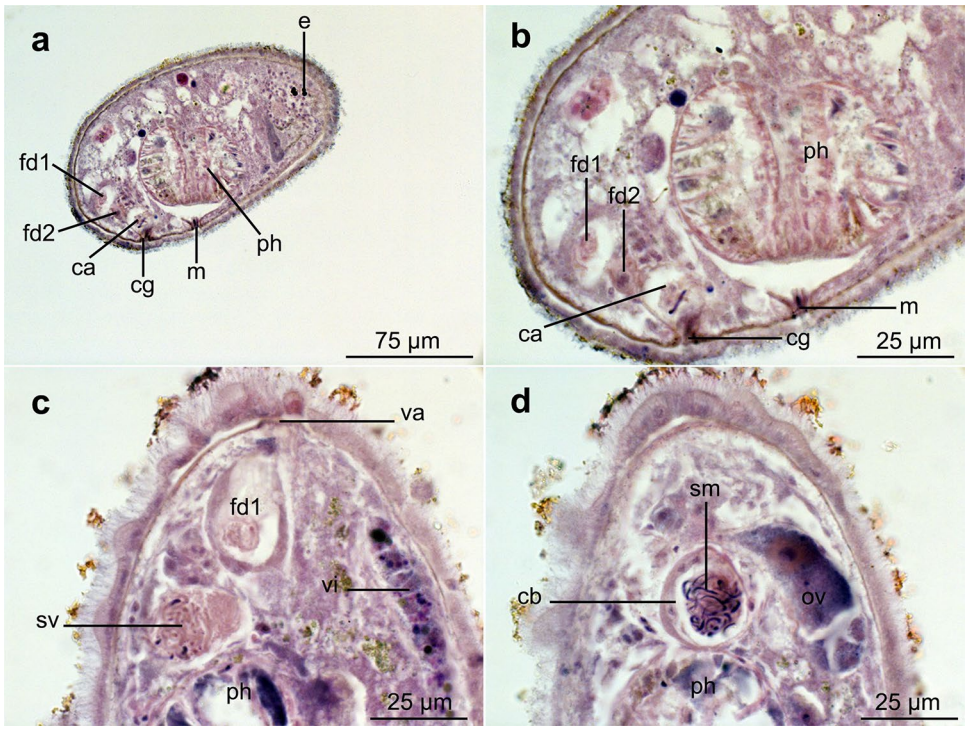

Fig. 2 *Schockaertia aprostatica* **gen. n. sp. n**. Micrograph of the sections. **a**, **b** Structures oriented with the anterior end toward the right side of the plate. **c**, **d** Structures oriented with the anterior end toward the bottom of the plate

mouth (Figs. 1c and 2a, b: m), which is surrounded by a sphincter (Fig. 1c: sph1). Three types of glands open in the distal half of the pharyngeal lumen: two types containing a fine-grained eosinophilic secretion (stained brownish and reddish, respectively) (Fig. 1c: phg1 and phg3, respectively) and one containing a coarse-grained basophilic secretion (stained dark blue-black) (Fig. 1c: phg2). The musculature of the pharynx includes a thick external layer of circular muscles (Fig. 1c: cm1) just inside of the septum. The pharynx lumen is lined by a syncytial epithelium (Fig. 1c: ep) and an inner circular muscle layer (Fig. 1c: cm2). Internal longitudinal muscles are present (Fig. 1c: ilm). Radial muscles (Fig. 1c: rm) run between the internal and the external walls. No muscles were observed outside of the septum or around the prepharyngeal cavity.

A pair of testes (Fig. 1 a and c: t) is located ventrally, anterior to the pharynx. The vasa deferentia form a pair of seminal vesicles caudal to the pharynx (Figs. 1c and 2c: sv). The seminal vesicles are lined by a nucleated epithelium. Distally, the seminal vesicles narrow and open into the copulatory bulb (Figs. 1b, c and 2d: cb). The copulatory bulb is an unarmed sac, filled with sperm (see Fig. 2d: sm) and hence functions as an unpaired seminal vesicle. It is lined with a nucleated epithelium and longitudinal muscles and enters the common genital atrium (Figs. 1c and 2a, b: ca) dorsally. A prostate vesicle is absent. Some sperm was also observed in the common genital atrium, which could be an artefact resulting from the fixation of the specimens or residual sperm from previous copulation events.

The paired vitellaria (Figs. 1a, c and 2c: vi) lie dorsally at each body side, between the brain (Fig. 1c: br) and the caudal body end. Each vitellarium connects to the respective oviduct (Fig. 1c: od) just distally to the ovary. The ovaries (Figs. 1a, c and 2d: ov) are kidney shaped, with the oocytes proximally diminishing in diameter. The oviducts are lined by a nucleated epithelium, and open into the sac-shaped female duct. The female duct is bipartite: The proximal globular part (Figs. 1a–c and 2a–c: fd1) is filled with sperm and lined by a thin anucleated epithelium. More distally, the female duct forms a second, smaller part: the stalk (Figs. 1c and 2a, b: fd2). The stalk is lined by a nucleated epithelium and longitudinal muscles and opens caudally into the common genital atrium. Muscles were not observed around the oviducts or the proximal part of the female duct. The proximal part of the female duct opens to the outside through a caudal vagina (Figs. 1c and 2c: va). The common genital atrium is lined by a low, nucleated epithelium and by longitudinal muscles. It receives fine-grained, eosinophilic glands (Fig. 1c: eg) through its caudal wall. The common gonopore (Figs. 1c and 2a, b: cg) is situated at 80% and is surrounded by a sphincter (Fig. 1c: sph2).

Neotyphloplanida Willems et al., 2006
Thalassotyphloplanida Willems et al., 2006
Kytorhynchidae Rieger, 1974
***Kytorhynchus* Rieger,** 1974
***Eukytorhynchus* Boyko,** 1996
***Kytorhynchus (Eukytorhynchus) microstylus* Rieger,** 1974

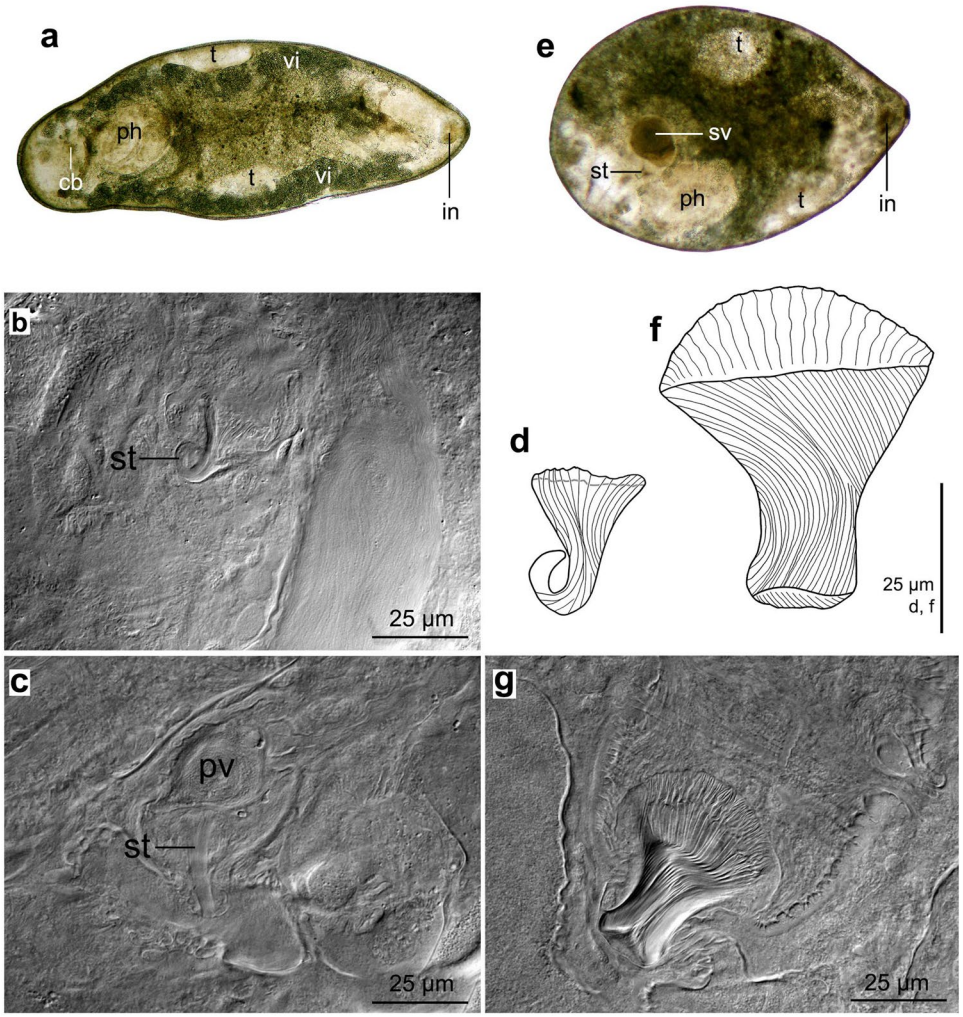

Fig. 3 *Kytorhynchus* (*Eukytorhynchus*) *microstylus* Rieger, 1974. **a** Body organisation (live animal). **b**, **c** Stylet (from a whole mount). *Kytorhynchus* (*Eukytorhynchus*) *yusdieli* **sp. n. d** Body organisation (live specimen). **e**, **f** Stylet (from the holotype). **a**, **d** Structures oriented with the anterior end toward the right side of the plate. **b**, **c**, **e**, **f** Structures are oriented with the anterior end toward the top of the plate

(Fig. 3a–d)
Kytorhynchus sp. 1 in Diez et al. (2023)

Known distribution. Beaufort, NC, USA, and Tobacco Bay, St. George, Bermuda (Rieger, 1974).
Material and distribution. Cuba: Observations on live animals, whole mounted afterwards. Five whole mounts from Siboney (7 February 2016 and 5 June 2017) (HU XIX.2.23–XIX.2.27); fine sand with organic matter, 0.5 m deep, salinity 32‰. Three whole mounts from Bueycabón (18 November and 14 December 2017; 6 February 2018) (HU XIX.2.28–XIX.2.30), fine silty sand, 0.5 m deep, salinity 31–33‰. One whole mount from Sardinero (30 ctober 2018) (HU XIX.2.31), fine sand, 1.4 m deep, salinity 32‰. Two specimens used for molecular analyses, one from Siboney and another from Chivirico.
Remarks. Habitus and internal organisation of the specimens from Cuba (Fig. 3a) are as described by Rieger (1974) in the original description. The funnel-shaped stylet (Fig. 3b, c: st, Fig. 3d), with longitudinal folds over its entire length and distally hook shaped, is 23–43 µm long ($\bar{x}$ = 34 µm; n = 9) and 10–27 µm wide proximally ($\bar{x}$ = 17 µm; n = 9). In some specimens, the stylet is complete straight (Fig. 3c).

***Kytorhynchus (Eukytorhynchus) yusdieli* sp. n. Diez, Reygel & Artois**
(Fig. 3e–g)
urn:lsid:zoobank.org:act: 31C7F10E-BB15-4918-B4AA-87101A70D5CC
Kytorhynchus sp. 2 in Diez et al. (2023)

Material and distribution. Cuba: Observations on live animals, whole mounted afterwards. One whole mount from Bueycabón (Type locality) (June 5, 2017), designated holotype (ZMH, No. V13678), fine silty sand, 0.5 m deep, salinity 31‰. Four whole mounts from Sardinero (October 30, 2018 and March 18, 2021) (HU XIX.2.32–XIX.2.35), one specimen collected subtidally, fine sand, 1.4 m deep, three specimens collected subtidally, 0.5 m deep, fine sand, salinity 32‰. Four whole mounts from Embarcadero

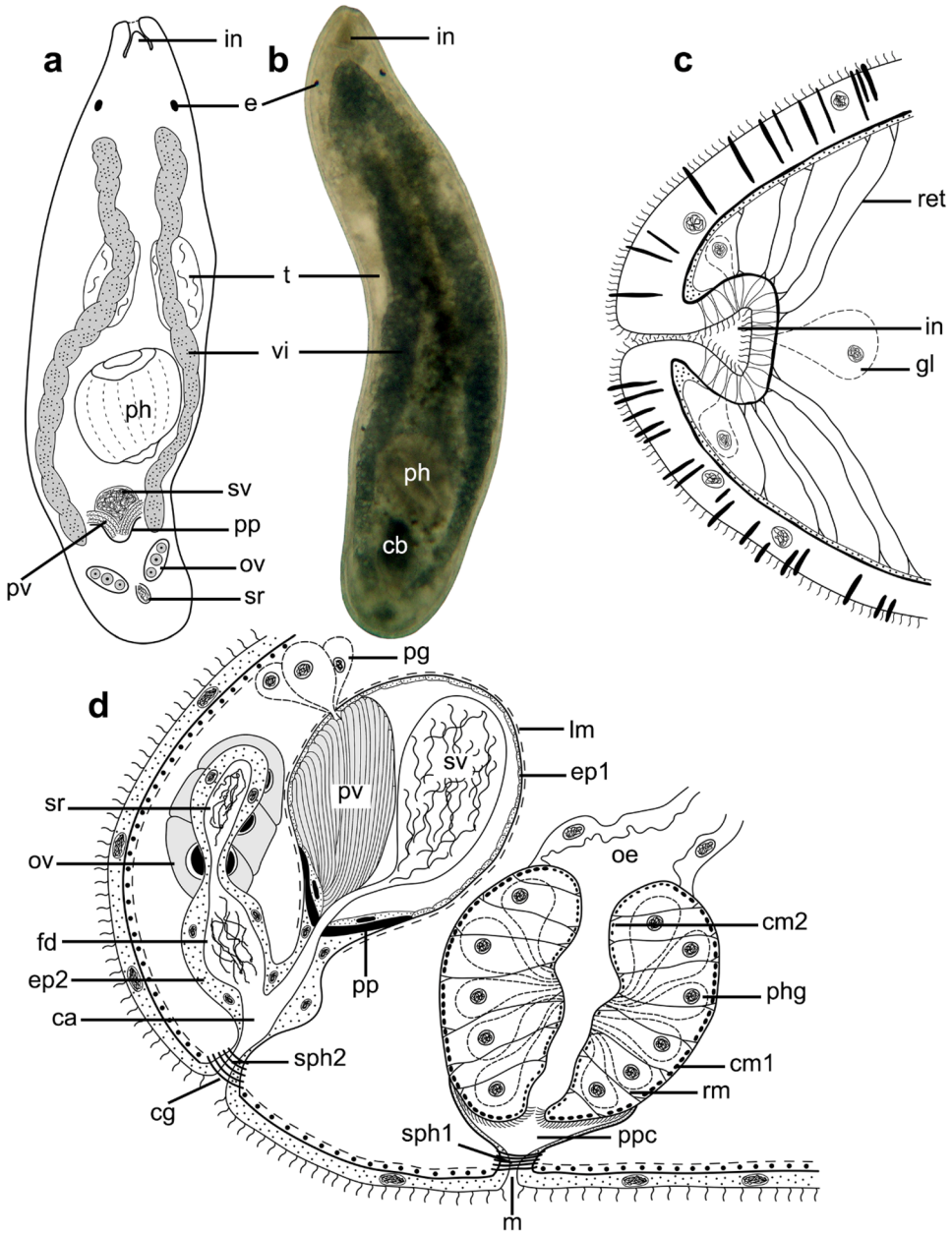

Fig. 4 *Neokytorhynchus pacificus* Ehlers & Ehlers, 1981. **a**, **b** Body organisation (live animals). **c** Schematic reconstruction from sagittal sections of the anterior invagination. **d** Schematic reconstruction from sagittal sections of pharynx and the genital systems from the right side; the left ovary and the vitellaria are not drawn. **a**, **b** Structures oriented with the anterior end toward the top of the plate. **c** Structures oriented with the anterior end toward the left side of the plate. **e** Structures oriented with the anterior end toward the right side of the plate

de Cayo Granma, Bahía de Santiago de Cuba (March 5, 2022) (HU XIX.2.36–XIX.2.39), sublittoral, 1 m deep, coarse and shelly sand with organic matter, salinity 35‰. One specimen used for molecular analyses, collected in Juraguá (11 May 2021); sublittoral, fine sand, 0.8 mm deep, salinity 34‰.

Etymology. Species dedicated to Dr. Yusdiel Torres-Cambas (Leibniz-Institute of Freshwater Ecology and Inland Fisheries, Germany), specialist in systematics and evolution of Odonata.

Diagnosis. Species of *Kytorhynchus* with a funnel-shaped stylet ~ 58 µm long, ~ 47 µm wide proximally, and ~ 20 µm wide distally, with longitudinal folds over its entire length.

Description. The live specimens (Fig. 3e) are about 1.2 mm long, translucent, without eyes. They are slightly brownish due to the presence of parenchymal glands. The anterior body invagination (Fig. 3e: in) is well developed, triangular and appears brown. The pharynx (Fig. 3e: ph) is 225 µm in diameter ($n = 1$) and located at 70–80%.

The testes (Fig. 3e: t) are located anterior to the pharynx. The vasa deferentia run backward and open proximally into the copulatory bulb. The copulatory bulb is located laterocaudal to the pharynx. The copulatory bulb encloses the seminal vesicle (Fig. 3e: sv), the prostate vesicle, and the stylet. The funnel-shaped stylet (Fig. 3e: st, f–g) is 53–62 µm long

($\bar{x}$ = 58 µm; n = 8), 34–53 µm wide proximally ($\bar{x}$ = 47 µm; n = 8), and 15–22 µm wide distally ($\bar{x}$ = 20 µm; n = 8). It shows longitudinal folds over its entire length.

The paired vitellaria run dorsally from the anterior part to the caudal body end. The globular ovaries are located caudally.

***Neokytorhynchus* Ehlers & Ehlers, 1981**
***Neokytorhynchus pacificus* Ehlers & Ehlers, 1981**
(Figs. 4 and 5)

Known distribution. Bahía Academy, Santa Cruz, Galapagos Islands (Ehlers & Ehlers, 1981).

Material and distribution. Canary Islands: Observations on live animals. Three whole mounts; ten sagittally; five horizontally; and six transversally oriented serial sections (HU XIX.2.40–XIX.2.50, XIX.3.01–XIX.3.13); and one specimen used for molecular analyses, collected in Lanzarote. Small bay just south of Orzola (7 October 2011), sheltered pool with a direct connection to the ocean; coarse sand with large pieces of lava rocks, 50–60 cm under water. Mala (October 13, 2011); intertidal, coarse, mixed, calcareous, volcanic sediment, upper 4–6 cm of sand, taken between rocks.

Remarks. The sectioned specimens are approximately 0.4 mm long, and 0.2 mm in width, smaller than that ones from The Galapagos (0.7 mm long; Ehlers & Ehlers, 1981). The structure of the epidermis, basal membrane, and subepidermal muscle layer is similar to what is described for other kytorhynchids (see Rieger, 1974). The anterior body invagination (Figs. 4a–c and 5a, b: in) and the pharynx (Figs. 4a, b, d and 5a, c: ph) are as that described for the specimens from The Galapagos.

The gonopore (Fig. 4d: cg) is located ventrally and subcaudally and opens into the common genital atrium (Figs. 4d and 5c: ca). No epithelial nuclei occur in this area. The epithelium is ruffled here, giving the appearance of cilia (pseudociliation). The round copulatory bulb (Figs. 4b and 5a, c: cb) is lined with a nucleated epithelium (Fig. 4d: ep1) and

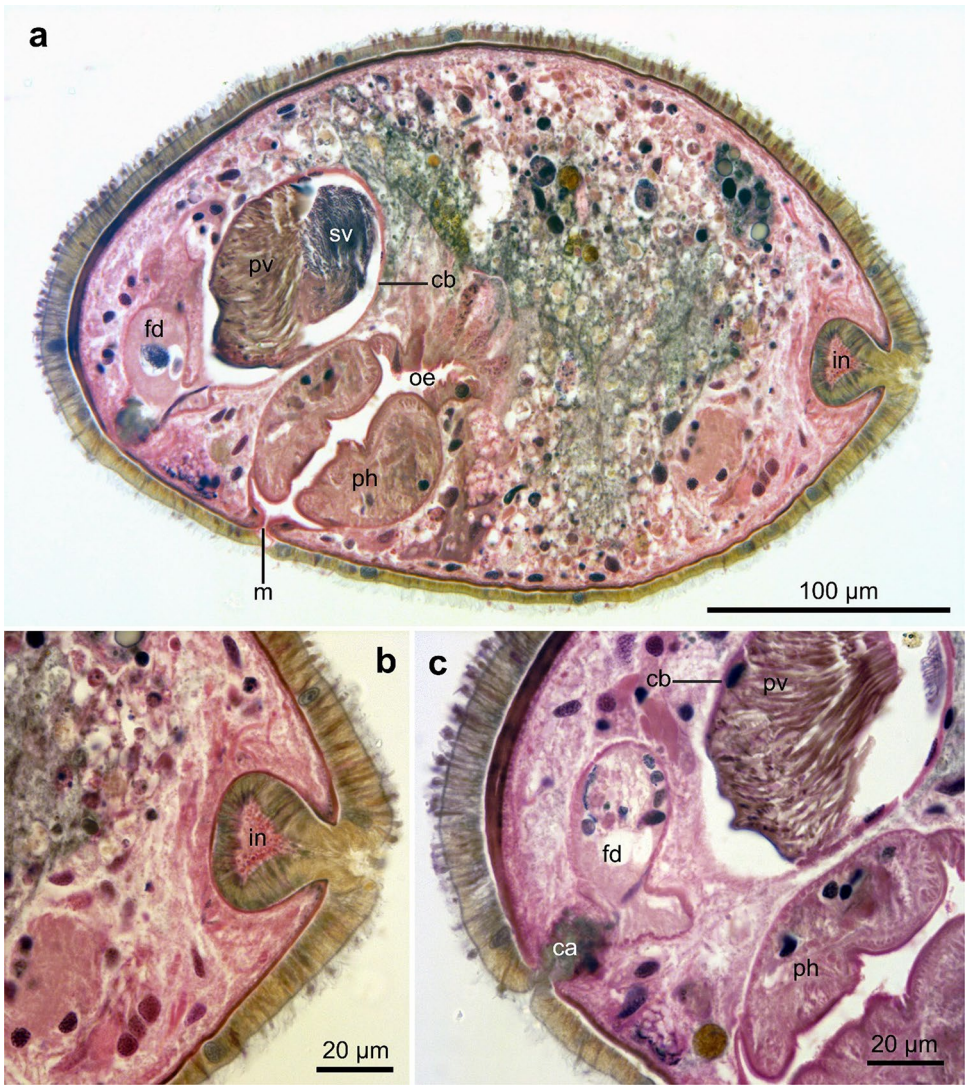

Fig. 5 *Neokytorhynchus pacificus* Ehlers & Ehlers, 1981. Micrograph of the sections. Structures oriented with the anterior end toward the right side of the plate

surrounded by a thin, longitudinal muscle layer (Fig. 4d: lm). The bulb contains the single seminal vesicle (Figs. 4a, d and 5a: sv) and a large prostate vesicle (Figs. 4a, d and 5a, c: pv), which empty into a broad, bowl-shaped penis papilla (Fig. 4a, d: pp). The penis papilla measures 25–34 µm in length and 33–44 µm in width ($n=2$), at its broadest point, and empties in a relatively large male atrium. According to Ehlers and Ehlers (1981), the length of the whole copulatory bulb of *N. pacificus* is 50 µm. The quality of the holotype of *N. pacificus* did not allow us to measure the penis papilla. Notwithstanding, this structure in the original drawing of Ehlers and Ehlers (1981: Fig. 15) is approximately 33 µm long, consonant with the measured range of the specimens from Lanzarote.

The paired ovaries (Fig. 4a, d: ov) are located at the caudal body end. The female duct (Figs. 4d and 5a, c: fd) is lined with a high, nucleated epithelium (Fig. 4d: ep2) and forms two seminal receptacles (Fig. 4d: sr), separated by a constriction. However, the bundles of glands entering the female duct and described from the specimens from The Galapagos were not observed in the specimens from Lanzarote.

Incertae sedis

***Gaziella* De Clerck & Schockaert, 1995**

***Gaziella cochleata* sp. n. Diez & Artois**

(Figs. 6a, b, 7a and 8a–c)

urn:lsid:zoobank.org:act: C1DF3F85-E74E-4848-B2C7-A46E97FA8AC5

Gaziella sp. 1 in Diez et al. (2023)

Material and distribution. Cuba: Observations on live animals, whole mounted afterwards. Two specimens used for

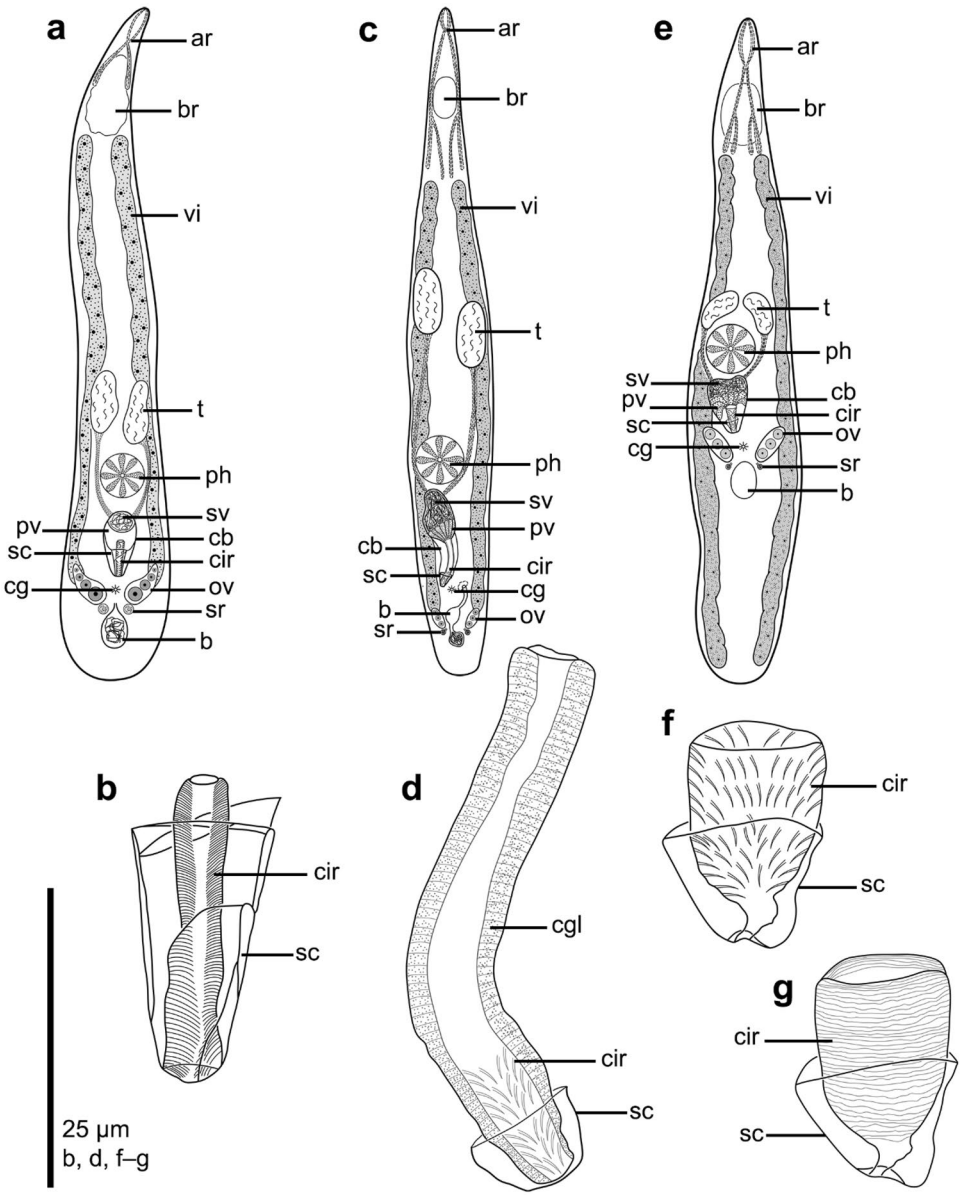

Fig. 6 Species of *Gaziella*. **a**, **b** *Gaziella cochleata* **sp. n. c**, **d** *G. glandulosa* **sp. n. e**–**g** *G. microcirra* **sp. n. a**, **c**, **e** Body organisation (live animals). **b**, **d**, **e**, **f** Cirrus and sclerotised cap from the holotypes. Structures oriented with the anterior end toward the top of the plate

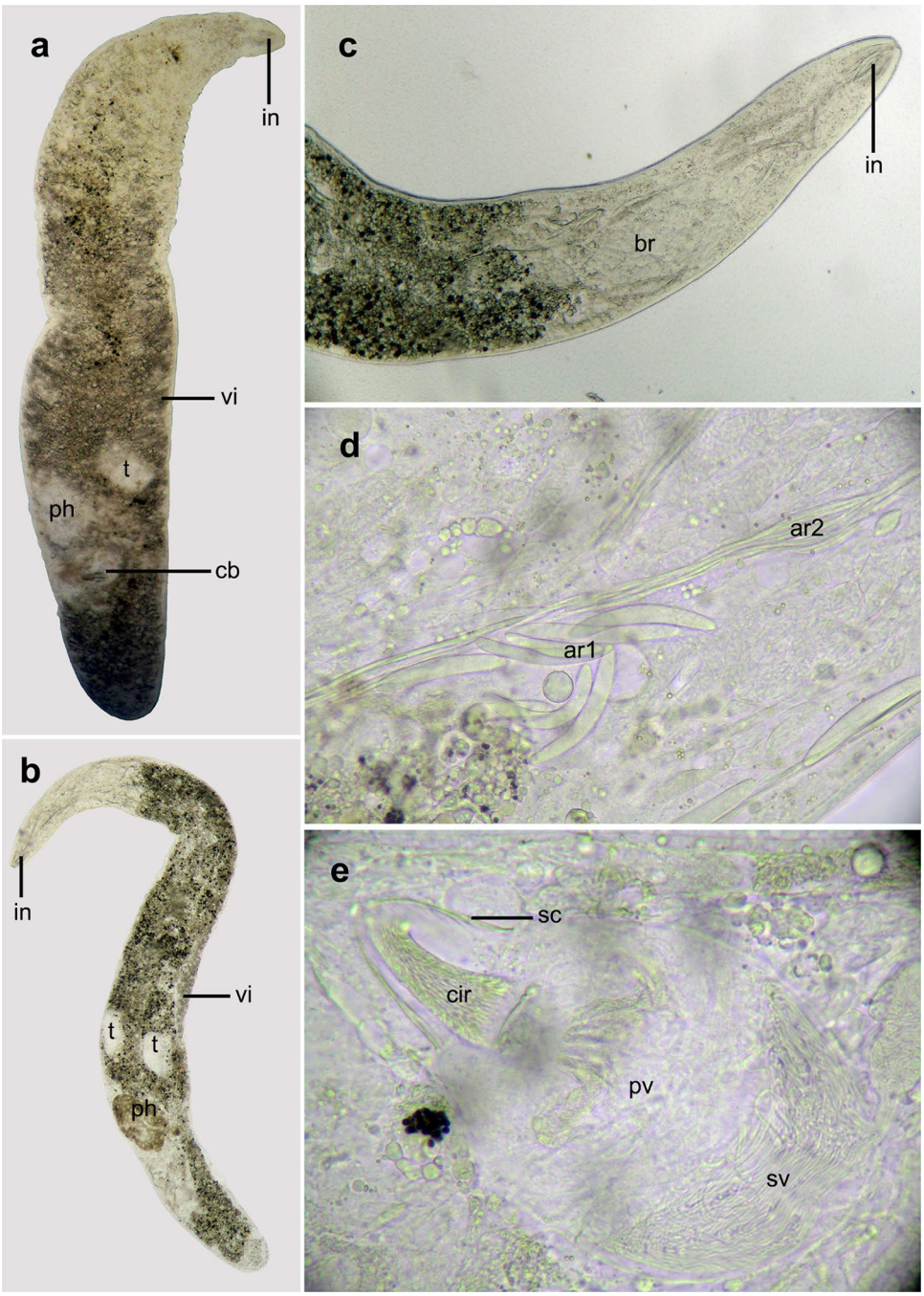

Fig. 7 Live specimens of species of *Gaziella*. **a** *Gaziella cochleata* **sp. n. b–e** *G. microcirra* **sp. n. a**, **b** Body organisation. **c**, **d** Details of the anterior region of the body and the rhabdite tracts. **e** Male copulatory bulb. **a**, **b** Structures oriented with the anterior end toward the top of the plate. **c–e** Structures oriented with the anterior end toward the right side of the plate

molecular analyses and four whole mounts from Bueycabón (type locality) (6 and 21 February 2018), one of which is designated holotype (ZMH, No. V13679) and the others paratypes (HU, No. 855–857); fine-grained sand with organic matter, 0.5 m deep, salinity 35‰. Four whole mounts from Playa Morales (January 4, 2017) (HU XIX.3.14–XIX.3.17); sandy-muddy bottom in a bed of *T. testudinum*, 0.5 m deep, salinity 35‰. One whole mount from Siboney (March 6, 2018) (HU XIX.3.28), sublittoral, 0.5 m deep, fine-grained sand rich in organic matter, salinity 33‰. Four whole mounts from Playa Caletón (26 January 2020) (HU XIX.3.18–XIX.3.21); sublittoral, 0.5 m deep, fine-grained sand around bed of *S. filiforme*, salinity 37‰. Three whole mounts from Juraguá (9 February 2020) (HU XIX.3.22–XIX.3.24); two specimens collected subtidally, 1 m deep, fine-grained sand, and one specimen collected intertidally, upper 20 cm of medium-grained sand, salinity 33‰. Three whole mounts from Hotel Guamá (October 21, 2020) (HU XIX.3.25–XIX.3.27); sublittoral, fine-grained and silty sand, 0.8 m deep, salinity 32‰.

Etymology. The epithet refers to the spiralised distal cap of the copulatory bulb. Lat. *Cochleatus*: spiral.

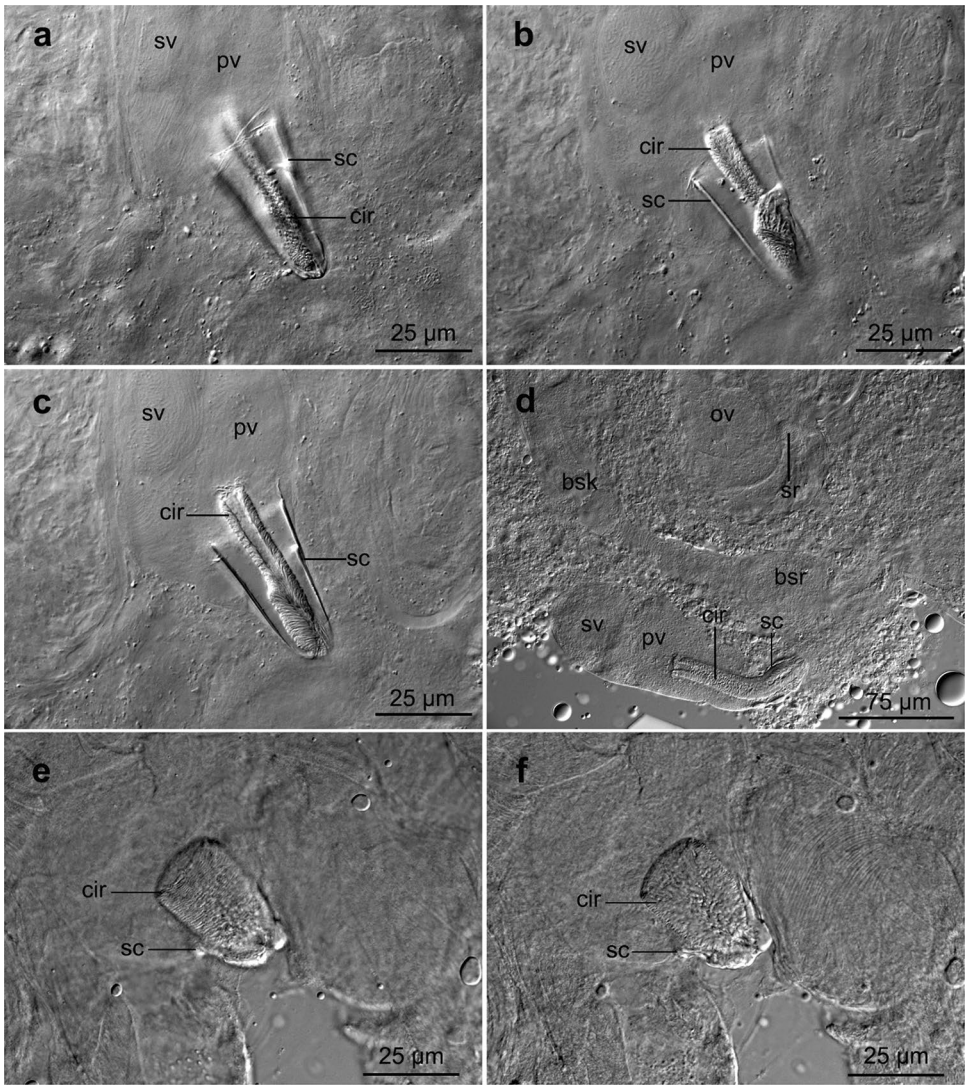

Fig. 8 Micrographs of the atrial organs of species of *Gaziella*, from the holotypes. **a–c**, *Gaziella cochleata* **sp. n. d** *G. glandulosa* **sp. n. e**, **f** *G. microcirra* **sp. n**. **a–c**, **e–f** Structures oriented with the anterior end toward the top of the plate. **d** Structures oriented with the anterior end toward the left side of the plate

Diagnosis. Species of *Gaziella* with a spiny cirrus ~ 44 µm long; spines ~ 5 µm long. The clerotized cap is a spiralised plate, ~ 41 µm long.

Description. The live animals are 2–2.5 mm long, slender, light-brown coloured due to parenchymal glands, and without eyes (Figs. 6a and 7a). Two types of strong frontal adenal rhabdites (Fig. 6a: ar) are present, opening in the anterior invagination (proboscis-like structure) (Fig. 7a: in). The pharynx (Figs. 6a and 7a: ph) is located at 75%.

The paired testes (Figs. 6a and 7a: t) are located anterolaterally from the pharynx. The thick seminal ducts run backwards and open independently into the single seminal vesicle (Figs. 6a and 8a–c: sv). The atrial organs are located caudal to the pharynx, in the distal body third. The copulatory bulb (Figs. 6a and 7a: cb) is inverted-pear shaped; it includes the seminal vesicle, the prostate vesicle (Figs. 6a and 7a–c: pv), a spiny cirrus (Figs. 6a, b and 8a–c: cir), and a distal clerotized cap (Figs. 6a, b and 8a–c: sc). The cirrus is 26–54 µm long ($\bar{x} = 44$ µm; $n = 14$) and 9–11 µm wide ($\bar{x} = 10$ µm; $n = 14$). The cirrus spines are fine, very close to each other, and 4–5 µm long ($\bar{x} = 5$ µm; $n = 28$). The clerotized cap is a spiralised plate, 32–62 µm long ($\bar{x} = 41$ µm; $n = 14$) and 17–27 µm wide proximally ($\bar{x} = 23$ µm; $n = 14$).

The paired vitellaria (Figs. 6a and 7a: vi) extend at both body sides, caudal to the brain (Fig. 6a: br) to the level of the pharynx. The paired kidney-shaped ovaries (Fig. 6a: ov) lie posterior to the male copulatory bulb; the oocytes are organised in a row, diminishing in diameter from the most distal to the most proximal. Each oviduct with a seminal reservoir vesicle (Fig. 6a: sr). The bursa (Fig. 6a: b) is located caudal to the ovaries. The common gonopore (Fig. 6a: cg) is located at about 80%, just caudal to the male copulatory organ.

Gaziella glandulosa sp. n. Diez & Artois

(Figs. 6c, d and 8d)

urn:lsid:zoobank.org:act: 838DF0F5-D6AB-4AC0-A341-41ECE429E8E5
Gaziella sp. 3 in Diez et al. (2023)

Material and distribution. Cuba: Observations on live animals. One whole mount, designated holotype (ZMH, No. V13680), and one specimen used for molecular analyses collected in Siboney (type locality) (June 5, 2017); intertidal, sand rich in organic matter, upper 10 cm of sediment, salinity 32‰.
Etymology. The epithet refers to the glandular proximal two-thirds of the cirrus. Lat. *Glandulae*: gland.
Diagnosis. Species of *Gaziella* with a cirrus 94 µm long, spiny in the distal 25% of its length; spines 5 µm long. The proximal 80% of the cirrus is glandular. Sclerotised cap 12 µm long and 18 µm wide proximally, it covers the distal 20% of the cirrus.
Description. The paired testes (Fig. 6c: t) are located some distance anterolaterally from the pharynx. The thick seminal ducts run backwards and open independently into de copulatory bulb (Fig. 6c: cb). The atrial organs are located caudal to the pharynx, in the last body third. The copulatory bulb encompasses the seminal vesicle (Figs. 6c and 8d: sv), the prostate vesicle (Figs. 6c and 8d: pv), the spiny cirrus (Figs. 6c–c and 8d: cir), and the clerotized cap (Figs. 6c, d and 8d: sc). The clerotized cap is 12 µm long and 18 µm wide proximally. It covers the spiny cirrus in the distal 20% of its length. The cirrus is 94 µm long and 13 µm wide; its walls are glandular (6d: cgl). The spines are distributed in the distal 23 µm of the cirrus length; they are fine and 3–6 µm long ($\bar{x}=5$ µm; $n=21$).

The paired vitellaria (Fig. 6c: vi) extend along the body sides, between the brain (Fig. 6c: br) and the pharynx. The paired oval-shaped ovaries (Figs. 6c and 8d: ov) lie posteriorly to the male copulatory bulb, with the oocytes in a row. Each oviduct has a seminal reservoir vesicle (Figs. 6c and 8d: sr). The bursa (Fig. 6c: b) is located caudal to the ovaries, with a long bursal stalk (Fig. 8d: bsk) and a proximal seminal reservoir vesicle (Fig. 8d: bsr). The walls of the bursa are thick and very muscular. The common gonopore opens at 90%, just caudal to the male copulatory organ.

***Gaziella microcirra* sp. n. Diez & Artois**
(Figs. 6e–g, 7b–e and 8e–f).
urn:lsid:zoobank.org:act: 49C98395-3F44-4FB2-99C9-F69A06E52947
Gaziella sp. 2 in Diez et al. (2023)

Material and distribution. Cuba: Observations on live animals, whole mounted afterwards. One whole mount from Bueycabón (type locality) (February 6, 2018) designated holotype (ZMH, No. V13681); sand with organic matter, 0.5 m deep, salinity 33‰. One whole mount from Guardalavaca (28 February 2017) (HU XIX.3.29); intertidal, upper layer of fine-grained sand, salinity 35‰. Two whole mounts from Playa Caletón (26 January 2020) (HU XIX.3.30–XIX.3.31); sublittoral, 0.5 m deep, fine-grained sand around bed of *S. filiforme*, salinity 37‰. One whole mount from Playa (27 January 2020) (HU XIX.3.32); sublittoral, 0.7 m deep, fine-grained sand, salinity 35‰. Two whole mounts from Siboney (6 March 2018) (HU XIX.3.33–XIX.3.34); sublittoral, 0.5 m deep, sand rich in organic matter, salinity 33‰. One whole mount from Juraguá (9 February 2020) (HU XIX.3.35), sublittoral, fine-grained sand, 1.5 m deep; salinity 33‰. One whole mount from Hotel Guamá (21 October 2020), sublittoral, 0.8 m deep, fine-grained and silty sand, in a bed of the turtlegrass *Thalassia testudinum* (HU XIX.3.36).
Etymology. The epithet reflects the fact that this species has the smallest cirrus among all known species of *Gaziella*.
Diagnosis. Species of *Gaziella* with a cirrus ~ 41 µm long, spines 3 µm long; surrounded distally by a ~ 28-µm-long sclerotised cap.
Description. The live animals are about 1.5 mm long, slender, translucent, and without eyes (Figs. 6e and 7b). Two types of strong frontal adenal rhabdites are present (Figs. 6c: ar and 7d: ar1 and ar2). The pharynx (Figs. 6e and 7b: ph) is located at 50–70%.

The paired testes (Figs. 6e and 7b: t) are located immediately anterolaterally to the pharynx. The thick seminal ducts run backwards and open independently into de copulatory bulb. The atrial organs are located caudal to the pharynx, in the second to the third body part. The copulatory bulb (Fig. 6e) is inverted-pear shaped. It encompasses the seminal vesicle (Figs. 6e and 7e: sv), the prostate vesicle (Figs. 6e and 7e: pv), the spiny cirrus (Figs. 6e–g, 7e and 8e–f: cir), and the distal sclerotised cap (Figs. 6e–g, 7e and 8e–f: sc). The sclerotised cap surrounds the spiny cirrus in its distal 1/2–1/3 length. The cirrus is 33–51 µm long ($\bar{x}=41$ µm; $n=7$) and 12–21 µm wide proximally ($\bar{x}=17$; $n=7$), and the sclerotised cap is 15–40 µm long ($\bar{x}=28$ µm; $n=5$) and 15–30 µm wide proximally ($\bar{x}=24$ µm; $n=7$). The specimen from Guardalavaca is much squeezed (cirrus 16 µm long and 12 µm wide; stylet broken and not measurable). The cirrus spines are very fine and positioned very close to each other, about 3 µm long.

The paired vitellaria (Figs. 6e and 7b: vi) extend at the body sides, caudal to the brain (Figs. 6e and 7c: br) to the distal body end. The paired oval-shaped ovaries (Fig. 6e: ov) lie posteriorly to the male copulatory bulb, with oocytes organised in a row. Each oviduct has a seminal reservoir vesicle (Fig. 6e: sr). The globular bursa (Fig. 6e: b) is caudally located to the ovaries. The common gonopore (Fig. 6e: cg) opens at 60–80%.

Byrsophlebidae Graff, 1905
***Byrsophlebs* Jensen,** 1878
***Byrsophlebs thalassicola* sp. n. Diez, Reygel & Artois**

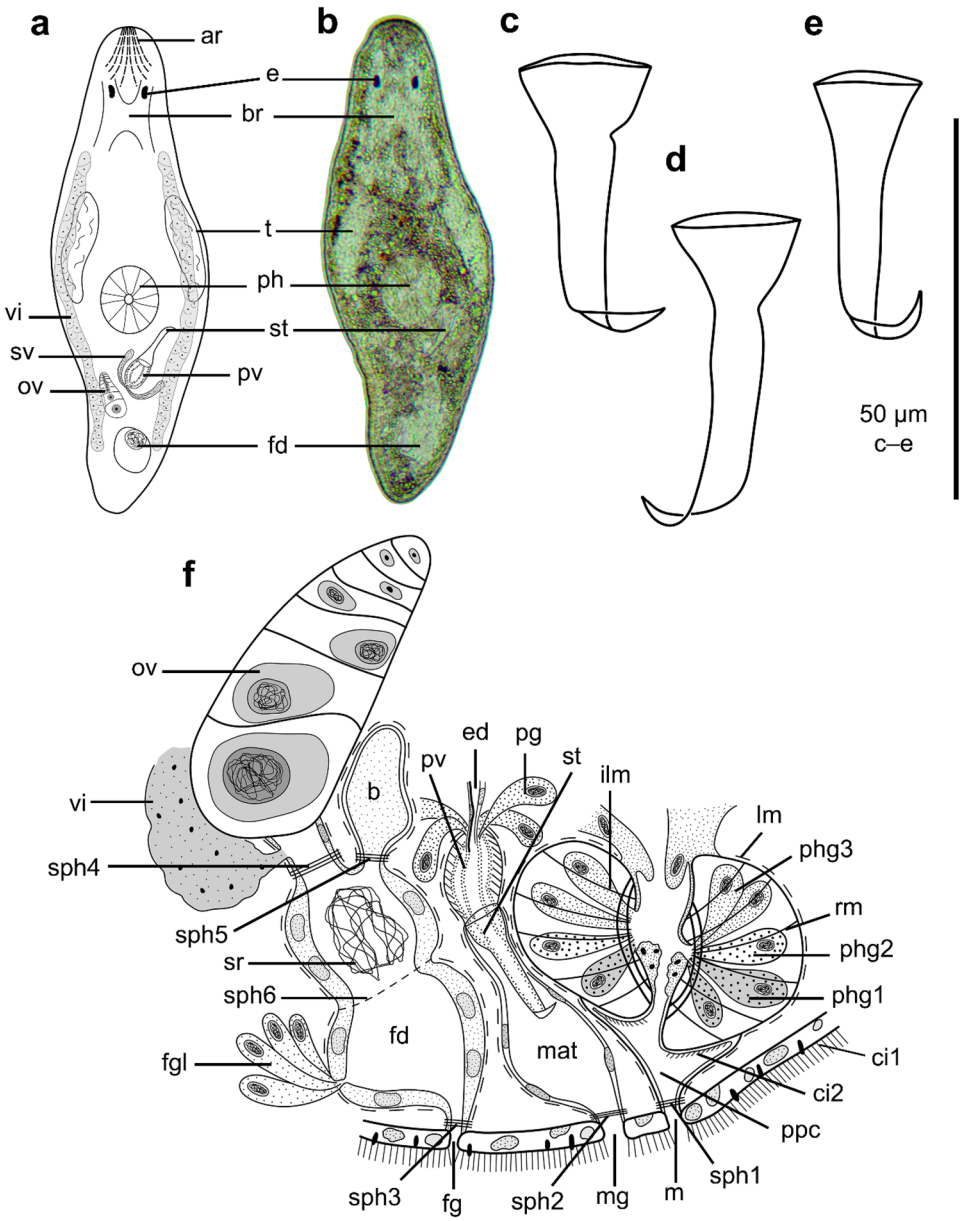

Fig. 9 *Byrsophlebs thalassicola* **sp. n. a**, **b** Body organisation (live animal). **c**–**e** Stylets. **f** Schematic reconstruction from sagittal sections of the pharynx and the genital systems from the right side. **c** From the holotype. **a**–**e** Structures oriented with the anterior end toward the top of the plate. **f** Structures oriented with the anterior end toward the right side of the plate

(Fig. 9)
urn:lsid:zoobank.org:act: BB6E81B4-7795-4BCD-B44E-D61E76E5B60F
Byrsophlebs sp. 1 in Diez et al. (2023)

Material and distribution. Cuba: Observations on live animals. Five whole mounts, one of which is designated holotype (ZMH, No. V13682) and the others paratypes (HU, No. 858–861), and one specimen used for molecular analyses collected in Bahía Larga (Type locality) (5 April and 25 May 2017); on leaves of *Thalassia testudinum* and the alga *Acanthophora spicifera*, 0.1–0.5 m deep, salinity 32–35‰. One whole mount from Chivirico (March 16, 2017) (HU XIX.3.37); sand with organic matter, 0.1 m deep, salinity 35‰. Four whole mounts (HU XIX.3.38–XIX.3.41) and eight serially sectioned specimens (HU XIX.3.42–XIX.3.49) collected in Bueycabón (6 and 21 February 2018); on leaves of *T. testudinum* and *Syringodium filiforme*, 0.5 m deep, and intertidal on the alga *Valoniopsis pachynema*, salinity 33‰.
Etymology. The epithet refers to the habitat of the species, namely leaves of *Thalassia testudinum*.
Diagnosis. Species of *Byrsophlebs* with a prostate stylet ~ 46 µm long. Proximal third of the stylet funnel shaped, middle third tubular, tapering to a distal sharp tip. Distal tip bends over 90°. Most external muscle layer surrounding the prostate vesicle longitudinal. Female duct bipartite, proximally differentiated into a seminal receptacle, which is separated from the distal part of the female duct by a sphincter. Bursa opens proximally into the female duct.

Description. The live specimens are about 0.5 mm long, translucent and have a pair of eyes (Fig. 9a, b: e). Adenal rhabdite tracts (Fig. 9a: ar) present, with the cell bodies caudal to the eyes, their necks in between the eyes and opening terminally at the anterior end of the body. The syncytial and fully ciliated epidermis is 4–6 µm thick; cilia (Fig. 9f: ci1) 4 µm long. It includes two types of vacuoles: translucent ones and ones filled with a dark-granular secretion. The rhabdites are 2–4 µm long.

The pharynx (Fig. 9a, b: ph) is located at 50%. The prepharyngeal cavity (Fig. 9f: ppc) is lined by a nucleated epithelium and a layer of longitudinal muscles. The mouth (Fig. 9f: m) is surrounded by a sphincter (Fig. 9f: sph1). Three types of glands open in the pharyngeal lumen from distal to proximal; these are as follows: coarse-grained eosinophilic (Fig. 9f: phg1), fine-grained eosinophilic (Fig. 9f: phg2), and fine-grained basophilic (Fig. 9f: phg3). The weak musculature of the pharynx is difficult to discern. There is a layer of longitudinal muscles just outside of the septum (Fig. 9f: lm). Radial muscles (Fig. 9f: rm) run between the internal and the external walls, and there are internal longitudinal muscles (Fig. 9f: ilm). The distal lips of the pharynx are ciliated; cilia ~ 2 µm long (Fig. 9f: ci2).

A pair of testes (Fig. 9a, b: t) is located anterior to the pharynx, whereas the rest of the genital system is situated caudal to the pharynx. Each vas deferens forms a seminal vesicle. The seminal vesicles (Fig. 9a: sv) fuse before entering the prostate vesicle. The prostate vesicle (Fig. 9a, f: pv) is spindle-shaped and is surrounded by an internal oblique and an external longitudinal muscle layer. The layer of longitudinal muscles is continuous with the layer that surrounds the male atrium (Fig. 9f: mat). The necks of the extracapsular prostatic glands (Fig. 9f: pg) enter the prostate vesicle proximally at the same point as the ejaculatory duct does, and contain a coarse-grained eosinophilic secretion. The prostatic ducts enter the stylet proximally and can be seen over the entire length of the stylet. The stylet (Figs. 3c–e and 9a, b, f: st) is located just caudal to the pharynx and has an anterior orientation. However, on much squeezed specimens (Fig. 9b), the stylet can turn towards either side or even have a posterior orientation. It is 43–52 µm long ($\bar{x}$ = 46 µm; n = 8) and 13–19 µm wide proximally ($\bar{x}$ = 15 µm; n = 6). The proximal third of the stylet is funnel-shaped; the mid-third is tubular and tapers to a distal sharp tip, which is bent over 90°. The male atrium is globular, lined by a nucleated epithelium and a layer of longitudinal muscles. The male gonopore (Fig. 9f: mg) is surrounded by a sphincter (Fig. 9f: sph2) and opens at 60%.

The paired vitellaria (Fig. 9 a and f: vi) lie laterally, between the brain and the caudal body end. The vitelloducts open into the most proximal part of the oviduct, which shows a sphincter just distally to the entrance of the vitelloducts (Fig. 9f: sph4). The long-drawn ovary (Fig. 9a, f: ov) is located dorsally, with the oocytes organised in a row, diminishing in diameter from the most distal one to the most proximal one. The female duct (Fig. 9a, b, f: fd) is bipartite, proximally forming a seminal receptacle (Fig. 9f: sr; terminology of Karling, 1985). The female duct is lined by a high nucleated epithelium and an external layer of longitudinal muscles which is continuous with the longitudinal layer surrounding the bursa. The seminal receptacle is distally delimited by a weak sphincter (Fig. 9f: sph6). A bundle of female glands (Fig. 9f: fg) enters caudally the most distal part of the female duct, and contains a fine-grained, eosinophilic secretion. The bursa (Fig. 9f: b) enters the female duct at the level of the seminal receptacle, contains a very fine secretion, and is lined by a syncytial epithelium; a sphincter (Fig. 9f: sph5) surrounds this connection. The female gonopore (Fig. 9f: fg) opens at 90% and is surrounded by a sphincter (Fig. 9f: sph3).

Incertae sedis

***Brinkmanniella* Luther, 1943**

***Brinkmanniella simplex* sp. n. Diez, Reygel & Artois**

(Fig. 10a, b, e)

urn:lsid:zoobank.org:act: 62C1E916-AE14-4571-AFD1-443E047266C3

Brinkmanniella sp. 1 in Diez et al. (2023)

Material and distribution. Cuba: Observations on one live animal, whole mounted afterwards, designated holotype (ZMH, No. V13683), collected in Bueycabón (type locality) (25 May 2018); on the alga *Digenea simplex*, 0.5 m deep, salinity 32‰.

Etymology. Species named after the simple morphology of its stylet. Lat. *simplex*: simple.

Diagnosis. Species of *Brinkmanniella* with a funnel-shaped 60-µm-long stylet, which is 29 µm wide proximally and 3 µm wide distally.

Description. The live animal is about 0.6 mm long, unpigmented, with a pair of eyes (Fig. 10a: e). The pharynx (Fig. 10a: ph) has a diameter of about 30% of the body length of the live specimen and is located caudally.

The testes (Fig. 10a: t) are located in the second body half, caudal to the ovaries. The vasa deferentia open separately into the copulatory bulb, where they join and form the single seminal vesicle (Fig. 10a: sv). The copulatory bulb is located beside the pharynx and apart from the large and rounded seminal vesicle. It also encloses the prostate vesicle which is connected to the stylet. The funnel-shaped stylet (Fig. 10a: st, b, e) is 60 µm long, 29 µm wide proximally, and 3 µm wide distally.

The ovaries (Fig. 10a: ov) are located anterior to the testes in the anterior half of the body.

***Brinkmanniella tenebrosa* sp. n. Diez, Reygel & Artois**

(Fig. 10c, d, f)

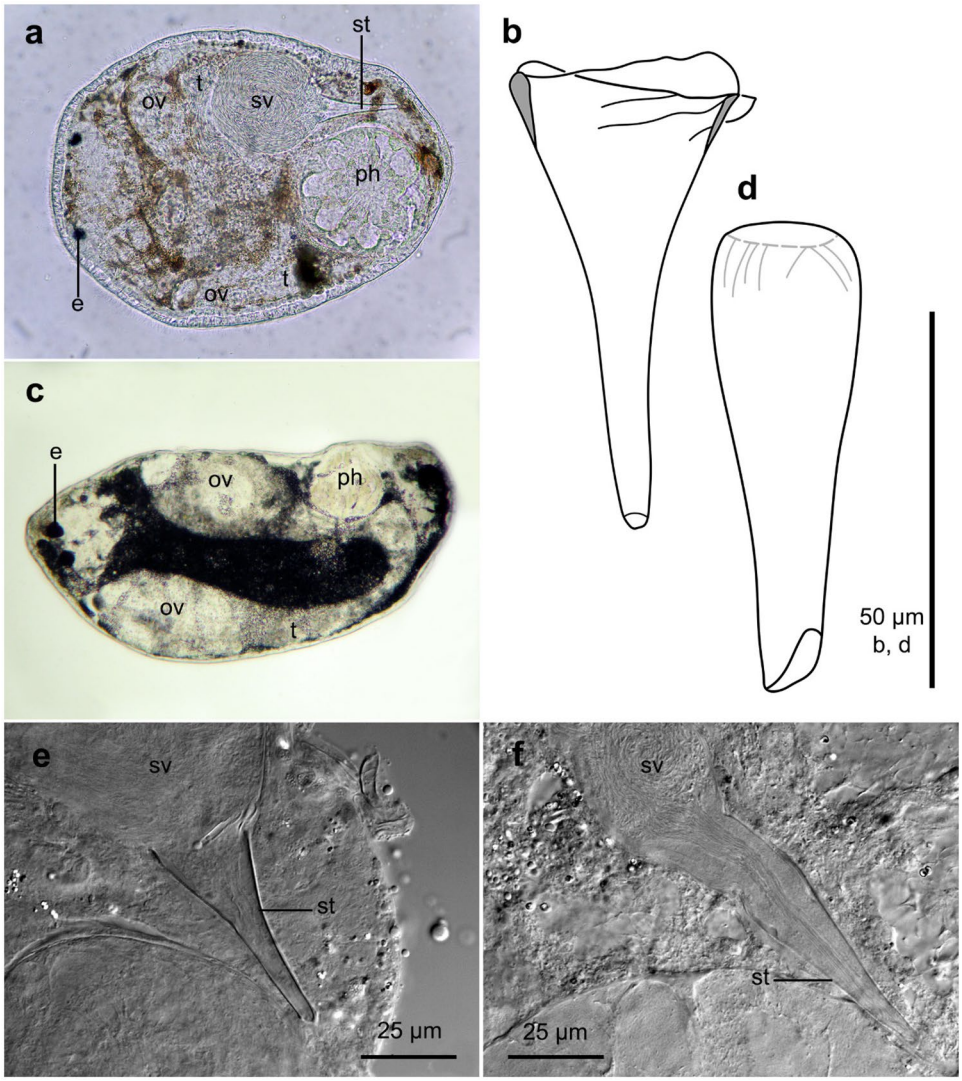

Fig. 10 *Brinkmanniella simplex* **sp. n. a** Body organisation. **b** Stylet. *Brinkmanniella tenebrosa* **sp. n. c** Body organisation. d, stylet. **b**, **d** From the holotype. **a**, **c** Structures oriented with the anterior end toward the left side of the plate. **b**, **d**–**f** Structures oriented with the anterior end toward the top of the plate

urn:lsid:zoobank.org:act: 4D693C04-8A69-4B99-A7E2-5D05FCB82F70
Brinkmanniella sp. 2 in Diez et al. (2023)

Material and distribution. Cuba: Observations on live animals. Four whole mounts from Bueycabón (type locality) (6 February 2018), one of which is designated holotype (ZMH, No. V13684) and the others paratypes (HU, No. 862–864), and one specimen used for molecular analyses; on leaves of *T. testudinum* and the alga *Galaxaura rugosa*, 0.5 m deep, salinity 33‰.

Etymology. The epithet refers to the dark pigmentation of the animal. Lat. *tenebrosus*: dark.

Diagnosis. Species of *Brinkmanniella* darkly pigmented, with a ~ 59-µm-long tubular stylet, which is ~ 17 µm wide proximally and ~ 7 µm wide distally.

Description. The live specimens are about 0.8 mm long, darkly pigmented, with a pair of eyes (Fig. 10c: e). Adenal rhabdite tracts present, with the cell bodies caudal to the eyes, their necks in between the eyes and opening terminally at the anterior end of the body. The pharynx (Fig. 10c: ph) is located at 75%. It has a diameter of 20% of the body length in the live animals.

Organisation of the genital and atrial organs as in *B. simplex* **sp. n.** The funnel-shaped stylet (Fig. 10d, f) is 55–63 µm long ($\bar{x}$ = 59 µm; n = 3), 16–18 µm wide proximally ($\bar{x}$ = 17 µm; n = 3), and 6–9 µm wide distally ($\bar{x}$ = 7 µm; n = 3).

The globular ovaries (Fig. 10c: ov) are located just caudal to the eyes and lie in the anterior body half.

Promesostomidae Luther, 1948
***Kymocarens* Ehlers & Ehlers,** 1981
***Kymocarens morrisi* sp. n. Diez, Reygel & Artois**
(Fig. 11)
urn:lsid:zoobank.org:act: 78F39A2A-509D-4DC5-9569-990DD14830FE
Kymocarens sp. in Diez et al. (2023)

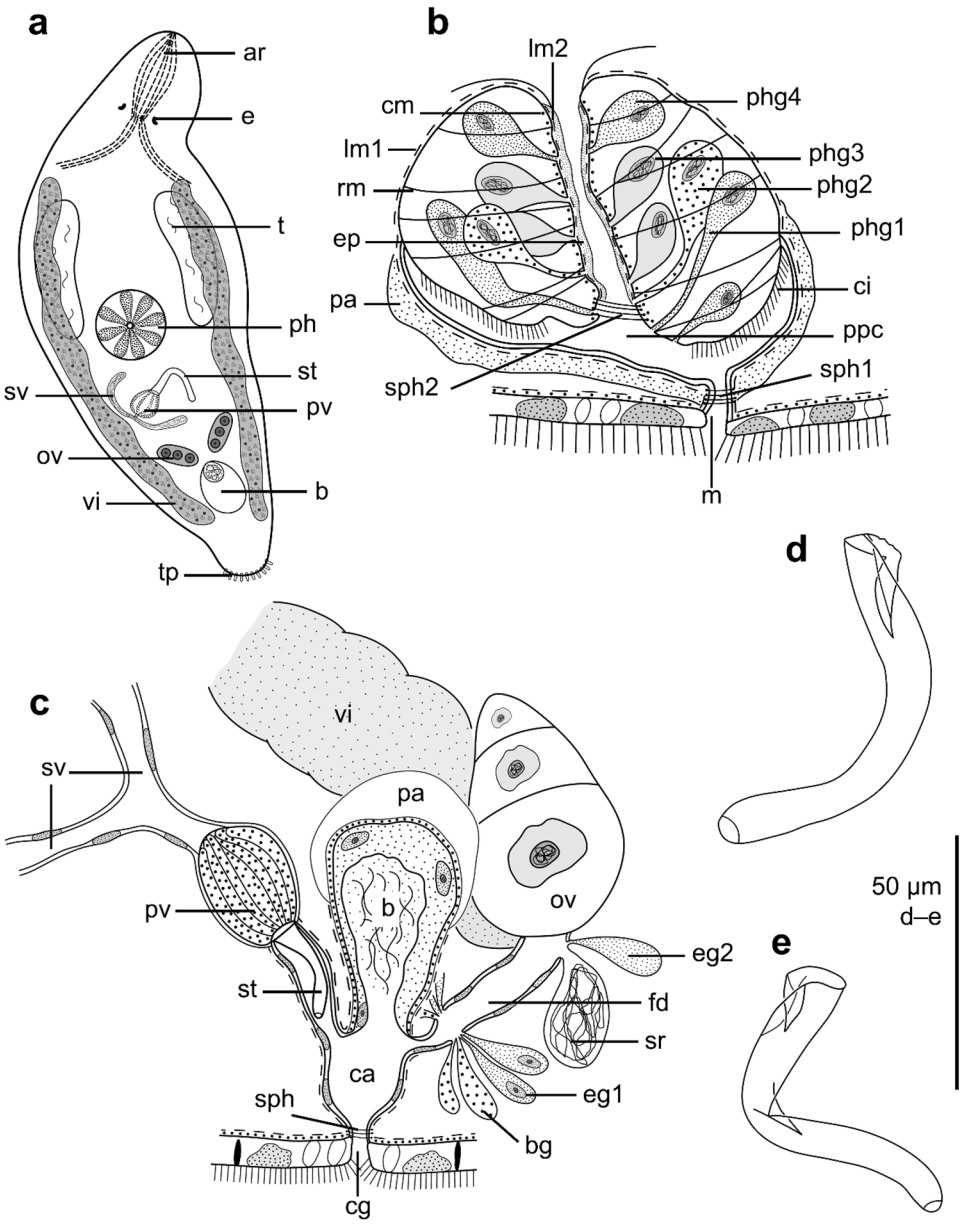

Fig. 11 *Kymocarens morrisi* **sp. n. a** Body organisation (live animal). **b** Schematic reconstruction from sagittal sections of the pharynx from the right side. **c** Schematic reconstruction from sagittal sections of the genital system from the left side; the right oviduct, ovary, and vitellarium are not drawn. **d**, **e** Stylet. **d** From the holotype. **a**, **d**–**e** Structures oriented with the anterior end toward the top of the plate. **b** Structures oriented with the anterior end toward the right side of the plate. **c** Structures oriented with the anterior end toward the left side of the plate

Material and distribution. Cuba: Observations on live animals, whole mounted afterwards. Seven whole mounts, one of which is designated holotype (ZMH, No. V13685) and the others paratypes (HU, No. 865–870), and eight serially sectioned specimens (UH XIX.3.50, XIX.4.01–XIX.4.07) collected in Aguadores (Type locality) (24 January 2017); intertidal, upper 20 cm of medium-grained sand, salinity 35‰. One whole mount from Belmares, Bahía de Santiago de Cuba (January 31, 2017) (UH XIX.4.08); intertidal, upper 10 cm of coarse shell gravel, salinity 35‰. One whole mount from Juraguá (February 9, 2020) (UH XIX.4.09); intertidal, upper 20 cm of medium-coarse sand, salinity 33‰. One whole mount from Chivirico, near Hotel Guamá, Guamá (October 21, 2020) (UH XIX.4.10); sublittoral, 0.8 m deep, fine-grained and silty sand, surrounded by the turtlegrass *Thalassia testudinum*, salinity 33‰.

Etymology. Species dedicated to Prof. Dr Humberto Joaquín Morris Quevedo (Universidad de Oriente, Santiago de Cuba, Cuba), nutraceutical specialist and dear friend of the first author.

Diagnosis. Species of *Kymocarens* with a pair of eyes. Tubular stylet ~ 81 µm long, with a longitudinal slit in its proximal end and a 90° bend at its mid-length. Internal bursal vesicle surrounded by a parenchymal sheath.

Description. The live animals are 0.5–0.7 mm long, translucent, with a pair of eyes (Fig. 11a: e). Adenal rhabdite tracts present (Fig. 11a: ar), with the cell bodies caudal to the eyes, their necks in between the eyes and opening terminally at the

anterior tip of the body. These rhabdites are 5–12 µm long ($\bar{x}$ = 7 µm; n = 11), measured on sections. The syncytial and fully ciliated epidermis is 6–9 µm thick dorsally, with rhabdites 5–7 µm long ($\bar{x}$ = 6 µm; n = 15). Ventrally, the epidermis is 2–3 µm thick, containing few ~ 2 µm-long rhabdites. The cilia are 3–4 µm long. Two types of vacuoles are present in the epidermis: some translucent and some filled with a granular secretion. The caudal body end is differentiated into a tail plate (Fig. 11a: tp), with conspicuous adhesive glands.

The pharynx (Fig. 11a: ph, b) is situated at 50%. At least four types of glands open into the pharyngeal lumen. These glands are, from distal to proximal, coarse-grained eosinophilic (stained reddish) (Fig. 11b: phg1), coarse-grained basophilic (stained dark blue-black) (Fig. 11b: phg2), and two fine-grained eosinophilic ones (stained brownish and yellowish, respectively) (Fig. 11b: phg3 and phg4). The musculature of the pharynx consists of a layer of longitudinal muscles just outside of the septum (Fig. 11b: lm1) and continuous with the longitudinal muscles of the prepharyngeal cavity. Apart from the radial muscles, we did not observe any other musculature inside the pharynx septum. Radial muscles run between the internal and external walls of the pharynx (Fig. 11b: rm). The pharynx lumen is surrounded by a thin, anucleated epithelium (Fig. 11b: ep), a longitudinal (Fig. 11b: lm2), and circular muscle layer (Fig. 11b: cm). The distal lips of the pharynx are ciliated (Fig. 11b: ci); cilia 2 µm long. The distal opening of the pharynx lumen is surrounded by a sphincter (Fig. 11b: sph2). The prepharyngeal cavity (Fig. 11b: ppc) is lined with a thin, anucleated epithelium and an external layer of longitudinal muscles. A layer of denser parenchyma (Fig. 11b: pa) surrounds the prepharyngeal cavity outside of the longitudinal muscle layer. The mouth (Fig. 11b: m) is surrounded by a sphincter (Fig. 11b: sph1).

The testes (Fig. 11a: t) are located ventrally, rostrolaterally from the pharynx. The vasa deferentia form the seminal vesicles (Fig. 11a, c: sv) caudal to the pharynx. The seminal vesicles fuse just before entering the copulatory bulb. They are lined by a nucleated epithelium. The prostate vesicle (Fig. 11a, c: pv) is globular and contains medium-grained, eosinophilic secretion. We did not observe a muscle layer surrounding the prostate vesicle. The tubular stylet (Fig. 11a, c: st, d–e) is 66–89 µm long ($\bar{x}$ = 81 µm; n = 9) and 8–15 µm wide proximally ($\bar{x}$ = 12 µm; n = 9). A longitudinal slit is present in its proximal end and the stylet is curved over 90° at its midpoint. The male atrium is lined by a nucleated epithelium and a layer of longitudinal muscles. It enters the common genital atrium anteriorly (Fig. 11c: ca).

The paired vitellaria (Fig. 11a, c: vi) extend dorsally along both sides of the body, from the eyes to the caudal body end. The ovaries (Fig. 11a, c: ov) are situated caudally in the ovovitellaria. They are oval shaped, with the oocytes organised in a row. Each oviduct proximally forms a seminal receptacle (Fig. 11c: sr), proximally of which a bundle of fine-grained, eosinophilic glands enter the oviduct (Fig. 11c: eg2). Both oviducts then unite to form the female duct, which receives two types of female glands: fine-grained, eosinophilic ones proximally (Fig. 11c: eg1) and coarse-grained, basophilic ones distally (Fig. 11c: bg). The oviducts and female duct are lined with a nucleated epithelium; muscles were not observed. The female duct enters the common genital atrium caudally. The bursa (Fig. 11a, c: b) is connected to the common genital atrium through its dorsal wall. This bursa is filled with sperm and a fine-grained, eosinophilic secretion. It is lined by a high, nucleated epithelium (~ 5 µm thick) and a circular muscle layer. The bursa is lined by longitudinal muscles in its distal half and a layer of dense parenchyma more proximally (~ 4 µm thick) (Fig. 11c: pa). The common genital atrium is lined by a nucleated epithelium and a layer of longitudinal muscles. The common gonopore (Fig. 11c: cg) is situated at 70% and surrounded by a sphincter (Fig. 11c: sph).

Promesostoma Graff, 1882

Promesostoma baculum sp. n. Diez, Reygel & Artois

(Figs. 12a–c and 15a)

urn:lsid:zoobank.org:act: 4FF78E7F-DCF0-40D8-8763-F73C7C15A93E

Promesostoma sp. 2 in Diez et al. (2023)

Material and distribution. Cuba: Observations on one live animal, whole mounted afterwards, designated holotype (ZMH, No. V13686), collected in Bueycabón (type locality) (February 21, 2018); sublittoral, on the alga *Gelidiella acerosa*, 0.5 m deep, salinity 33‰.

Etymology. Species named after the walking-stick-shaped stylet. Lat. *Baculum*: walking stick.

Diagnosis. Species of *Promesostoma* with eyes. Copulatory bursa present. Seminal vesicle, prostate vesicle and male atrium with stylet located latero-caudal to the pharynx. Slightly curved stylet 93 µm long, with the proximal funnel bent over about 90°. Tubular part of the stylet 2–3 µm wide, ending in a widened (5 µm) and oblique distal tip. Seminal vesicle oriented forward, surrounded by a strong sphincter at the connection to the prostate vesicle.

Description. The overall organisation is comparable to that of other species of *Promesostoma* (see Luther, 1943; Ax, 1951, 1952; Karling, 1967). The live animal is about 1 mm long, translucent, with two eyes (Fig. 12a: e). Anterior adenal rhabdite tracts present (Fig. 12a: ar). The pharynx (Fig. 12a: ph) is located at 50%.

The testes (Fig. 12a: t) are located anterior to the pharynx. The vasa deferentia fuse and form a single seminal vesicle. The seminal vesicle, the prostate vesicle and the stylet are located latero-caudal to the pharynx. On the whole mount it was impossible to infer whether or not

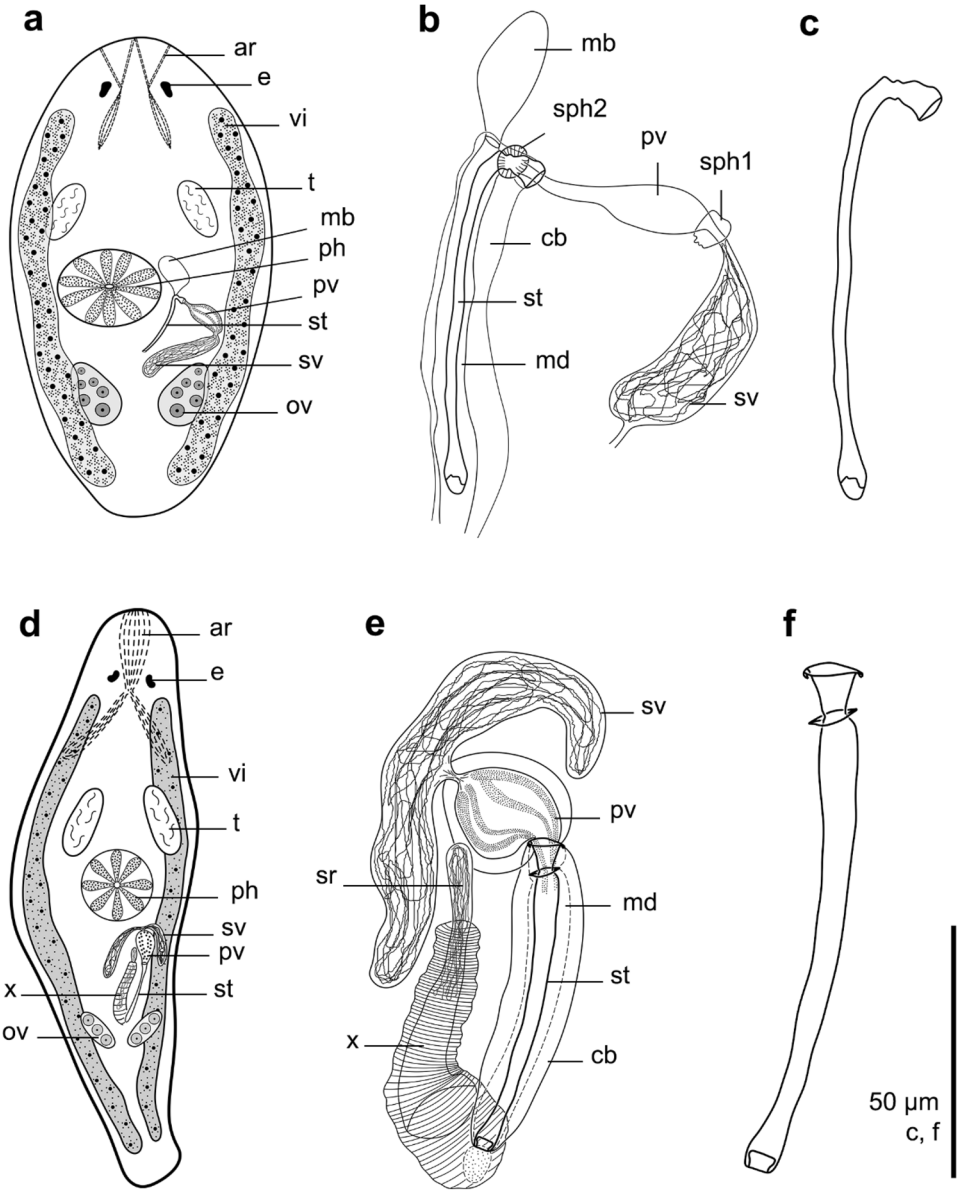

Fig. 12 **a**–**c** *Promesostoma baculum* **sp. n. d**, **e** *Promesostoma cubanum* **sp. n. a**, **d** Body organisation. **b**, **e** Schematic reconstruction of the male genital structures. **c**, **e** Stylet (from the holotype). Structures oriented with the anterior end toward the top of the plate

the seminal vesicle is surrounded by a muscle layer. The seminal vesicle (Fig. 12a, b: sv) is oriented forwards and opens into the prostate vesicle, running axially through it (Fig. 12a, b: pv). A sphincter (Fig. 12b: sph1) surrounds the connection between the seminal and the prostate vesicle. The slightly curved stylet (Figs. 12a, b and 15a: st 12c) is 93 µm long, with the proximal funnel bent over ~ 90° relative to the tubular part. The funnel is 9 µm long, 6 µm wide proximally, and 3 µm wide distally. The base of the funnel is surrounded by a sphincter (Fig. 12b: sph2). The tubular part of the stylet is 2–3 µm wide and ends in a widened (5 µm), oblique tip. At the location where the stylet bends, the male atrium (Fig. 12b: cb) receives the male copulatory bursa (Fig. 12a, b: mb; terminology of Karling, 1967).

The paired vitellaria (Fig. 12a: vi) extend laterally, from the eyes to the caudal body end. The globular ovaries (Fig. 12a: ov) are located caudal to the pharynx.

***Promesostoma cubanum* sp. n. Diez, Reygel & Artois**
(Figs. 12d–f and 15b)
urn:lsid:zoobank.org:act: 121E1264-4D1A-4DA5-B4BA-EFD5321BDCD0
Promesostoma sp. 1 in Diez et al. (2023)

Material and distribution. Cuba: Observations on live animals, whole mounted afterwards. Three whole mounts from Bueycabón (type locality) (6 February and 25 May 2018), one of which is designated holotype (ZMH, No. V13687) and the others paratypes (HU, No. 871–872), and one specimen used for molecular analyses; on leaves of *T. testudinum*

and *S. filiforme* and the alga *G. rugosa*, 0.5 m deep, salinity 32‰. Two whole mounts from Sardinero (March 18, 2021), sublittoral, 0.5 m deep, on leaves of the turtlegrass *Thalassia testudinum*, salinity 32‰ (HU XIX.4.11–XIX.4.12).

Etymology. Species named after the island of Cuba.

Diagnosis. Species of *Promesostoma* with eyes. Copulatory bursa lacking. Seminal vesicles, prostate vesicle, and male atrium with stylet located caudal to the pharynx. Slightly curved stylet ~ 106 µm long, with a circular extension surrounding the stylet proximally and ending in a slightly swollen, rounded tip. A bipartite structure runs adjacent to the male atrium; consisting of a pronounced muscular part and a smaller, sperm-containing vesicle devoid of musculature.

Description. The overall organisation is comparable to that of other species of *Promesostoma* (see Luther, 1943; Ax, 1951, 1952; Karling, 1967). Measured on the whole mounts, animals are 0.5–1 mm long ($\bar{x}$ = 0.7 mm; n = 3), translucent, with a pair of kidney-shaped eyes (Fig. 12d: e). Anterior adenal rhabdite tracts present (Fig. 12d: ar), with the cell bodies caudal to the eyes, their necks in between the eyes and opening terminally at the anterior end of the body. The pharynx (Fig. 12d: ph) is located at 50%, with a diameter of 68–114 µm ($\bar{x}$ = 94 µm; n = 3), measured on the whole mounts.

The testes (Fig. 12d: t) are located anterior to the pharynx. The seminal vesicles, the prostate vesicle, and the male duct (Fig. 12e: md) are located caudal to the pharynx. The seminal vesicles (Figs. 12d–e and 15b: sv) are oriented backward and fuse just before entering the prostate vesicle (Figs. 12d–e and 15b: pv), forming a seminal duct that runs axially through the prostate vesicle. It is not clear from the available material whether or not the seminal vesicles are surrounded by a muscle layer. The slightly curved stylet (Figs. 12d–e and 15b: st, 12f) is 93–103 µm long ($\bar{x}$ = 106 µm; n = 5). Its proximal funnel is 7–10 µm long ($\bar{x}$ = 9 µm; n = 5), 11–18 µm wide proximally ($\bar{x}$ = 17 µm; n = 5), and 4–6 µm wide distally ($\bar{x}$ = 5 µm; n = 5). Its proximal rim is slightly folded backwards. Somewhat distally to the funnel, a circular extension surrounds the stylet. Distally to this extension, the stylet is tubular, 7–8 µm wide proximally ($\bar{x}$ = 7 µm, n = 5), 5–6 µm wide medially ($\bar{x}$ = 5 µm; n = 5), and 6–8 µm wide distally ($\bar{x}$ = 7 µm; n = 5). The distal tip of the stylet is a bit wider, with the opening exactly terminal.

A very muscular and cylindrical structure (Figs. 12d–e and 15b: x) runs adjacent to the copulatory bulb. From the whole mounts, it is impossible to discern whether this structure is part of the male or the female system. Proximally, this structure continues in a non-muscular receptacle containing sperm (Fig. 12e: sr). The paired vitellaria (Fig. 12d: vi) extend along both sides of the body, from the eyes to the caudal body end. The oval ovaries (Fig. 12d: ov) are located caudal to the copulatory bulb.

***Promesostoma cubitum* sp. n. Artois & Diez**

(Figs. 13a, b and 15c)

urn:lsid:zoobank.org:act: EF102DE1-EB7D-42A9-95F7-99C083E04918

Material and distribution. Panama: Five specimen studied alive and whole mounted, one of which is designated holotype (ZMH, No. V13688) and the others paratypes (HU, No. 873–876), collected in Bahía Can Can (type locality), near to Portobelo, Atlantic side of Panama (29 February 2016). Two specimens, including the holotype, collected subtidally in a lagoon, in fine-grained sand with some organic matter taken in between sea grass, 0.2 m deep at low tide; the other three specimens collected intertidally, in well-sorted and fine sand from channels in mangroves.

Etymology. Species named after the fact that the stylet shows an elbow-like proximal extension. Lat. *Cubitum*: elbow.

Diagnosis. Species of *Promesostoma* with eyes. Copulatory bursa present. Seminal vesicle, prostate vesicle, and male atrium with stylet located caudal to the pharynx. Slightly curved stylet ~ 118 µm long, with a pointed elbow-shaped, angular projection just distally to the proximal funnel-shaped part.

Description. The overall organisation is comparable to that of other species of the genus *Promesostoma* (see Luther, 1943; Ax, 1951, 1952; Karling, 1967). Measured on the whole mounts, the animals are 1–1.1 mm long (n = 2), translucent, with a pair of eyes (Fig. 13a: e). Anterior adenal rhabdite tracts are present (Fig. 13a: ar). The pharynx is located at 50% (Fig. 13a: ph); it is 117–182 µm in diameter ($\bar{x}$ = 152 µm; n = 3) measured on the whole mounts.

A pair of testes (Fig. 13a: t) is located anterior to the pharynx. The seminal vesicle, the prostate vesicle, and stylet are located caudal to the pharynx. The vasa deferentia run caudal and fuse to form a single seminal vesicle (Figs. 13a and 15c: sv), which narrows distally to enter the prostate vesicle (Figs. 13a and 15c: pv) and runs axially through it. On the whole mounts it was impossible to assess whether or not the seminal vesicle is surrounded by a muscle layer. The prostate vesicle itself connects to the stylet. The male atrium receives the well-developed male copulatory bursa and the stylet. The stylet (Figs. 13a and 15c: st, 13b) is 108–123 µm long ($\bar{x}$ = 118 µm; n = 5). Proximally it is funnel shaped, 8–10 µm wide ($\bar{x}$ = 9 µm; n = 5). Caudal to the funnel, the stylet shows a pointed angular projection, which is somewhat elbow shaped. The distal end of the stylet is widened, with the distal opening of the stylet completely at the end. The male copulatory bursa (Figs. 13a and 15c: mb; terminology of Karling, 1967) is located beside the pharynx and opens into the male atrium at the level of the projection of the stylet.

The paired vitellaria (Fig. 13a: vi) extend along both body sides, from the eyes to the caudally located, oval-shaped ovaries (Fig. 13a: ov).

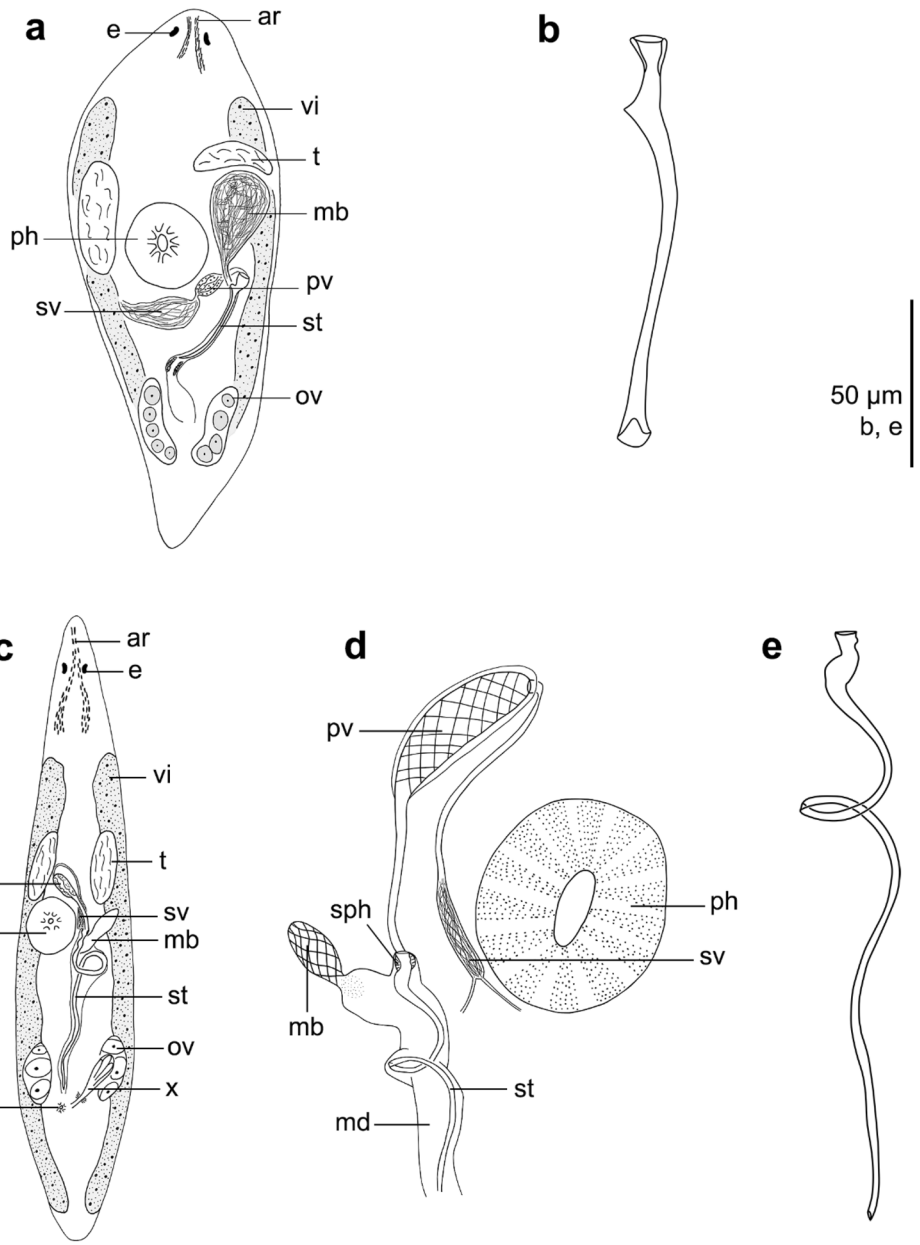

Fig. 13 **a**, **b** *Promesostoma cubitum* **sp. n. c–d**, *Promesostoma panamensis* **sp. n. a**, **c** Body organisation. **b**, **e** Stylet (from the holotype). **d** Schematic reconstruction of the male genital structures. Structures oriented with the anterior end toward the top of the plate

***Promesostoma panamaense* sp. n. Artois & Diez**
(Figs. 13c–e and 15d)
urn:lsid:zoobank.org:act: 56E29EE6-46C3-4A04-9B27-A96E1478CD86

Material and distribution. Panama: Observations on live animals, whole mounted afterwards. Seven whole mounts, one of which is designated holotype (ZMH, No. V13689) and the others paratypes (HU, No. V877–882), collected in Taboga (type locality), Taboga Island, Pacific side of Panama (9 December 2011); intertidal, fine sand with the alga *Caulerpa* sp., salinity 30‰.
Etymology. Species named after its occurrence in Panama.

Diagnosis. Species of *Promesostoma* with eyes. Copulatory bursa present. Prostate vesicle located anterior to the pharynx, the seminal vesicle located beside the pharynx, and the male atrium with stylet caudal to the pharynx. Stylet ~ 88 µm long and twisting 360° at about its proximal third; distal end rounded to oblique. Seminal vesicle oriented forward and prostate vesicle backward.
Description. The overall organisation is comparable to that of other species of the genus *Promesostoma* (see Luther, 1943; Ax, 1951, 1952; Karling, 1967). Measured on the whole mounts, the animals are 0.5–1.1 mm long ($\bar{x}$ = 0.8 mm; n = 4) translucent, with a pair of eyes (Fig. 13c: e). Anterior rhabdite tracts present (Fig. 13a: ar). The pharynx (Figs. 13c,

d and 15d: ph) is located at 50–60%, and in the whole mounts is 82–102 µm in diameter ($\bar{x}$ = 94 µm; n = 3).

A pair of testes (Fig. 13c: t) is located anterior to the pharynx. The vasa deferentia open into a single seminal vesicle (Figs. 13c, d and 15d: sv), which is located beside the pharynx. Whether or not the seminal vesicle is surrounded by a muscle layer is unclear from the whole mounted material. From this vesicle, the seminal duct runs forward and opens into the prostate vesicle, which is located anterior to the pharynx. The prostate vesicle (Figs. 13c, d and 15d: pv) connects to the stylet through a relatively long duct. The stylet (Figs. 13c, d and 15d: st, 13e) is positioned caudal to the pharynx. It is 81–92 µm long ($\bar{x}$ = 88 µm; n = 7), with a proximal, funnel-shaped part 2–3 µm wide ($\bar{x}$ = 2 µm; n = 7), surrounded by a sphincter (Fig. 13d: sph). At about its proximal third the stylet makes a 360° turn. Its distal end is blunt, its opening sometimes appearing a bit oblique. The male copulatory bursa (Figs. 13c, d and 15d: mb; terminology of Karling, 1967) is located latero-proximally from the stylet, entering the male atrium at the level of the turn of the stylet.

The paired vitellaria (Fig. 13c: vi) extend laterally, between the brain and the caudal body end. The oval-shaped ovaries (Fig. 13c: ov) are located latero-caudal to the male atrium. A glandular structure (Fig. 13c: x), presumably part of the female system, is located between the ovaries. The common gonopore (Fig. 13c: cg) opens at 80%.

***Promesostoma roseapharynx* sp. n. Diez, Reygel & Artois**
(Figs. 14a–c and 15e)

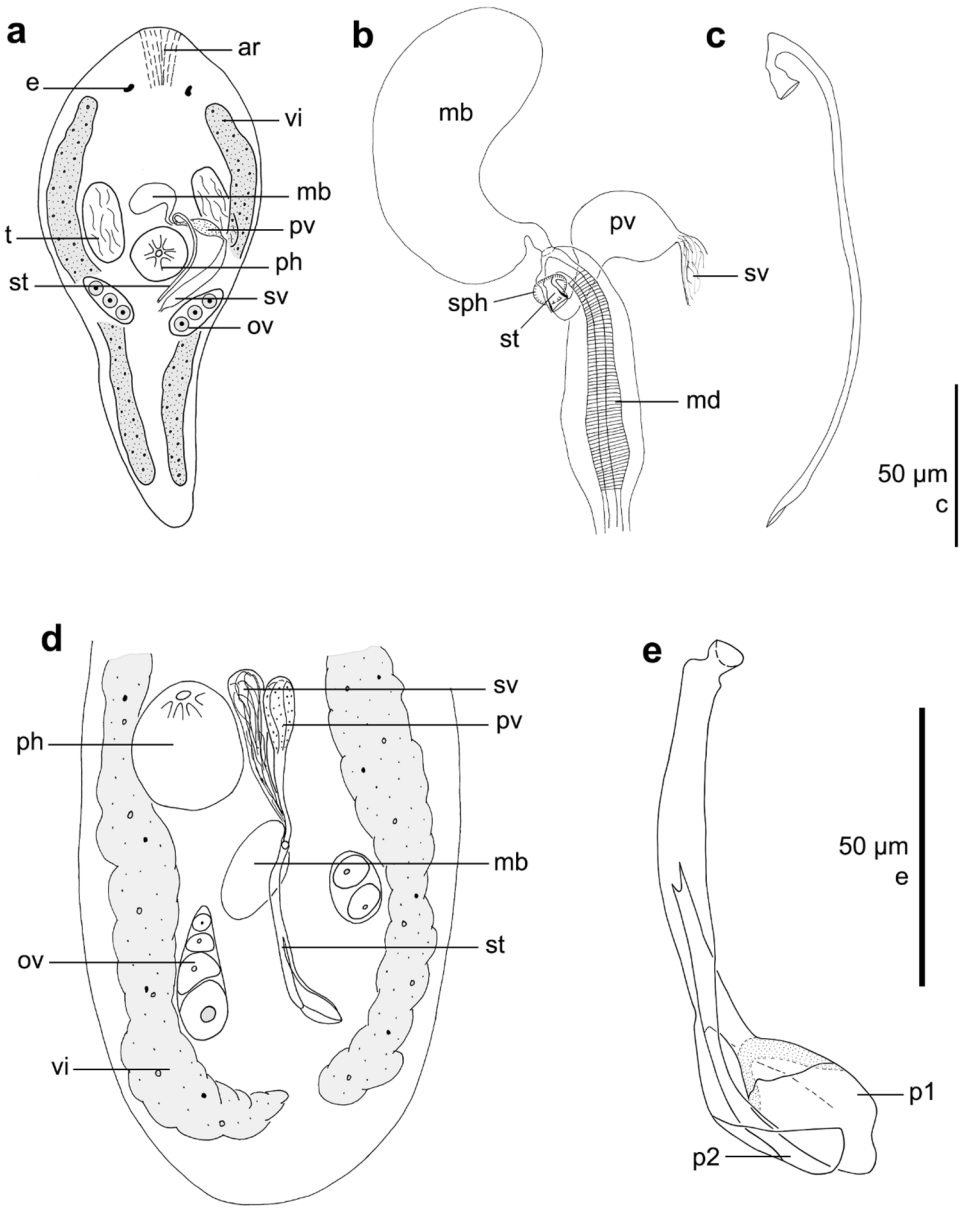

Fig. 14 **a–c**, *Promesostoma roseapharynx* **sp. n. d–e**, *Promesostoma toryne* **sp. n. a**, **d** Body organisation. **b** Schematic reconstruction of the male genital structures. **c**, **e** Stylet (from the holotype). Structures oriented with the anterior end toward the top of the plate

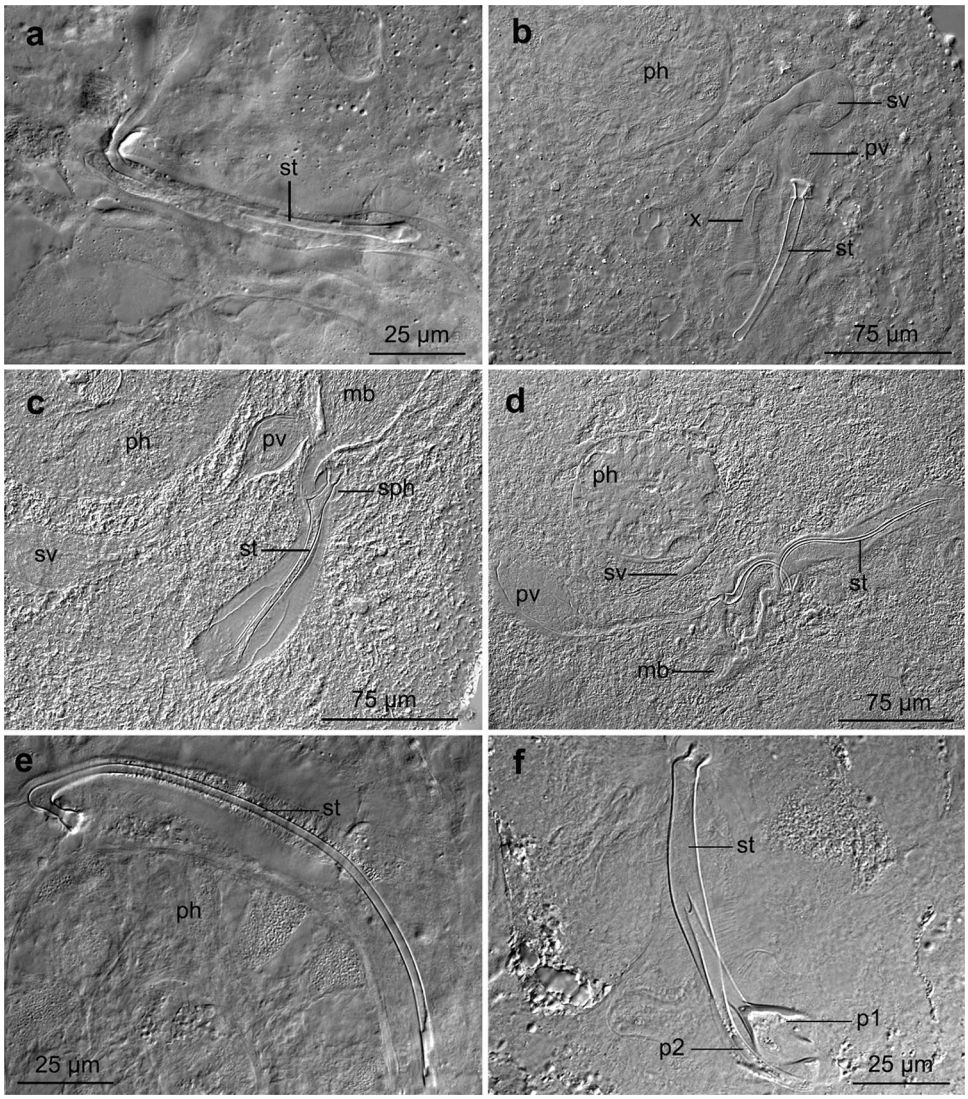

Fig. 15 Male genital structures in the new species of *Promesostoma* (from the holotype). **a** *Promesostoma baculum* **sp. n. b** *Promesostoma cubanum* **sp. n. c** *Promesostoma cubitum* **sp. n. d** *Promesostoma panamaense* **sp. n. e** *Promesostoma roseapharynx* **sp. n. f** *Promesostoma toryne* **sp. n. a**, **d–e** Structures oriented with the anterior end toward the left side of the plate. **b**, **c**, **f** Structures oriented with the anterior end toward the top of the plate

urn:lsid:zoobank.org:act: 53511906-ED97-4332-924F-1AF9FB99C04D

Promesostoma sp. 3 in Diez et al. (2023)

Material and distribution. Cuba: Observations on live animals. Three whole mounts from Las Sardinas (type locality) (21 June 2017), one of which is designated holotype (ZMH, No. V13690) and the others paratypes (HU, No. 883–884); on the alga *Dictyota menstrualis* covered with silty sand, 0.5 m deep, salinity 32‰. Two whole mounts and one specimen used for molecular analyses from Chivirico (March 16, 2017) (HU XIX.4.13–XIX.4.14); on the alga *Halimeda* sp. covered with silt, 0.6 m deep, salinity 35‰. Seven whole mounts from Bueycabón (February 6 & 21, & May 25, 2018) (HU XIX.4.15–XIX.4.21); on algae (*V. pachynema* covered with red filamentous algae, *Amphiroa fragilissima*, *G. rugosa*, and *G. acerosa*), 0.5 m deep, salinity 32‰.

Etymology. Species named after the pinkish glands of the pharynx observed on live animals. Lat. *roseus*: pink.

Diagnosis. Species of *Promesostoma* with eyes. Male copulatory bursa present. Curved stylet situated beside the pharynx, ~ 177 µm long, with the proximal funnel bent over ~ 180°. Tubular part of the stylet ~ 2 µm wide and ends in a sharp and oblique tip. Seminal vesicle situated caudally and laterally from the pharynx, oriented forward. Prostate vesicle anterior to the pharynx, directed backwards.

Description. The overall organisation is comparable to that of other species of the genus *Promesostoma* (see Luther, 1943; Ax, 1951, 1952; Karling, 1967). Measured on the whole mounts, the animals are 0.6–1 mm long ($\bar{x}$ = 0.8 mm; n = 3), translucent, with a pair of eyes (Fig. 14d: e). Adenal rhabdite tracts present anteriorly (Fig. 14a: ar). The pharynx (Figs. 14a and 15e: ph) is located at 50%, 105–136 µm in diameter ($\bar{x}$ = 119 µm; n = 4), measured on the whole mounts, containing pinkish glands in live animals.

A pair of testes (Fig. 14a: t) is located anterior to the pharynx. The vasa deferentia open into a large seminal vesicle

situated caudal to the pharynx. On the whole mounts it was not possible to infer whether or not the seminal vesicle is surrounded by a muscle layer. The seminal vesicle (Fig. 14a, b: sv) is oriented forwards and opens into the prostate vesicle (Figs. 14a, b: pv), which itself is located anterior to the pharynx and oriented backwards. The male duct (Fig. 14b: md) receives the stylet and the male copulatory bursa (Figs. 14a, b: mb; terminology of Karling, 1967). The curved stylet (Figs. 14a, b and 15e: st, 14c) lies next to the pharynx. It is 168–189 µm long ($\bar{x}$ = 177 µm; n = 12), with a proximal funnel bent over ~ 180°. This funnel is 9–15 µm long ($\bar{x}$ = 12 µm; n = 7) and 6–8 µm wide proximally ($\bar{x}$ = 7 µm; n = 7). A sphincter surrounds the base of the funnel. The tubular part of the stylet is 2–3 µm wide ($\bar{x}$ = 2 µm; n = 12), and distally ends in a sharp, oblique tip. The proximal half of the stylet is surrounded by a sheath of circular muscles.

The paired vitellaria (Fig. 14a: vi) extend laterally from the eyes to the caudal body end. The oval-shaped ovaries (Fig. 14a: ov) are located caudal to the pharynx. The common gonopore opens at 70–75%.

Promesostoma toryne sp. n. Artois & Diez

(Figs. 14d, e and 15f)

urn:lsid:zoobank.org:act:8EB37E6D-8BBD-40D8-9C37-12A1C1119108

Material and distribution. Panama: One specimen studied alive and whole mounted, designated holotype (ZMH, No. V13691), collected in Las Perlas (type locality), Archipelago Las Perlas, Pacific side of Panama (December 6, 2011); coarse sand with shell gravel and sponge spicules, 20 m deep, salinity 30‰.

Etymology. The name refers to the fact that one of the distal parts of the stylet is spoon shaped. Gr.: spoon.

Diagnosis. Species of *Promesostoma* without eyes. Copulatory bursa present. Seminal vesicle and prostate vesicle located beside the pharynx; male atrium with stylet caudal to the pharynx. Seminal vesicle and prostate vesicle open separately into the copulatory bulb. Stylet 109 µm long, distally split into two branches. Larger branch distally widened (16 µm wide) and spoon shaped, with a very broad distal aperture. Second branch 52 µm long and 7 µm wide.

Description. The overall organisation is comparable to that of other species of the genus *Promesostoma* (see Luther, 1943; Ax, 1951, 1952; Karling, 1967). The live animal is about 1 mm long, translucent, without eyes. Adenal rhabdite tracts

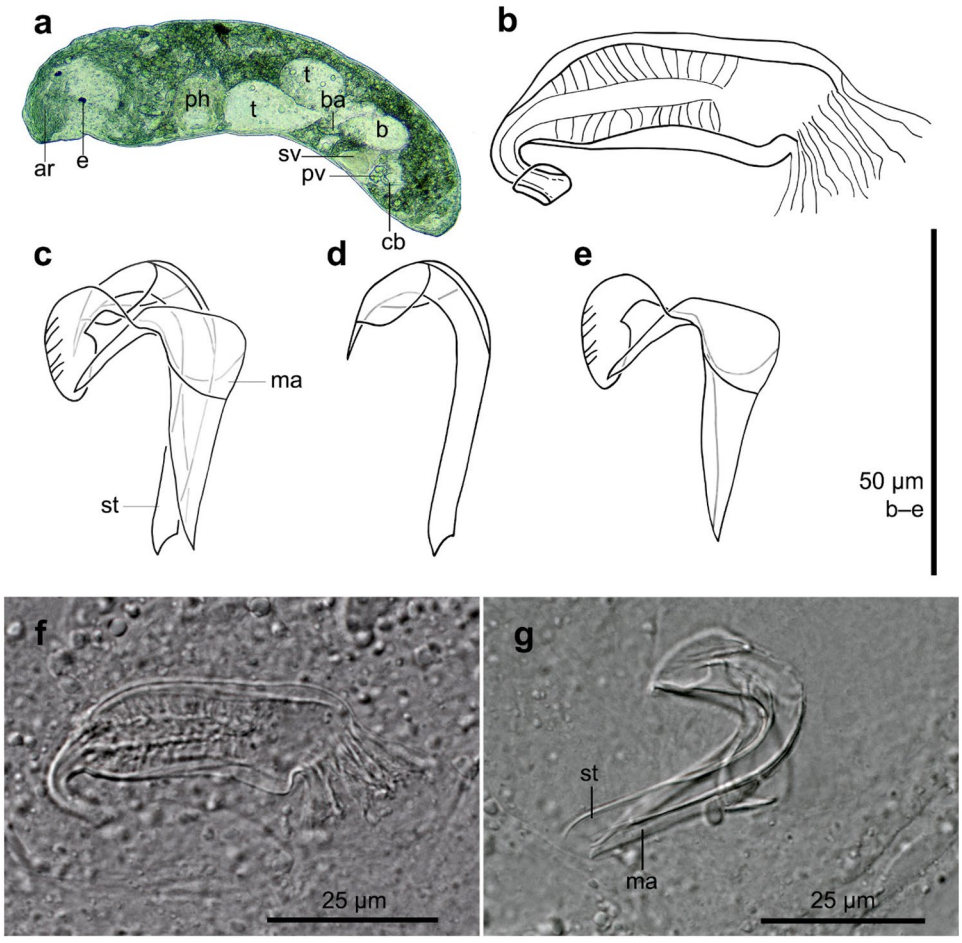

Fig. 16 *Ceratopera paragracilis* Ehlers & Ax, 1974. **a** Body organisation (live animal). **b**, **f** Bursal appendage. **c**, **g** Hard structures of the copulatory bulb. **d** Stylet. **e** Mantle. **a**–**b**, **f** Structures oriented with the anterior end toward the left side of the plate. **c**–**e**, **g** Structures oriented with the anterior end toward the top of the plate

present anteriorly. The pharynx (Fig. 14d: ph) is 74 µm in diameter in the whole mount, located at 50%.

The testes are located anterior to the pharynx. The vasa deferentia open into a single seminal vesicle (Fig. 14d: sv), located beside the pharynx. It was not clear from the whole mounted specimen whether or not the seminal vesicle is surrounded by a muscle layer. The prostate vesicle (Fig. 14d: pv) is located beside the pharynx and next to the seminal vesicle. Both the seminal vesicle and prostate vesicle open separately into the male atrium. The male atrium also receives the male copulatory bursa (Fig. 14d: mb; terminology of Karling, 1967). The stylet (Figs. 14d and 15f: st, 14e) is 109 µm long and distally split in two branches. The larger branch (Figs. 14e and 15f: p1) is distally widened (16 µm wide) and spoon shaped, with a very broad distal aperture. The second blanch (Figs. 14e and 15f: p2) is 52 µm long and 7 µm wide.

The paired vitellaria (Fig. 14d: vi) extend laterally, from the brain to the caudal body end. The globular to kidney-shaped ovaries (Fig. 14d: ov) are located beside the stylet.

Trigonostomidae Graff, 1905
***Ceratopera* Hartog,** 1964
***Ceratopera paragracilis* Ehlers & Ax,** 1974
(Fig. 16)
Ceratopera sp. in Diez et al. (2023)

Known distribution. Isabela, Archipelago Colon, Galapagos Islands (Ehlers & Ax, 1974). St. George's West, Biological Station landing, Bermuda Islands, Bermuda (Karling, 1978).
Material and distribution. Cuba: Observations on live animals. Two whole mounts from Bahía Larga (April 5, 2017) (HU XIX.4.22–XIX.4.23); on leaves of the seagrass *T. testudinum*, 1 m deep, salinity 34‰. One whole mount from Bueycabón (21 February 2018) (HU XIX.4.24), on leaves of *T. testudinum* and *S. filiforme*, 0.5 m deep, salinity 33‰. One specimen used for molecular analyses collected in Sardinero (18 March 2021); sublittoral, on leaves of *T. testudinum*, 0.6 m deep, salinity 34‰.
Remarks. The habitus and overall internal organisation of the specimens from Cuba correspond to the description of Ehlers and Ax (1974). Specimens are about 1 mm long, unpigmented and have a pair of eyes (Fig. 16a: e). Large adenal rhabdite tracts are present anteriorly (Fig. 16a: ar), with the cell bodies caudal to the eyes, their necks in between the eyes and opening terminally at the anterior end of the body. The stylet (Fig. 16c, g: st, 16d) is 44–58 µm long ($\bar{x}=51$ µm; $n=3$), and 3–4 µm wide in the middle ($\bar{x}=4$ µm; n = 3). The mantle (Fig. 16c, g: ma, 16e) is 53 µm long ($n=3$). The bursal appendage (Fig. 16 a: ba; b; f) is 60–64 µm long in the specimens from Bahía Larga ($\bar{x}=62$ µm; $n=2$) and 105 µm long in the specimen from Bueycabón, 14–16 µm wide medially ($\bar{x}=15$ µm; $n=3$), and 5 µm wide in the distal tubular

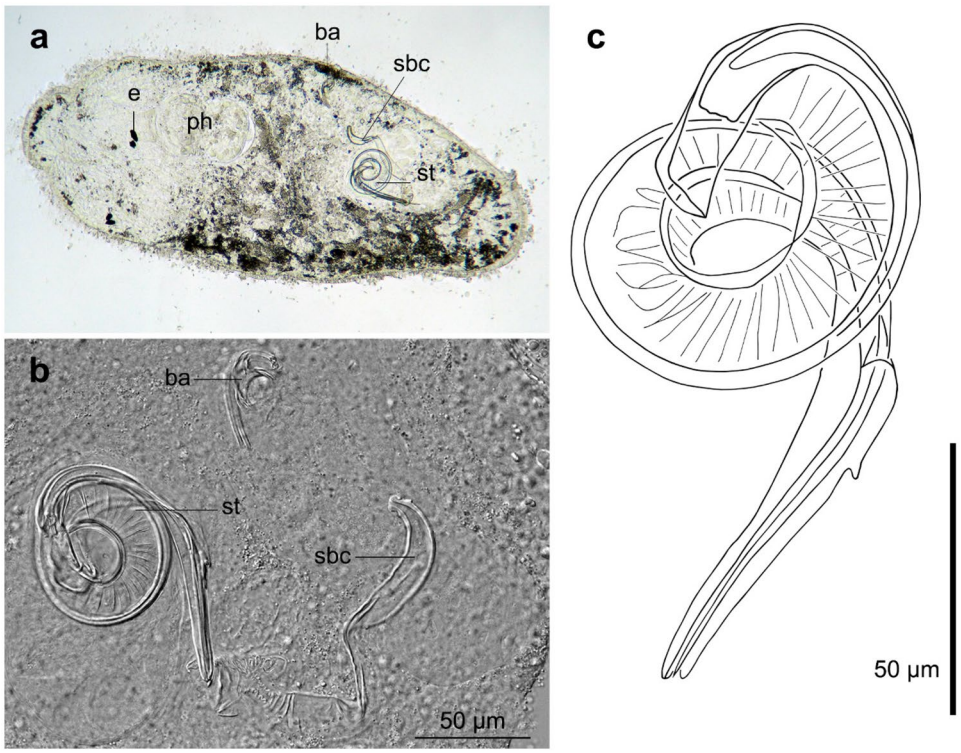

Fig. 17 *Trigonostomum armatum* (Jensen, 1878) Gamble, 1900. **a** Body organisation (live animal). **b** Atrial organs. **c** Stylet. **b**, **c** From a whole mount. **a** Structures oriented with the anterior end toward the left side of the plate. **b–c** Structures oriented with the anterior end toward the top of the plate

part ($n=2$). In the specimen from Bueycabón, two distal tubes were observed, which are 31 µm long and 2 µm wide.

***Trigonostomum* Schmidt,** 1852
***Trigonostomum armatum* (Jensen,** 1878**) Gamble,** 1900
(Fig. 17)
Trigonostomum sp. 1 in Diez et al. (2023)

Known distribution. Norway (Graff, 1882; Jensen, 1878; Westblad, 1954; Willems et al., 2004b), English Channel (Gamble, 1893), North Sea (Attems, 1897; Meixner, 1924, 1925), Ireland (Gamble, 1893, 1900; Southern, 1912, 1915, 1936), Faeroe Islands (Steinböck, 1931), Iceland (Steinböck, 1938), Baltic Sea (Ax, 1952). United Kingdom, Sweden, Wimeroux (France), Curaçao, New South Wales, Arrawarra (Australia), Nouméa (New Caledonia), and South Georgia (Willems et al., 2004b).
Material and distribution. Cuba: Observations on live animals. Nine whole mounts and one specimen for molecular analyses from Siboney (22 March and 5 June 2017) (HU XIX.4.25–XIX.4.33); sublittoral, on algae (*Ulva lactuca*, *U. flexuosa*, and *Gracilaria* sp.), 0.5 m deep, salinity 32–35‰. One whole mount from Bueycabón (6 February 2018) (XIX.4.34), sublittoral, 0.5 m deep, on the red alga *Galaxaura rugosa*, salinity 33‰. One whole mount from Playa Caletón (24 January 2020) (XIX.4.35), sublittoral, 0.5 m deep, on leaves of the seagrass *Syringodium filiforme*, salinity 37‰.
Remarks. For a detailed treatment of this species, see Willems et al. (2004b) and references therein. The live specimens collected in Cuba are about 0.8–1 mm long. The body is translucent, with anterior spots consisting of dark pigment granules. Each eye (Fig. 17a: e) is observed as two pigmented spots due to squeezing. The stylet (Fig. 17a, b: st, 17c) is 333–369 µm long ($\bar{x}=352$ µm; $n=8$). The bursal appendage (Fig. 17a, b: ba) is 84–100 µm long ($\bar{x}=89$ µm; $n=6$). The bursal channel is sclerotised (Fig. 17a, b: sbc).

***Trigonostomum franki* Willems et al.,** 2004b
(Fig. 18)
Trigonostomum sp. 2 in Diez et al. (2023)

Known distribution. Curaçao (Dutch Antilles), Florida (USA), Mombasa (Kenya), Zanzibar (Tanzania), Nouméa (New Caledonia) (Willems et al., 2004b).
Material and distribution. Cuba: Observations on one live animal, whole mounted afterwards (HU XIX.4.36), collected in Bahía Larga (April 5, 2017); on leaves of *T. testudinum*, 1 m deep, salinity 34‰.
Remarks. The general habitus of the specimen collected in Cuba fits the description provided by Willems et al. (2004b). The stylet (Fig. 18a: st, 18b, d) is 103 µm long, and the bursal appendage (Fig. 18a: ba; c, e) is 97 µm long. The dimensions of stylet and bursal appendage are within the range recorded in literature: 86–111 µm long and 62–166 µm long, respectively (Willems et al., 2004b).

***Trigonostomum vanmecheleni* Artois et al.,** 2013
(Fig. 19)
Trigonostomum sp. 3 in Diez et al. (2023)
Known distribution. Venice, Italy (Artois et al., 2013).

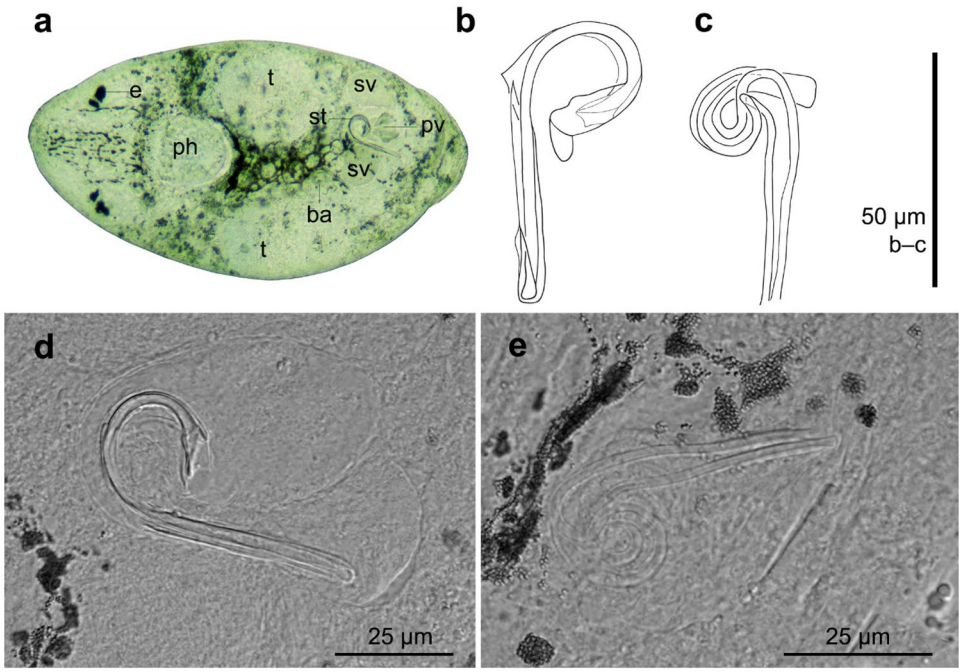

Fig. 18 *Trigonostomum franki* Willems et al., 2004b. **a** Body organisation (live animal). **b**, **d** Stylet. **c**, **e** Bursal appendage. **b–e** From the whole mount. **a**, **d**, **e** Structures oriented with the anterior end toward the left side of the plate. **b**, **c** Structures oriented with the anterior end toward the top of the plate

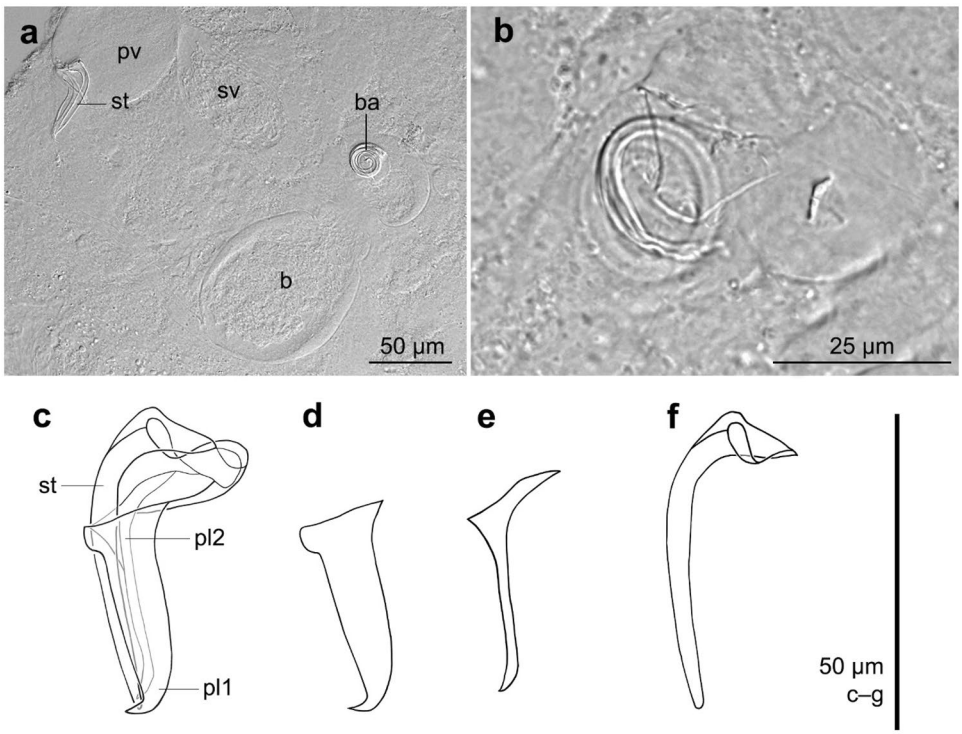

Fig. 19 *Trigonostomum vanmecheleni* Artois et al., 2013. **a** Atrial organs. **b** Bursal appendage. **c** Hard structures of the copulatory bulb. **d**, **e** Mantle plates. **f** Stylet. **a**, **f** From whole mounts. Structures oriented with the anterior end toward the top of the plate

Material and distribution. Cuba: Observations on live animals. Five whole mounts and one specimen for molecular analyses from Bahía Larga (May 25, 2017) (HU XIX.4.37–XIX.4.41); on leaves of *T. testudinum*, 0.5 m deep, salinity 32‰. Six whole mounts from Bueycabón (25 May 2018 and 20 May 2021) (HU XIX.4.42–XIX.4.47); on leaves of *T. testudinum* and *S. filiforme*, 0.5 m deep, salinity 32‰.
Remarks. The stylet proper (Fig. 19a, c: st, 19f) is 48–54 µm long ($\bar{x}$ = 52 µm; n = 4), 10–17 µm wide proximally ($\bar{x}$ = 15 µm; n = 4), and 3 µm wide at its midpoint (n = 5). The broader plate (Fig. 19c: pl1, 19d) of the mantle is 31–36 µm long ($\bar{x}$ = 33 µm; n = 3) and 12–19 µm wide proximally ($\bar{x}$ = 15 µm; n = 3). The narrower plate (Fig. 19c: pl2, e) is 28–35 µm long ($\bar{x}$ = 32 µm; n = 3) and 13–21 µm wide proximally ($\bar{x}$ = 17 µm; n = 3). The bursal appendage is 111–115 µm long ($\bar{x}$ = 113 µm; n = 2) and 15–23 µm wide proximally ($\bar{x}$ = 19 µm; n = 2). In one specimen, the distal part of the bursal appendage (Fig. 19a: ba, 19b) appears to be branched in four thin tubes, and in other specimens, clearly in six.

***Trigonostomum yoandrisi* sp. n. Diez, Reygel & Artois**
(Fig. 20)
urn:lsid:zoobank.org:act: 5950B008-9B1F-4F5E-96FE-7467E881C6CD
Trigonostomum sp. 4 in Diez et al. (2023)

Material and distribution. Cuba: Observations on live animals, whole mounted afterwards. Two whole mounts from Siboney (Type locality) (December 6, 2017), one of which is designated holotype (ZMH, No. V13692) and the other paratype (HU, No. V885); sublittoral, on the alga *Dictyota* sp., 4 m deep, salinity 33‰.
Etymology. Species named after Prof. Dr Yoandri Suárez Megna (Universidad de Oriente, Cuba), specialist in freshwater beetles.
Diagnosis. Species of *Trigonostomum* with a copulatory organ which consist of a stylet and two mantle plates. Funnel-shaped stylet ~ 24 µm long. One mantle plate is ~ 28 µm long and 17–18 µm wide proximally, tapering to a distal sharp tip. Second plate X shaped, ~ 21 µm long and 17–18 µm wide proximally; distally, it forms two sharp hooks, ~ 12 µm long. Bursal appendage 19–20 µm long as a whole, distally branching in two coiled tubes ~ 48 µm long and ~ 3 µm in diameter.
Description. The animals are 0.47–0.51 mm long ($\bar{x}$ = 0.49 mm; n = 2), measured on the whole mounts, translucent, with a pair of eyes (Fig. 20a, b: e). The pharynx (Fig. 20a, b: ph) is 74–80 µm long ($\bar{x}$ = 77 µm; n = 2), as measured on whole mounts, and located in the first body half.

The paired testes (Fig. 20a: t) are located at the body's midpoint. The atrial organs are located in the second body half. The vasa deferentia form seminal vesicles that open into the copulatory bulb. The copulatory bulb encloses the prostate vesicle and copulatory organ. The sclerotised parts of the copulatory organ consist of the stylet proper and two mantle pieces. The funnel-shaped stylet (Fig. 20a, d–f: st) is 22–25 µm long ($\bar{x}$ = 24 µm; n = 2) and 11–12 µm wide proximally. It tapers to a blunt distal tip. One plate of the mantle (Fig. 20d–f: pl1) is 26–29 µm long ($\bar{x}$ = 28 µm; n = 2) and 17–18 µm wide proximally; distally, it forms a triangular tip. The second plate of the mantle (Fig. 20d–f: pl2) is X shaped,

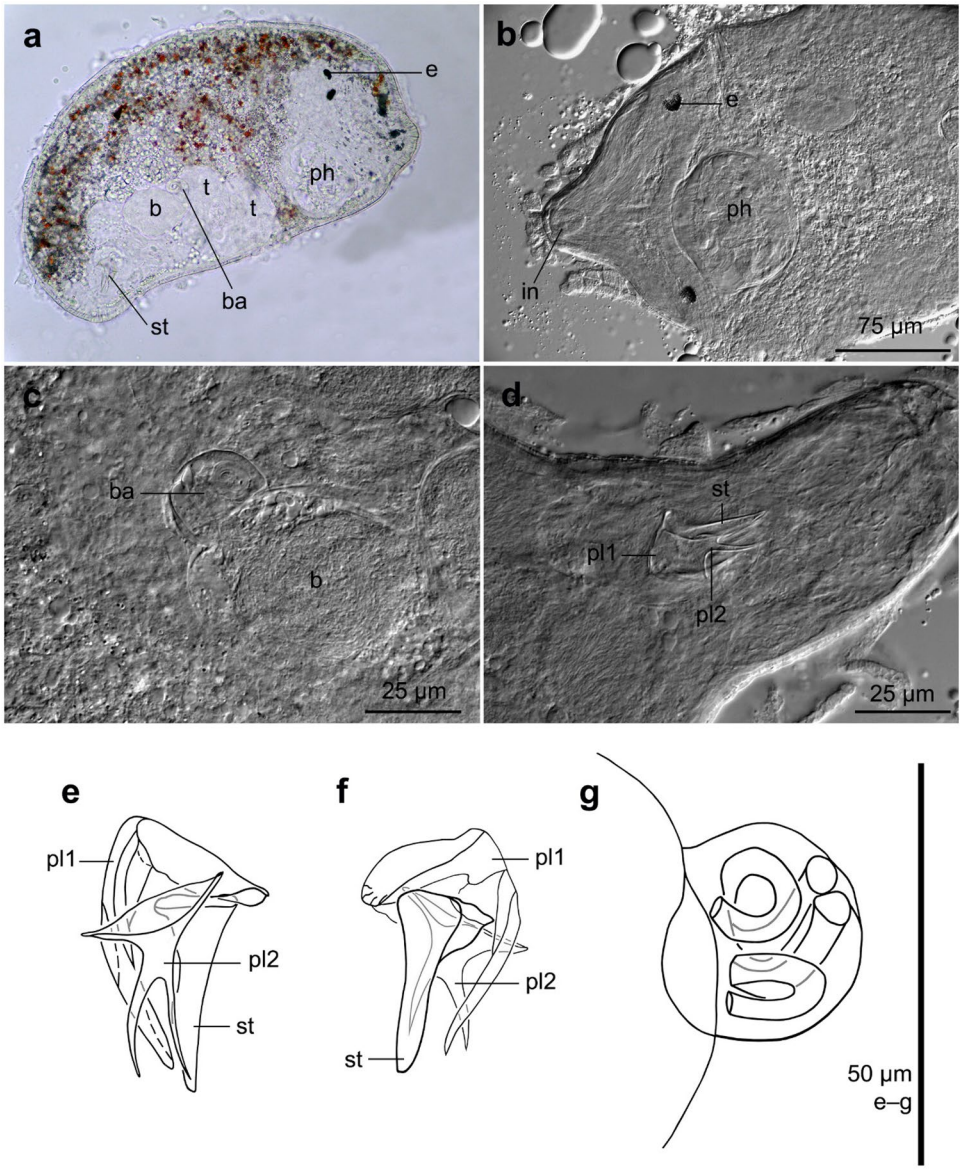

Fig. 20 *Trigonostomum yoandrisi* **sp. n. a** Body organisation (live animal). **b** Anterior body end. **c**, **g** Bursal appendage. **d**–**f** Copulatory organ. **b**–**e**, **g** From the holotype. **a**, **g** Structures oriented with the anterior end toward the right side of the plate. **b**–**d** Structures oriented with the anterior end toward the left side of the plate. **e**–**f** Structures oriented with the anterior end toward the top of the plate

18–24 µm long ($\bar{x}$ = 21 µm; n = 2) and 17–18 µm wide proximally. Distally, it displays two triangular projections, 9–15 µm long ($\bar{x}$ = 12 µm; n = 4) which end in a pointed tip.

The paired vitellaria extend laterally between the pharynx and copulatory bulb. The bursal appendage (Fig. 20a; c: ba; g) is 19–20 µm long (n = 2), and consists of a proximal case and two distal, coiled tubes (~ 360°), measuring 46–49 µm ($\bar{x}$ = 48 µm; n = 2) in length and ~ 3 µm in diameter.

Molecular phylogenetic account

The dataset of Dalytyphloplanida included sequences of 244 specimens, belonging to 238 taxa, 14 of which were sequenced for the first time. After removing ambiguously aligned positions, the 18S and 28S rDNA alignments were 1778 and 1570 bp long, respectively, resulting in a concatenated alignment of 3341 bp. After trimming, the 18S rRNA, 28S rRNA, and *cox1* mtDNA alignments of *Promesostoma* comprised 18 taxa, including three of the outgroup, and 1705 bp, 1664 bp, and 612 bp, respectively (concatenated dataset 3920 bp). Similarly, the 18S rRNA, 28S rRNA, and *cox1* mtDNA alignments of *Trigonostomum* comprised 15 taxa, including three of the outgroup, and 1791 bp, 1681 bp, and 642 bp, respectively (concatenated dataset 4068 bp). Bayesian and ML topologies were congruent after collapsing of weakly supported clades.

The resulting phylogeny of the analysis of Dalytyphloplanida is shown in Fig. 21. However, we restrict our analysis to the clade of Neodalyellida including *Schockaertia aprostatica* **gen. n. sp. n.** and all Thalassotyphloplanida. *Schockaertia aprostatica* **gen. n. sp. n.** is recovered as the

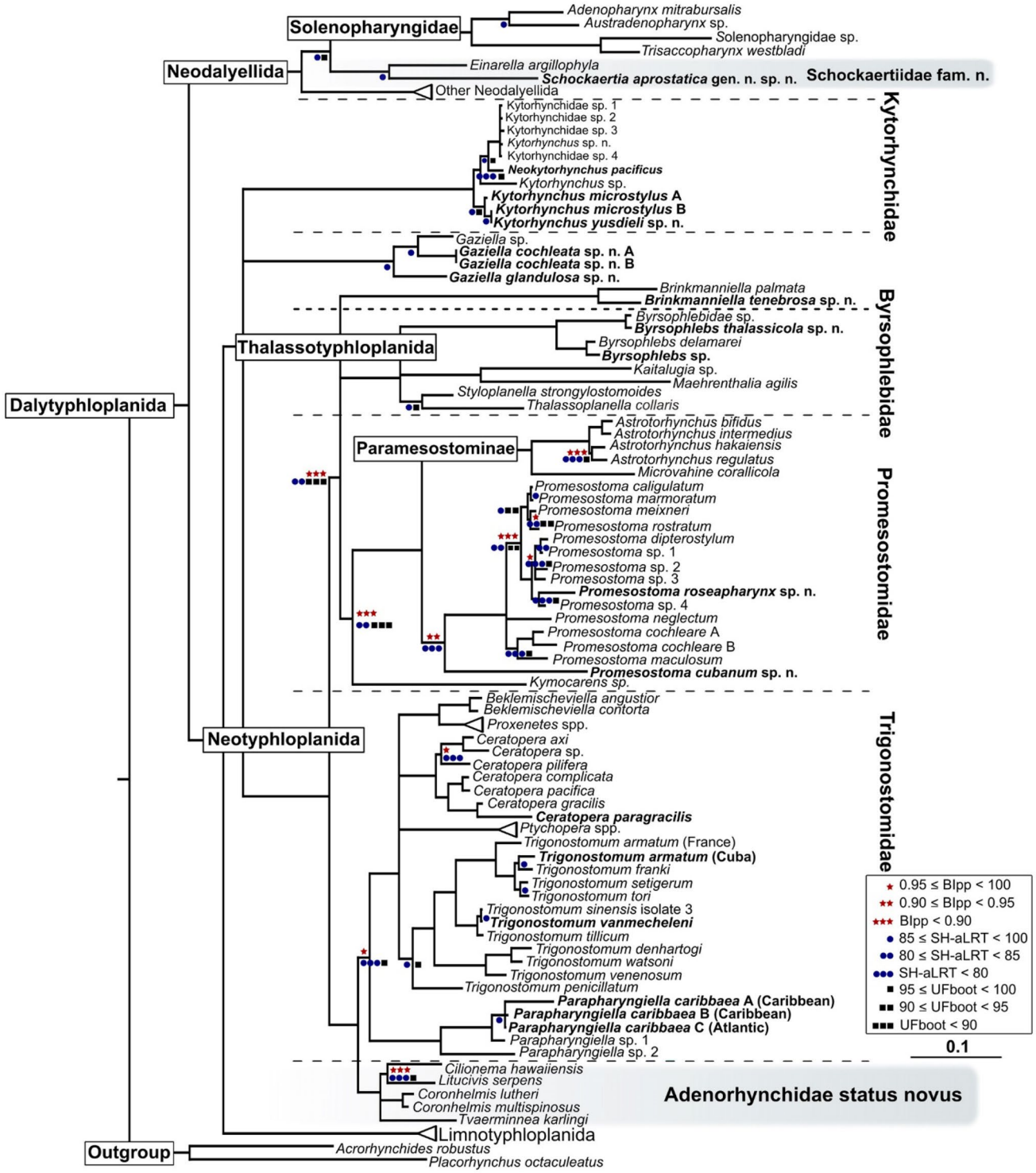

Fig. 21 Majority-rule consensus tree from the Bayesian analysis of the concatenated 18S+28S rDNA dataset of Dalytyphloplanida. Branches with support values below the thresholds in the legend of the three analyses were collapsed. Symbols above branches represent posterior probabilities (★: 0.98 ≤ pp < 100;★★: 0.95 ≤ pp < 0.98;★★★: pp < 0.95). Symbols below branches indicate SH-aLRT (●: 85 ≤ SH-aLRT < 100 ;●●: 80 ≤ SH-aLRT < 85;●●●: SH-aLRT < 80) and ultrafast bootstrap values (■: 95 ≤ UFboot < 100; ■■: 90 ≤ UFboot < 95; ■■■: UFboot < 90) from the maximum likelihood analysis. Branches without symbols have pp = 1, SH-aLRT = 100, and UFboot = 100). Taxa from which new sequences were obtained for this study are highlighted in bold

sister taxon of *Einarella argillophyla* (pp = 1, SH-LRT = 99, UFboot = 100), and this clade is sister to representatives of Solenopharyngidae Graff, 1882 (pp = 1, SH-LRT = 95, UFboot = 99).

Within the monophyletic Thalassotyphloplanida (pp = 1, SH-LRT = 98, UFboot = 100), three fully supported clades form a polytomy: Kytorhynchidae, *Gaziella* spp., and all the other thalassotyphloplanids (currently classified within Byrsophlebidae, Promesostomidae, and Trigonostomidae). In the fully supported family Kytorhynchidae (pp = 1, SH-LRT = 100, UFboot = 100), species of *Kytorhynchus* collected in Cuba form a well-supported clade (pp = 1, SH-LRT = 92, UFboot = 99) which is the sister to all other kytorhynchids (pp = 0.76, SH-LRT = 56, UFboot = 99). *Kytorhynchus microstylus* appears paraphyletic due to one specimen of this species being sister to a clade including another specimen of *K. microstylus* and *K. yusdieli* **sp. n.** (pp = 1, SH-LRT = 91, UFboot = 100). *Neokytorhynchus pacificus* clusters with unidentified species of Kytorhynchidae and *Kytorhynchus* (collected in the Eastern Atlantic, Mediterranean, and Hawaiian coasts) (pp = 1, SH-LRT = 91, UFboot = 99).

Both Trigonostomidae and Promesostomidae are polyphyletic. Species of *Gaziella* (Promesostomidae) make up a separate clade of thalassotyphloplanids. Species of *Astrotorhynchus* Graff, 1905 and *Microvahine corallicola* Karling et al., 1972 (Trigonostomidae, Paramesostominae) together form a monophyletic clade with *Promesostoma* (Promesostomidae, Promesostominae) (pp = 1; SH-aLRT = 100; UFboot = 100). *Litucivis serpens* Ax & Heller, 1970, a promesostomid species classified within Adenorhynchinae Ax & Heller, 1970, forms a fully supported clade with four species traditionally classified within Brinkmanniellinae: *Coronhelmis lutheri* Ax, 1951, *C. multispinosus* Luther in Purasjoki, 1945, *Tvaerminnea karlingi* Luther, 1943 and *Cilionema hawaiiensis* Karling et al., 1972 (pp = 1; SH-aLRT = 100; UFboot = 100). This group fully clusters with Trigonostominae (pp = 1; SH-aLRT = 100; UFboot = 100).

In the fully supported clade containing species of *Gaziella*, *G. glandulosa* **sp. n.** is the sister taxon to a clade (pp = 1, SH-LRT = 94, UFboot = 100) containing two specimens of *G. cochleata* **sp. n.** (pp = 1, SH-LRT = 100, UFboot = 100) and *Gaziella* sp. The other traditional thalassotyphloplanid families are recovered in the tree forming a fully supported clade (pp = 1, SH-LRT = 94, UFboot = 100): Byrsophlebidae, Promesostomidae, and Trigonostomidae. However, the position of their representatives differs from the traditional morphological classification. Within this group of species, a monophyletic clade including most of the Trigonostomidae and some formally considered Promesostomidae (*Coronhelmis lutheri*, *C. multispinosus*, *Cilionema hawaiiensis*, *T. karlingi*, and *L. serpens*) cluster together (pp = 1, SH-LRT = 100, UFboot = 100). The previous mentioned clade is sister to a clade containing most Promesostomidae, representatives of Byrsophlebidae and some formally considered Trigonostomidae (*Astrotorhynchus* spp. and *M. corallicola*) (pp = 0.8, SH-LRT = 81, UFboot = 63).

The relationships within the last-mentioned clade are not fully resolved and it contains three clades. The first one includes two species of *Brinkmanniella* (pp = 1, SH-LRT = 100, UFboot = 100). The second one includes representatives of Byrsophlebidae and some taxa previously considered *insertae sedis* within Thalassotyphloplanida (*Kaitalugia* Willems et al., 2005a; *Styloplanella* Findenegg, 1924; and *Thalassoplanella* Luther, 1946) (pp = 0.88, SH-LRT = 80, UFboot = 56). The third clade contains *Kymocarens* sp., *Promesostoma* spp., *Astrotorhynchus* spp., and *Microvahine corallicola*.

Within Byrsophlebidae three monophyletic clades can be recognised: one including *Kaitalugia* sp. together with *Maehrenthalia agilis* (Levinsen, 1879) Graff, 1905 (pp = 1, SH-LRT = 100, UFboot = 100), and a second one consisting of *Byrsophlebs thalassicola* **sp. n.**, *B. delamarei*, *Byrsophlebs* sp., and Byrsophlebidae sp. (pp = 1, SH-LRT = 100, UFboot = 100). The third clade includes *Styloplanella strongylostomoides* Findenegg, 1924, and *Thalassoplanella collaris* Luther, 1946 (pp = 1, SH-LRT = 90, UFboot = 99). In the clade containing most promesostomids, *Kymocarens* sp. is sister to a clade containing all species of *Promesostoma* (pp = 0.95; SH-aLRT = 70; UFboot = 100) and a clade containing *Astrotorhynchus* spp. and *M. corallicola* (formerly Trigonostomidae, Paramesostominae) (pp = 1, SH-LRT = 100, UFboot = 100).

Within Trigonostominae (pp = 0.95; SH-aLRT = 65; UFboot = 98), the clade including species of *Parapharyngiella* (pp = 1; SH-aLRT = 100; UFboot = 100) is sister to all other trigonostominids (pp = 1; SH-aLRT = 100; UFboot = 100). *Parapharyngiella* sp. 2 is the sister taxon to a clade including *Parapharyngiella* sp. 1, and *P. caribbaea* (pp = 1; SH-aLRT = 100; UFboot = 100). Three specimens of *P. caribbaea* cluster together (pp = 1; SH-aLRT = 95; UFboot = 100). Four other monophyletic groups form a polytomy within all other Trigonostominae: *Proxenetes* + *Beklemischeviella* Luther, 1943 (pp = 1; SH-aLRT = 100; UFboot = 100), *Ceratopera* (pp = 1; SH-aLRT = 100; UFboot = 100); *Trigonostomum* (pp = 1; SH-aLRT = 94; UFboot = 98); and *Ptychopera* den Hartog, 1964 (pp = 1; SH-aLRT = 100; UFboot = 100).

The monophyly of the genus *Promesostoma* is well supported (Figs. 21 and 22). In the internal analysis of the genus, *P. cubanum* **sp. n.** is the sister taxon of a clade formed by all other species of *Promesostoma* (pp = 0.96; SH-aLRT = 91; UFboot = 94). Within *Promesostoma*, three monophyletic clades can be recognised. Clade 1 '*cochleare*' (Fig. 22) includes *P. cochleare* Karling, 1935, and *P.*

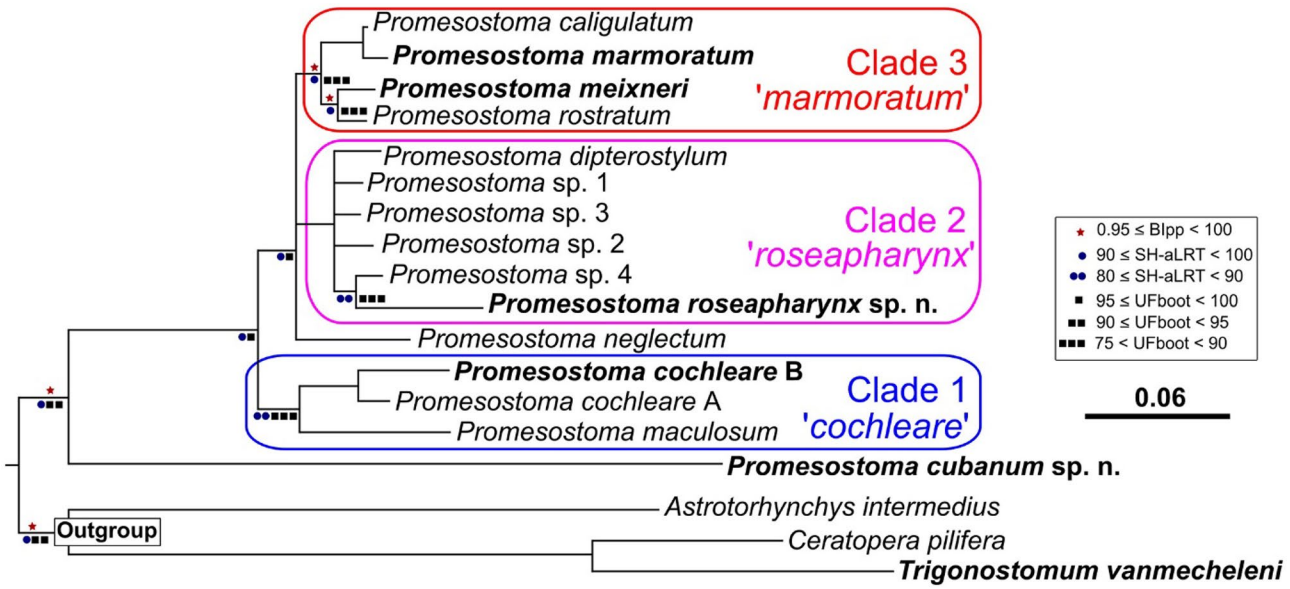

Fig. 22 Majority-rule consensus tree from the Bayesian analysis of the concatenated 18S rDNA + 28S rDNA + *cox1* dataset of *Promesostoma*. Branches with support values below the thresholds in the legend of the three analyses were collapsed. Symbols above branches represent posterior probabilities (★: 0.95 ≤ pp < 100;★★: 0.85 ≤ pp < 0.95;★★★: pp < 0.85). Symbols below branches indicate SH-aLRT (●: 80 ≤ SH-aLRT < 100;●●: SH-aLRT < 80) and ultrafast bootstrap values (■: 95 ≤ UFboot ≤ 100; ■■: 90 ≤ UFboot < 95; ■■■: UFboot < 90) from the maximum likelihood analysis. Branches without symbols have pp = 1, bootstrap = 100, and UFboot = 100). Taxa from which new sequences were obtained for this study are highlighted in bold

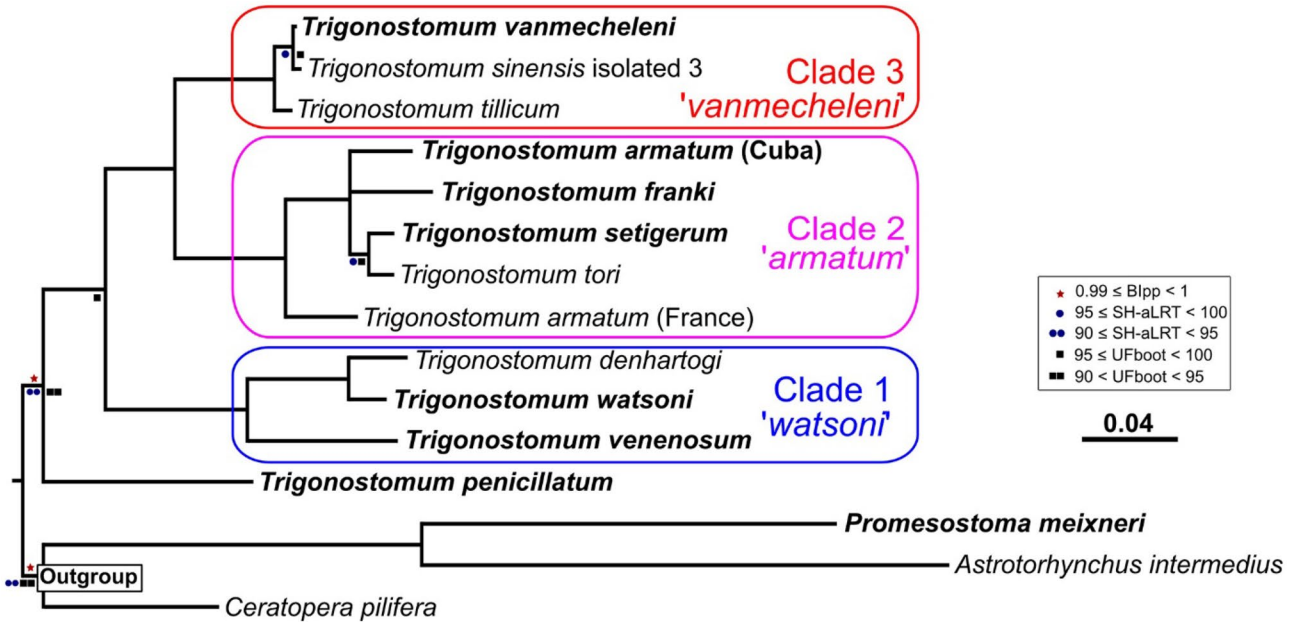

Fig. 23 Majority-rule consensus tree from the Bayesian analysis of the concatenated 18S rDNA + 28S rDNA + *cox1* of *Trigonostomum*. Branches with support values below the thresholds in the legend of the three analyses were collapsed. Symbols above branches represent posterior probabilities (★: 0.90 ≤ pp < 0.95). Symbols below branches indicate SH-aLRT (●: 99 ≤ SH-aLRT < 100;●●: 85 ≤ SH-aLRT < 95;●●●: 70 ≤ SH-aLRT < 75) and ultrafast bootstrap values (■: 98 ≤ UFboot < 100; ■■: 85 ≤ UFboot < 95; ■■■: 70 ≤ UFboot < 75) from the maximum likelihood analysis. Branches without symbols have pp = 1, bootstrap = 100, and UFboot = 100). Taxa from which new sequences were obtained for this study are highlighted in bold

maculosum Ax, 1956 (pp = 1; SH-aLRT = 83; UFboot = 83). A well-supported group includes all other species of *Promesostoma* (pp = 1; SH-aLRT = 97; UFboot = 97). However, deep internal relationships are not resolved in this clade. It contains *P. neglectum* Karling, 1967 and two clades (clades 2 '*roseapharynx*' and 3 '*marmoratum*' in Fig. 22). Clade '*roseapharynx*' includes *P. dipterostylum* Karling, 1967, *P. roseapharynx* **sp. n.**, and four undescribed species of *Promesostoma* with unknown morphology (pp = 1; SH-aLRT = 100; UFboot = 100). Clade '*marmoratum*' includes *P. caligulatum* Ax, 1952; *P. marmoratum* (Schultze, 1851) Graff, 1882; *P. meixneri*; and *P. rostratum* Ax, 1951 (pp = 0.98; SH-aLRT = 99; UFboot = 78).

Within the monophyletic *Trigonostomum* (pp = 0.99; SH-aLRT = 92; UFboot = 90), three monophyletic subclades can be recognised that together form a monophyletic clade (pp = 1; SH-aLRT = 100; UFboot = 99) with *T. penicillatum* (Schmidt, 1857) Micoletzky, 1910 as sister taxon (Fig. 23). Clade 1 '*watsoni*' includes three species: *T. venenosum*; *T. watsoni* Willems et al., 2004b; and *T. denhartogi* (pp = 1; SH-aLRT = 100; UFboot = 100). Clade 2 '*armatum*' encompasses five species: *T. franki*, *T. setigerum*, *T. tori*, and two populations identified as *T. armatum* (pp = 1; SH-aLRT = 100; UFboot = 100). Within this clade the population of *T. armatum* from France is the sister of a fully-supported clade consisting of all other taxa, including the population of *T. armatum* from Cuba (pp = 1; SH-aLRT = 100; UFboot = 100). *Trigonostomum setigerum* and *T. tori* are sister taxa (pp = 1; SH-aLRT = 98; UFboot = 97). Finally, clade 3 '*vanmecheleni*' encompasses three species: *T. tillicum* Van Steenkiste & Leander, 2018, *T. vanmecheleni*, and *T. sinensis* (pp = 1; SH-aLRT = 100; UFboot = 100). *Trigonostomum tillicum* is the sister taxon of *T. vanmecheleni* and *T. sinensis* (pp = 1; SH-aLRT = 96; UFboot = 98).

The inter- and intraspecific genetic distances (Supplementary Table 1) calculated for species of *Trigonostomum* showed very high similarity among the species belonging to clade '*vanmecheleni*'. Both sequenced specimens of *T. sinensis* have a ML distance of 0.001 from each other and with respect to *T. vanmecheleni*. The phylogenetic distance is 0.010 between *T. tillicum* and *T. vanmecheleni*/*T. sinensis*. The phylogenetic distance is higher among all other species of *Trigonostomum* (Supplementary Table 1).

Discussion

Extensive phylogenetic analyses of Dalytyphloplanida were conducted by Van Steenkiste et al. (2013) and Van Steenkiste and Leander (2017), exploring the deep relationships within this group for the first time. In addition, Stephenson et al. (2019) also contributed to elucidate the interrelationships among neodalyellids. In this contribution, we mainly focus on interrelationships at the lowest taxonomic level. We explore the relationships of the newly sequenced taxa with their congeners, and in this context discuss the newly described species. Moreover, we examine the intrageneric relationships of two of the largest genera of Thalassotyphloplanida, *Promesostoma* and *Trigonostomum*, in detail.

Based on molecular phylogeny and morphology, we propose a new classification for Thalassotyphloplanida. Until now, four thalassotyphloplanid families where recognised (Kytorhynchidae, Byrsophlebidae, Promesostomidae, and Trigonostomidae). Our analyses also support these four families and, furthermore, recognise Adenorhynchidae Ax & Heller, 1970 **status novus**. A new family is proposed to contain two species of neodalyellids with a pharynx rosulatus: Schockaertiidae **fam. n**. Species of *Gaziella* form a polytomy with Kytorhynchidae and the remaining thalassotyphloplanids. Species of *Brinkmanniella* form a polytomy with Byrsophlebidae and Promesostomidae and, therefore, remain *incertae sedis*. The only subfamily taxon supported in our analyses is Paramesostominae, leading to the suppression of the remaining subfamily taxa.

Schockaertiidae fam. n. and *Schockaertia* gen. n., a new family and a new genus of Neodalyellida

While we mainly focus on members of Thalassotyphloplanida, we also include a new marine neodalyellid species in this work: *Schockaertia aprostatica* **gen. n. sp. n**. The new taxon resembles *Einarella argillophila*, a species traditionally classified within Trigonostomidae (Luther, 1948) and later Promesostomidae (Den Hartog, 1964). However, Willems et al. (2006) and Van Steenkiste et al. (2013) demonstrated that *E. argillophila* is a neodalyellid related to Solenopharyngidae. In our inferred phylogeny, *S. aprostatica* **gen. n. sp. n.** is recovered as the sister taxon of *E. argillophila*. This clade contains the only known species of neodalyellids that have a pharynx rosulatus. In addition, both species possess a male copulatory bulb devoid of any hard structures. A copulatory bulb devoid of hard structures is encountered in two other neodalyellid taxa: *Pseudograffilla* Meixner, 1938 and *Paravortex* Wahl, 1906, which are contained in 'Other Neodalyellida' in Fig. 21. Representatives of both these taxa differ from *Einarella* and *Schockaertia* **gen. n.** by the location of the gonads and atrial organs in the anterior body half, they are ovoviviparous, and their pharynx is of the doliiform type. Moreover, all species of *Paravortex* are specialised parasites of bivalves (Brusa et al., 2006, 2011) and fish (Cannon & Lester, 1988; Fernández et al., 2015). In *Bresslauilla relicta* Reisinger, 1929, also lacks a stylet, but has a slightly sclerotised ejaculatory duct. However, it can be differentiated from *Einarella* and *Schockaertia* **gen. n.** by an anteriorly located male copulatory bulb and a single ovary (Reisinger, 1929). Many species of Umagillidae also lack

sclerotised genital structures. Notwithstanding, umagillids are specialised endosymbiotic/endoparasitic flatworms with a doliiform pharynx (Stunkard & Collins, 1951; Cannon, 1981), and they belong to a group of neodalyellids that is sister to the clade including Solenopharyngidae (see Van Steenkiste et al., 2013) and Schockaertiidae **fam. n**.

Based on the above, we propose a new family to encompass *Einarella argillophyla* and *Schockaertia aprostatica*: Schockaertiidae **fam. n**. Representatives of this family are easily distinguished from their nearest evolutionary relatives in Solenopharyngidae due to their pharynx morphology: in Solenopharyngidae, the pharynx is elongated (similar to plicatus) and associated with well-developed extrapharyngeal glands (Ehlers, 1972; Luther, 1963). *Einarella argillophyla* is formally transferred from Promesostomidae to Schockaertiidae **fam. n.**

Several features allow us to distinguish between *Einarella* and *Schockaertia* **gen. n**. The presence of a second connection with the exterior through a vagina is a unique feature of *Schockaertia* **gen. n.**, lacking in *Einarella* and all other neodalyellids. However, a bursa with a vagina may be present in *Orostylis timucuorum* Smith III in Gobert et al., 2022, a species belonging to a genus characterised by the male aperture associated with the mouth (Gobert et al., 2022). Moreover, the female duct in *S. aprostatica* **gen. n. sp. n.** is bipartite and consists of two globular parts, whereas it is a straight duct without differentiations in *E. argilophylla*. *Einarella argilophylla* possesses a bursa (or receptaculum seminis; see Luther, 1948), which is not the case in *S. aprostatica* **gen. n. sp. n.** *Einarella* and *Schockaertia* **gen. n.** also differ in the detailed morphology of the male system. In *S. aprostatica* **gen. n. sp. n.**, a pair of extracapsular seminal vesicles is located ventro-caudal to the pharynx. Seminal ducts open into the copulatory bulb, which is a simple sac without prostate vesicle. In *E. argillophila*, vasa deferentia are widened caudal to the pharynx, forming false seminal vesicles. These open into a single seminal vesicle enclosed by the copulatory bulb. The copulatory bulb of *E. argillophila* also contains a prostate vesicle, partially surrounding the male duct (see Luther, 1948), which is lacking in *S. aprostatica* **gen. n. sp. n**. Furthermore, *S. aprostatica* **gen. n. sp. n.** has a pair of eyes, which are lacking in *Einarella*.

New insights on the interrelationships of Thalassotyphloplanida

The topology of the newly obtained trees largely corroborates the results of Van Steenkiste et al. (2013). Inclusion of new taxa and sequences solved several previously unclear relationships. A general conclusion is that the presence of a proboscis-like anterior invagination of the body wall is a feature found in several unrelated taxa throughout the tree: Kytorhynchidae, *Gaziella*, *Trigonostomum*, *Astrotorhynchus*, and *Microvahine corallicola*. As such, this structure seems to have evolved several times independently in the evolutionary history of thalassotyphloplanids.

Representatives of Brinkmanniellinae (Promesostomidae) are scattered throughout our tree, clustering with trigonostomids and promesostomids, and species of *Brinkmanniella* (type genus of the subfamily) form a polytomy with byrsophlebids and most promesostomids (excluding the taxa now included in Adenorhynchidae **status novus**); therefore, we propose to suppress Brinkmanniellinae. Representatives of this subfamily are allocated to other taxa as follow: *Cilionema* Karling et al., 1972; *Coronhelmis* Luther, 1948; and *Tvaerminnea* Luther, 1943 are transferred to Adenorhynchidae **status novus**, *Gaziella* is a taxon *incertae sedis* within Thalassotyphloplanida, and all other representatives now in Brinkmanniellinae remain within Promesostomidae (except *Brinkmanniella*), awaiting inclusion in further molecular phylogenetic analyses.

As *Microvahine* and *Astrotorhynchus* (Paramesostominae, Trigonostomidae) form a monophyletic clade with species of *Promesostoma*, we transfer Paramesostominae to Promesostomidae. Paramesostominae also includes *Gandalfia* Willems et al., 2005b, and *Paramesostoma* Attems, 1896 (type genus), which were not included in the analysis. However, this is a homogeneous group of species characterised by several distinctive traits: The vitellaria are separated from the ovaries, the bursa possesses a double connection, the male sclerotised copulatory organ consists of a stylet, there is one extracapsular seminal vesicle, and the distal half of the pharynx is ciliated (Luther, 1948; Karling et al., 1972).

According to Karling et al. (1972), there is only one taxonomically important feature common to all the subfamilies of Trigonostomidae: the presence of a second connection of the bursa with the common oviduct (the insemination canal), also mentioned by Den Hartog (1964) and Ax and Heller (1970). However, Karling et al. (1972) questioned the taxonomic value of this feature as this connection appears convergently in many taxa. These authors proposed to retain the division of Trigonostomidae into three subfamilies, but stated that this classification is not satisfactory and needs re-evaluation considering a higher number of taxa. Our phylogenetic work is congruent with the most recent results of Van Steenkiste and Leander (2022), and we recover Trigonostomidae as a monophyletic grouping, including only representatives of Trigonostominae. Therefore, we suppress the use of Trigonostominae and consider the double connection of the bursa a synapomorphy for Trigonostomidae. We transferred the subfamily Paramesostominae to Promesostomidae, whereas Van Steenkiste and Leander (2022) updated the status of Mariplanellinae to Mariplanellida (the sister taxon of all other Rhabdocoela).

In the following sections, we provide an in-depth taxonomic discussion of all new and previously described thalassotyphloplanids. The value of the respective morphological

traits used to delineate species and genera are discussed in the framework of the newly presented phylogeny.

Kytorhynchidae

The family Kytorhynchidae is best known from the seminal article by Rieger (1974), containing the first descriptions of two genera, *Kytorhynchus* and *Kytorhynchella* Rieger, 1974, each with three species from the Atlantic coast of North America. Since that publication, only one other (monotypic) kytorhynchid genus was described: *Neokytorhynchus pacificus* Ehlers & Ehlers, 1974 from Galapagos Islands. However, the distribution of the family is much wider, as specimens of several new species were collected in Lanzarote, Sardinia, and Andalusia by members of Hasselt University group, some species of which were already included in the phylogenetic analysis by Van Steenkiste et al. (2013). With the findings of this paper, the distribution of Kytorhynchidae is extended to the Caribbean Sea.

The length of the stylet of *K. microstylus* in the specimens from Cuba (23–43 µm long) broadens the range of 30–35 µm thus far mentioned in literature (Rieger, 1974). This author reported some degree of intraspecific variation in the morphology of the stylet, mainly in the distal part: it is either straight and slender, forms a pronounced hook or even is bifurcate in one specimen from Bermuda. Also in the specimens from Cuba, the same type of variation can be observed: some stylets show a distal hook (Fig. 3b, d), while others are more straight (Fig. 3c). These differences, however, are likely due to a difference in degree of squeezing, as the stylet is thin-walled and flexible. Nevertheless, *K. microstylus* appears paraphyletic in our analysis indicating that it might represent a species complex. The sequenced specimen indicated as '*K. microstylus* B' in our phylogeny was collected in Siboney and the specimens from this locality show a stylet with a typical distal hook (Fig. 3b, d), matching the diagnostic characteristics of the species provided by Rieger (1974). On the other hand, specimens from Bueycabón, where the specimen '*K. microstylus* A' of our phylogeny was also collected, present an almost straight stylet (Fig. 3c). These morphological and molecular phylogenetic differences suggest that *K. microstylus*, may constitute an unresolved species complex.

Kytorhynchus (*Eukytorhynchus*) *yusdieli* **sp. n.** fits the features of both the genus (testes located ventrally from the vitellaria, male genital canal short) and subgenus (no eyes, anterior invagination triangular, with a sclerotised and funnel-shaped stylet with longitudinal folds) (Boyko, 1996; Rieger, 1974). Other features typical of the subgenus such as the single connection between ovary and atrium and the fact that the proximal, glandular part of the female genital canal is enlarged are only observable on sectioned material, which is currently not available for the Cuban populations. *Kytorhynchus yusdieli* **sp. n.** appears as the sister taxon of *K. microstylus* in our phylogeny.

The new species can easily be distinguished from *K. microstylus*, the only other species within the subgenus, based on stylet morphology: The stylet is 53–62 µm long in *K. yusdieli* **sp. n.** and 23–43 µm long in *K. microstylus* (Rieger, 1974; our data on this work). Moreover, the funnel-shaped stylet of *K. microstylus* tapers to a distal blunt, curved hook, whereas in *K. yusdieli* **sp. n.**, the stylet is much wide distally (20 µm), lacking such as a hook.

Gaziella and *Moevenbergia*

The monophyly of the genus *Gaziella* is demonstrated after the inclusion of two new species in our phylogenetic analysis, which cluster together with a previously sequenced and undescribed species. All species of *Gaziella* share the diagnostic features of the genus as established by De Clerck and Schockaert (1995): the presence of a single seminal vesicle contained within the male copulatory bulb and an anterior proboscis-like and glandular invagination. Now five species of *Gaziella* are known, three of which are described in this contribution. The two previously known species, *G. lacertosa* De Clerck & Schockaert, 1995 and *G. pileola* De Clerck & Schockaert, 1995, were described from the eastern coast of Africa (Kenya, Western Indian Ocean) (De Clerck & Schockaert, 1995). An unidentified species of *Gaziella* from the Mediterranean was included in the phylogenetic analysis of Van Steenkiste et al. (2013). Therefore, the known distribution of the genus is extended to the Caribbean and Atlantic coasts of Cuba.

A common characteristic of the three new species described from Cuba is the presence of two types of anterior rhabdite tracts. One type presents filiform rhabdites (Fig. 7d: ar2) and in the other type the rhabdites are thicker (Fig. 7d: ar1). The presence of different types of anterior rhabdite tracts was not mentioned in the description of the other two previously known species (see De Clerck & Schockaert, 1995). The general internal morphology of all species of *Gaziella* is similar and they mostly differ in the detailed morphology of the male copulatory bulb. Although the position of the pharynx is not a strong characteristic to differentiate among species of *Gaziella*, this structure is located at mid body (*G. pileola* and *G. microcirra* **sp. n.**) or in the second body half (*G. lacertosa*, *G. cochleata* **sp. n.**, and *G. glandulosa* **sp. n.**).

Gaziella pileola is readily distinguished from its congeners by its very long cirrus (249–305 µm; $\bar{x}$ = 270 µm), which is smaller in the other four species: *G. glandulosa* **sp. n.** 94 µm, *G. lacertosa* 48–78 µm ($\bar{x}$ = 64 µm), *G. cochleata* **sp. n.** 26–54 µm ($\bar{x}$ = 44 µm), and *G. microcirra* **sp. n.** 33–51 µm ($\bar{x}$ = 41 µm). From these measurements, it is clear that also *G. glandulosa* **sp. n.** is well recognised by its cirrus length.

Similarly, in both *G. pileola* and *G. glandulosa* **sp. n.** the sclerotised cap surrounds the most distal end of the cirrus (10% and 20% of its length, respectively). In *G. cochleata* **sp. n.** and *G. microcirra* **sp. n.**, the sclerotised cap surrounds at least the distal 60% of the cirrus, whereas in *G. lacertosa*, it surrounds the distal 30%. A unique feature of *G. glandulosa* **sp. n.** is the fact that the proximal 80% of its cirrus is devoid of spines and shows thick glandular walls. In all other species of *Gaziella*, the cirrus is fully covered by spines.

Gaziella cochleata **sp. n.** is the only species of the genus where the distal cap of the copulatory bulb is a spiralised plate, a clear diagnostic feature of this species. *Gaziella microcirra* **sp. n.** exhibits a cirrus similar in morphology to that of *G. lacertosa*. However, the average length of the cirrus of *G. lacertosa* (64 µm) is larger than that of *G. microcirra* **sp. n.** (41 µm). Furthermore, a distinguishing feature of *G. microcirra* **sp. n.** is the fact that the walls of its cirrus are partially sclerotised and form distinct, lamellar-like structures (see Figs. 6g and 8e).

Representatives of *Moevenbergia* Armonies & Hellwig, 1987 (formally Promesostomidae, Brinkmanniellinae), are morphologically similar to *Gaziella*. These genera differ from each other by the presence of two extracapsular seminal vesicles and a pair of seminal reservoirs on each oviduct in *Moevenbergia* (Armonies & Hellwig, 1987), whereas there is a single intracapsular seminal vesicle and a single seminal reservoir on each oviduct in *Gaziella* (De Clerck & Schockaert, 1995). Recently, Armonies (2017) described a second species of *Moevenbergia*: *M. oculofagi* Armonies, 2017. However, *M. oculofagi* exhibits two traits typical of *Gaziella*: the presence of a strong, anterior, proboscis-like structure and a single and well-developed, intracapsular seminal vesicle (Armonies, 2017). Species of *Moevenbergia* do not have an anterior, proboscis-like structure (Armonies & Hellwig, 1987).

Seminal receptacles were not observed in *M. oculofagi*, but the development of these structures depends on the reproductive state of the specimens and sometimes are not observable (i.e., when not filled with sperm). Therefore, we suggest *M. oculofagi* to be transferred to *Gaziella* (now *G. oculofagi* **comb. n.**). *Gaziella oculofagi* **comb. n.** is similar to *G. microcirra* **sp. n.**; however, the former has a smaller cirrus ($\bar{x}$ = 32 µm long) and does not exhibit the sclerotised lamellae in the cirrus characteristic for *G. microcirra* **sp. n.**

Following this reasoning, *Gaziella* now contains six species, three of which are described in this paper. Further molecular phylogenetic analyses are necessary to elucidate the relationships between *Gaziella* and *Moevenbergia*.

Brinkmanniellinae and *Brinkmanniella*

Brinkmanniella is the type species of the promesostomid subfamily Brinkmanniellinae Luther, 1948. As stated previously, representatives of Brinkmanniellinae appear scattered throughout the inferred tree and species of *Brinkmanniella* represent a monophyletic clade clustering with Byrsophlebidae and the other promesostomids. Species of *Brinkmanniella* strongly differ from the representatives of other genera included within Brinkmanniellinae by the fact that they are the only thalassotyphloplanids with the ovaries located anterior to the testes, and by the absence of female atrial organs (Karling, 1986; Luther, 1943). Therefore, considering both phylogeny and morphology, we suppress the use of the subfamily name Brinkmanniellinae. Hence, *Brinkmanniella* is considered a taxon *incertae sedis* within Thalassotyphloplanida.

The inclusion of a second species of *Brinkmanniella* (*B. tenebrosa* **sp. n.**) in the phylogenetic analyses provides the first evidence for the monophyly of this genus (pp = 1, SH-LRT = 100, UFboot = 100). All representatives of *Brinkmanniella*, including the two new species included in this work, are characterised by the anterior position of the ovaries, the absence of specific female atrial organs apart from the female duct, and the caudally located pharynx (Luther, 1943; Schockaert & Martens, 1985).

All species of *Brinkmanniella* possess a more or less funnel-shaped stylet, the detailed morphology of which is the main feature to distinguish between them. In *B. macrostomoides* Luther, 1948, and *B. procerastyla* Ehlers, 1974, the stylet is curved and tapers toward a sharp distal tip, which clearly distinguishes them from all other species of the genus, including the ones described in this contribution. The ruffled stylet tip of *B. augusti* Marcus, 1951; *B. obtusa* Luther, 1948; and *B. palmata* Karling, 1986 is typical of these three species and is not seen in the new species. *Brinkmanniella microps* Schockaert & Martens, 1985, possesses a straight stylet, although the distal tip of the stylet in the holotype is bent, which is caused by the fixation procedure (for a discussion, see Schockaert & Martens, 1985).

The shape of the stylet in *B. microps* most closely resembles that of the two new species, but it is much smaller: 30 µm vs 60 µm in *B. simplex* **sp. n.** and ~ 59 µm in *B. tenebrosa* **sp. n**. The stylet of *B. australiensis* Willems et al., 2004a, is similar in length (57 µm) to that of the new species. However, it is 32 µm wide proximally, funnel shaped and constricted at about its midpoint, which is not the case in the new species from Cuba. The two new species can be distinguished from each other by the fact that the stylet of *B. tenebrosa* **sp. n.** is more tubular, with its widest part located a short distance from its proximal end, a feature unique among all species of *Brinkmanniella*. The stylet of *B. simplex* **sp. n.** consists of a wide proximal funnel, gradually tapering towards a rounded tip.

Dark pigmentation as observed in *B. tenebrosa* **sp. n.** has only been reported in *B. microps*. However, in the latter species, the pigmentation is dark grey-brown, while in *B. tenebrosa* **sp. n.**, it is black. In *B. augusti*, the pale-yellow colouration of the specimens is caused by fine pigment

distributed in the parenchyma (Marcus, 1951), whereas, in *B. tenebrosa* **sp. n.** is caused by fine epidermal granules. The pale-yellow colouration of *B. australiensis* is probably also due to such a pigment type as in *B. augusti*. The pronounced proterandry observed in some species of *Brinkmanniella* was once considered a typical feature of the genus (see Karling, 1986). However, Schockaert and Martens (1985) did not observe protandry in *B. microps*, nor is it the case for *B. australiensis* (see Willems et al., 2004a). Also in the two new species, male and female gonads are fully developed simultaneously, providing further evidence that pronounced proterandry cannot be considered a general or diagnostic trait of *Brinkmanniella*.

Byrsophlebidae

The position of *Kaitalugia* within Byrsophlebidae has implications for the taxonomic value of the number of gonopores as a synapomorphy. Previously, Byrsophlebidae was distinguished from Typhloplanidae Graff, 1905 (Limnotyphloplanida), by the presence of two gonopores in the former taxon. However, as species of *Kaitalugia* possess a single, common gonopore this is no longer a defining feature of Byrsophlebidae. *Kaitalugia* is recovered as the sister taxon to *Maehrenthalia* Graff, 1905, but a clear morphological synapomorphy cannot be identified. The female system of *Maehrenthalia* includes a bursa with a seminal reservoir, whereas these structures are absent in species of *Kaitalugia* (Willems et al., 2005a, b). The main features shared by members of Byrsophlebidae are the presence of a single ovary and a bursa with a single connection to the female duct.

The newly described species, *Byrsophlebs thalassicola* **sp. n.**, can unambiguously be placed in Byrsophlebidae as it shows the above-mentioned characteristics of the family. The position of *B. thalassicola* **sp. n.** within *Byrsophlebs* was confirmed by the phylogenetic analysis. *Byrsophlebs thalassicola* **sp. n.** constitutes a monophyletic clade together with an unidentified species of Byrsophlebidae, *Byrsophlebs* sp., and *Byrsophlebs delamarei* (Ax, 1956) Karling, 1985. In addition, the new species possesses a bursa, a feature present only in two genera of byrsophlebids: *Byrsophlebs* and *Maehrenthalia*. These genera can be distinguished from each other by the morphology of the female reproductive system: species of *Maehrenthalia* lack a seminal receptacle in the female duct and their bursa is bipartite, consisting of a uterus and a terminal resorptive vesicle; representatives of *Byrsophlebs* have a female duct with a seminal receptacle and a bursa without resorptive vesicle (see Karling, 1985). The Cuban specimens exhibit the latter morphology, corroborating their placement in *Byrsophlebs*. *Byrsophlebs* and *Maehrenthalia* also differ in the morphology of the male copulatory bulb, being globular-oviform with two layers of strong spiral muscle fibres in *Byrsophlebs*, and cylindrical with a single layer of strong spiral muscle fibres in *Maehrenthalia*. However, in *B. thalassicola* **sp. n.**, the external muscle layer has a longitudinal orientation, a unique pattern of compared with all other species of *Byrsophlebs*.

All species of *Byrsophlebs* possess a simple, funnel-like-to-tubular stylet. In *B. thalassicola* **sp. n.**, the distal tip of the stylet is hook shaped. This is the case in most species of this genus, except for *B. dubia* (Ax, 1956) Karling, 1985, and *B. graffi* Jensen, 1878. Those species with a distal hook on the stylet differ from each other in the detailed morphology of the stylet and other atrial organs. In *B. dubia*, *B. delamarei*, and *B. graffi*, the stylet gradually tapers to a distal tip, as occurs in some of our specimens (Fig. 9e), whereas in other specimens of *B. thalassicola* **sp. n.**, the stylet has a well-differentiated, proximal funnel-like and distal tubular part (Fig. 9c, d). A similar stylet morphology is seen in *B. caligulachaena* and *B. lutheri* (Marcus, 1952) Karling, 1985.

The stylet of *B. thalassicola* **sp. n.** is ~ 46 µm long, compared to a length of ~ 36 µm in *B. caligulachaena* (Ehlers & Ehlers, 1981) and ~ 43 µm in *B. lutheri* (Marcus, 1952). While the stylet length of *B. thalassicola* **sp. n.** corresponds to that of *B. lutheri*, its stylet is more similar in shape to that of *B. caligulachaena*. The distal tip of the stylet of *B. lutheri* resembles a fishing hook, with the tip pointing forward; in *B. thalassicola* **sp. n.** and *B. caligulachaena*, the distal tip is directed sideways. In one specimen of *B. thalassicola* **sp. n.** (Fig. 9e), the distal tip of the stylet points forward. However, considering the delicate construction of the stylet, this situation is most likely a fixation artefact. Indeed, in the live specimen, the stylet had the same morphology as that of the other specimens. The distal tip of the stylet is pointed in *B. thalassicola* **sp. n.**, while it is blunter in *B. caligulachaena*.

As mentioned before, a unique feature of *B. thalassicola* **sp. n.** is the longitudinal orientation of the external muscle fibres surrounding the prostate vesicle, whereas it is oblique in all other species of *Byrsophlebs*. Another diagnostic trait of *B. thalassicola* **sp. n.** is the fact that the bursa opens proximally into the female atrium, whereas this connection occurs more distally in its congeners. The presence of a bursal sphincter at the connection with the female duct in *B. thalassicola* **sp. n.** is uncommon in *Byrsophlebs* and has only been described for *B. delamarei* (Ax, 1956). The seminal receptacle as a differentiation of the proximal part of the female duct, apart from the new species, has only been reported in *B. caligulachaena*. The sphincter surrounding the distal part of the oviduct is a feature shared by *B. thalassicola* **sp. n.** and *B. uncinata*.

Kymocarens

Representatives of *Kymocarens* are characterised by large and conspicuous anterior rhabdite tracts, a caudal adhesive tail plate, paired testes situated anterior to the pharynx, paired

seminal vesicles, a tubular stylet, paired ovovitellaria with the ovaries most caudally, an atrial bursa connected to the common genital atrium, and each oviduct with a seminal receptacle (Ehlers & Ehlers, 1981). All these features are present in the specimens from Cuba, justifying inclusion in the genus *Kymocarens*. However, in *K. morrisi* **sp. n.**, the position of the ovaries is not completely clear. The ovaries seem to be located just caudal to the male copulatory organ (Fig. 11a: ov).

The only molecular data available for *Kymocarens* is the sequence of the 18S rDNA gene of *Kymocarens* sp. (Van Steenkiste et al., 2013). Unfortunately, we failed to amplify the 18S gene for *K. morrisi* and only the amplification of the 28S gene was succesful. Therefore, we did not include *K. morrisi* in the phylogenetic analyses. Consequently, we cannot address the monophyly of *Kymocarens* and the discussion of the new species is based on comparative morphology.

Three species of *Kymocarens* have previously been described, and *K. morrisi* **sp. n.** can be distinguished from these by the morphology of the stylet. In *K. proxenetoides* Ehlers & Ehlers, 1981, the elongated and funnel-shaped stylet is 49–50 µm long, whereas in *K. tibialis* Ehlers & Ehlers, 1981, it is 30 µm long with a complex distal end (see Ehlers & Ehlers, 1981; Willems et al., 2005a). In *K. kanakorum* Willems et al., 2005a, the stylet is 56 µm long and shows a typical transverse ridge distally (Willems et al., 2005a). *Kymocarens morrisi* **sp. n.** displays a longitudinal slit in the proximal end of the stylet. This feature combined with the fact that the stylet bends over 90° at its midpoint are diagnostic for the new species. Furthermore, measuring 66–89 µm long, the new species possesses the longest stylet ever reported for a species of *Kymocarens*.

The general morphology of the atrial organs of *K. morrisi* **sp. n.** does not differ from that in *K. proxenetoides* and *K. tibialis*. However, the parenchymal sheath surrounding the bursa is unique for *K. morrisi* **sp. n.** Also, the sphincter on the distal aperture of the pharynx has never been reported in any other representative (but note that both features are unknown for *K. kanakorum*, as no sectioned material of this species exists).

Promesostoma

Currently, 37 species of *Promesostoma* are described (WoRMS, 2023). They all have a stylet that basically is a single-walled tube, situated in an elongated male atrium that is widened proximally. The male atrium is constricted by at least one sphincter (Karling, 1967; Luther, 1943). Species of *Promesostoma* are distinguished from each other based on size and shape of the stylet, and some easily observable features of the male genital system, such as the presence of a copulatory bursa (Karling, 1967). Unfortunately, apart from that of *P. marmoratum* (studied by Luther, 1943), the internal morphology is not known in detail for any of the species, as most species are only described on observations on live animals and on the detailed morphology of the stylet (Karling, 1967). This lack of knowledge impedes the elaboration of sound hypotheses on the evolution of morphological traits within this speciose genus.

Within *Promesostoma*, Karling (1967) delimited some more or less homogeneous species groups based on features of the male genital system, including stylet shape (straight, curved, spiralised, branched, proximally bent or not) and position (lying completely caudal to the pharynx or next to it, or with the proximal end anterior to the pharynx and the distal end caudal to it). Two additional important taxonomic features are the presence or absence of the male copulatory bursa and of a seminal receptacle. The latter two features are easily observable in live specimens. The species groups proposed by Karling (1967) could not be retrieved in our phylogeny (see our clade '*cochleare*', for example). However, our study corroborates Karling's hypothesis about the ancestral morphological state of the male atrial organs in *Promesostoma*. This affirmation is supported by the fact that *P. cubanum* **sp. n.** is recovered as the sister taxon of all other species of *Promesostoma* in our phylogeny as this species shows the hypothetical ancestral characteristics mentioned by Karling (1967): 1, prostate vesicle provided with a short and straight stylet; 2, prostate vesicle oriented backwards and its axis is the same of that of the stylet; and 3, proximally, the stylet enlarge to a funnel with an annular thickening.

Because of the fact that their stylet is straight to slightly curved, without spines, and located caudal to the pharynx, *Promesostoma cubanum* **sp. n.** and *P. cubitum* **sp. n.** resemble *P. bilineatum* Pereyaslawzewa, 1892; *P. gallicum* Ax, 1956; *P. kergroixense* Ehlers & Sopott-Ehlers, 1989; *P. norvegicum* Karling, 1967; *P. serpentistylum* Ax, 1952; and *P. tenebrosum* Ax & Ehlers, 1973. Unfortunately, except for *P. cubanum* **sp. n.**, none of these species could be included in our phylogenetic analysis. *Promesostoma cubanum* **sp. n.** and *P. cubitum* **sp. n.** are unique by the fact that their prostate vesicle is located caudal to the pharynx and is connected by a short duct to the stylet, whereas the prostate vesicle is located anterior to the pharynx and is connected to the stylet by a very long duct in the other forementioned species. In this group, *P. bilineatum* and *P. kergroixense* are the only species where the stylet carries one distal wing, a feature not seen in our specimens, nor in any other species of this group. The longest stylet among these species is found in *P. bilineatum* and *P. gallicum* (240–250 µm long) (Ax, 1952, 1956). The stylet of *P. cubitum* **sp. n.** (108–123 µm) is slightly smaller than that of *P. norvegicum* (130 µm), but longer than that of *P. cubanum* **sp. n.** (93–114 µm), *P. kergroixense* (95–100 µm), and *P. tenebrosum* (45–48 µm). There are no measures available in literature for the stylet in *P. serpentistylum*. However, it differs from that of *P. cubanum* **sp. n.** by the fact it is slender, with

the same width all over its length, and has an oblique distal end (see Ax, 1952; Karling, 1967; Ehlers, 1974).

Promesostoma cubitum **sp. n.** is the only species of this species group that has only one seminal vesicle, whereas there is a pair of them in all other species. Furthermore, the proximal elbow-shaped projection of the stylet of *P. cubitum* **sp. n.** (Figs. 13b and 15c) is also unique.

Apart from the differences mentioned above, *P. cubanum* **sp. n.** differs from each of the other species in this group in several details. It is the only species of the group without male bursa, and it is the only one that has a muscular bulb with a proximal sperm-containing vesicle connected to the genital atrium (Fig. 13d: x). *Promesostoma norvegicum* has a strongly curved stylet, with the distal end irregularly club shaped and a tooth-like edge, which is not the case in *P. cubanum* **sp. n.** In *P. tenebrosum* the stylet has a proximal funnel surrounded by three sphincters and an oblique distal end. Moreover, it is the only species within the group that lacks eyes. The combination of these features unambiguously differentiates *P. tenebrosum* from *P. cubanum* **sp. n.,** which has eyes, a single proximal sphincter around the funnel of the stylet, and a stylet with a rounded distal end.

Clade '*cochleare*' of *Promesostoma* (Fig. 22) encompasses two species that Karling (1967) included in two different morphological groups (*P. cochleare* and *P. maculosum*). In both species, the stylet is positioned caudal to the pharynx, a copulatory bursa is present, and a seminal receptacle is absent, a combination of features that also occurs in species from other clades. The same combination of features is shown by *P. toryne* **sp. n.**, which has a distally split stylet. Therefore, we hypothesise that this species belongs to clade '*cochleare*'. A stylet with a distally split end is also found in *P. balticum* Luther, 1918; *P. bipartitum* Ax, 1956; *P. furcatum* Armonies, 2023; *P. paracochlearis* Ax, 1952; and *P. wehrenbergi* Armonies, 2018. Because of this combination of characters, we conjecture that the previously mentioned species belong to clade '*cochleare*'. However, *P. balticum* has a seminal receptacle, distinguishing it from the other species mentioned above.

The species belonging to clade '*cochleare*' differ from each other as to stylet length and relative position of the distal split in the stylet (see Armonies, 2018, 2023). The largest stylet occurs in *P. paracochleare* (210–233 µm; Ax, 1952) and the smallest in *P. bipartitum* (80 µm; Ax, 1956). The stylet of *P. toryne* **sp. n.** (109 µm long) is of the same length as that in *P. furcatum* and similar to that of *P. wehrenbergi* (110–112 µm). Stylet length highly varies in *P. balticum* (55–135 µm; Luther, 1918) and *P. cochleare* (120–155 µm; Karling, 1935; Ax, 1952; Luther, 1962). The fact that the stylet splits near its midpoint is characteristic for *P. toryne* **sp. n.**, *P. bipartitum*, and *P. wehrenbergi*, whereas it splits more distally in *P. furcatum*. Furthermore, the stylet of *P. toryne* **sp. n.** is spoon-shaped distally, which, apart from this species, is only the case in *P. bipartitum*. However, both species can easily be distinguished from each other as *P. bipartitum* has paired seminal vesicles and an interposed prostate vesicle, whereas *P. toryne* **sp. n.** has a single seminal vesicle and a free prostate vesicle, the last feature being unique within the genus. The stylet of *P. furcatum* differs from that of *P. toryne* **sp. n.** in its proximal S-shaped end and the fact that the branched plate surrounds the main tubular stylet and does not reach its distal end. The lack of eyes also differentiates *P. toryne* **sp. n.** from *P. bipartitum*, *P. paracochleare*, and *P. wehrenbergi*; however, *P. balticum* also lacks eyes.

The sister group of clade '*cochleare*' comprises a trichotomy of *P. neglectum* and two monophyletic clades ('*roseapharynx*' and '*marmoratum*'; Fig. 22). Karling (1967) placed *P. neglectum* in a group of species characterised by a proximally coiled stylet, four of which form the clade '*marmoratum*'. In addition to this typical stylet, these four species also share a well-developed male copulatory bursa and a relatively small seminal receptacle, incorporated in, or positioned next to, the bursa. Other species showing this unique combination of traits are *P. ensifer* (Uljanin, 1870) Pereyaslawzewa, 1892; *P. gracile* Ax, 1951; *P. karlingi* Ehlers, 1974; *P. kristenseni* Ax, 1993; and *P. sartagine* Ax & Ehlers, 1973. However, Karling (1967) excluded *P. gracile* from this group because its stylet is curved, not coiled, and excluded *P. ensifer* from his discussion because of the lack of detailed morphology of the stylet. The phylogenetic analyses, however, cannot unambiguously confirm the position of *P. neglectum* within this group, as its position remains unresolved. According to Karling (1967), *P. neglectum* is different from the other species in this group because of the presence of a glandular organ opening near the aperture of the male atrium to the common atrium, as occurs in *P. norvegicum* and *P. spiriferum* Karling, 1967. Unfortunately, these species were not included in the phylogenetic analysis and future studies will be needed to reveal if the presence of this glandular organ is a synapomorphy of these three species.

Because of its morphological resemblance with some species in clade '*marmoratum*' (*P. caligulatum* and *P. meixneri*), it can be conjectured that also *P. panamaense* **sp. n.** belongs to this clade. Indeed, *P. panamaense* **sp. n.** also possesses a proximally coiled stylet and a copulatory bursa. However, the absence of a seminal receptacle in *P. panamaense* **sp. n.** distinguishes it from the other species in clade '*marmoratum*'. Other species resembling *P. panamaense* **sp. n.** are *P. infundibulum*, and *P. minutum*; the former, however, lacks a copulatory bursa. The stylet is very long and involves several coils in *P. meixneri* (710–720 µm) and two to three coils in *P. caligulatum* (1.170–1.350 µm) and *P. infundibulum* (296–307 µm long). In *P. panamaense* **sp. n.** and in *P. minutum*, the stylet involves a single coil (Fig. 13e). *Promesostoma panamaense* **sp. n.** can be

distinguished from the latter (and the other three) species as its stylet is much shorter (~ 88 µm) compared to the 430–490 µm reported for *P. minutum* (Ax, 1956). *Promesostoma panamaense* **sp. n.** also differs from *P. minutum* in the morphology of the distal end of the stylet, which bears a wing and a pointed projection in the later species. In *P. panamaense* **sp. n.**, the stylet end is oblique or rounded and no wing is present.

From the above, it is still unclear which morphological characters are indeed diagnostic for clade '*marmoratum*' and which species can be included there. This can only be solved by incorporating more species into the molecular analyses and/or additional morphological markers.

The two species with a known morphology included in clade '*roseapharynx*' (*P. dipterostylum* and *P. roseapharynx* **sp. n.**) each possess a well-developed male copulatory bursa. Apart from that, it is difficult to pinpoint morphological characters diagnostic for this clade. Moreover, this feature is not unique for these two species (see discussion above). In *P. roseapharynx* **sp. n.**, the prostate vesicle is oriented forward, entering the stylet, which shows a proximal > 90° bent. This is also the case in six other species of *Promesostoma*: *P. alaskanum* Ax & Armonies, 1990; *P. dennisalleni* Ax, 1995; *P. digitosum* Ax, 1995; *P. fibulatum* Ax & Armonies, 1987; *P. nynaesiense* Karling, 1957; and *P. teshirogii* Ax, 1992. In two of these species, *P. digitosum* and *P. fibulatum*, the stylet is distally branched, distinguishing it clearly from the unbranched stylet of *P. roseapharynx* **sp. n.** Measuring ~ 177 µm in length, the stylet of *P. roseapharynx* **sp. n.** is shorter than that *P. nynaesiense* (363–399 µm), *P. alaskanum* (250 µm), and *P. teshirogii* (200 µm), but larger than that of *P. dennisalleni* (120–130 µm long). Furthermore, the stylet of *P. dennisalleni* shows an asymmetric thickening of its distal opening (Ax, 1995) and it is proximally rolled up in *P. alaskanum* (Ax & Armonies, 1990), which is not the case in *P. roseapharynx* **sp. n.** In *P. teshirogii*, the copulatory bursa is elongated, oriented forward, and reaches the caudal part of the brain, whereas in *P. roseapharynx* **sp. n.**, it is globular, located just anterior to the pharynx and is oriented sideways.

The stylet of *Promesostoma baculum* **sp. n.** is approximately 90° bent proximally and in that respect comparable with that of *P. bilobatum* Ax & Armonies, 1987; *P. dipterostylum* Karling, 1967; *P. nynaesiense* Karling, 1957; and *P. teshirogii*. The stylet of *P. baculum* **sp. n.** does not carry distinctive ornamentations, such as the distal spoon-shaped oval plates in *P. bilobatum* (see Ax & Armonies, 1987), or the proximal wing-like structures in *P. dipterostylum* (see Karling, 1967). The stylet of *P. baculum* **sp. n.** is 93 µm long, much shorter than that of *P. nynaesiense* (363–399 µm), *P. dipterostylum* and *P. teshirogii* (~ 200 µm), and *P. bilobatum* (~ 210 µm).

Ceratopera

The morphological similarities between *C. gracilis* (Graff, 1882) Den Hartog, 1964, and *C. paragracilis* (Ehlers & Ax, 1974) are also reflected in the phylogenetic relationships of both species, which form a fully supported clade. Specimens of *C. paragracilis* collected in Cuba are similar in overall morphology to those in other populations of this species. However, some intraspecific variability has been reported (Karling, 1978), to which we here add new data. With a length of ~ 51 µm, the stylet of the Cuban specimens is longer than that reported in populations from Bermuda (40 µm; Karling, 1978) and the Galapagos (36 µm; Ehlers & Ax, 1974). These measurements recorded in literature considered the stylet as a whole, including the mantle in all instances. The bursal appendage also varies in length; in the specimen from Bermuda, it is 90 µm long (the bursal part being 60 µm long; the tubular part 30 µm) (Karling, 1978), while Ehlers and Ax (1974) mention a total length of 45 µm in the specimens from the Galapagos.

Also, the populations in Cuba differ substantially from each other as to the length of the bursal appendage, ranging from ~ 62 µm in the population from Bahía Larga to 105 µm in the specimen from Bueycabón. Moreover, the specimen from Bueycabón shows a bursal appendage with two distal tubes, as was also mentioned for the specimens from Bermuda (Karling, 1978). In the populations from Bahía Larga and Galapagos Islands (Ehlers & Ax, 1974), only one distal tube is present. Considering these size differences and the wide distribution of the species, it might be that *C. paragracilis* comprises a species complex. Also in *C. axi*, a variable number of distal tubes is reported, which even lead to the recognition of two different species: *C. axi* (1 distal tube) and *C. bifida* Ehlers & Ax, 1974 (2 distal tubes). However, Willems et al. (2004a) considered both species to be one and the same (*C. axi*), a view we follow here. Yet, Willems et al. (2005b) and other authors (e.g. Van Steenkiste & Leander, 2018) also expressed the possibility that *C. axi* is a species complex. Following this logic, and because the number of specimens is low for all sampled populations, we opt to keep all populations of *C. paragracilis* in one species for the time being. To bring more clarity, an extensively sampled dataset including sufficiently fast-evolving markers and representing specimens of all species from different localities is needed.

Parapharyngiella

As well as in the analysis by Van Steenkiste et al. (2013) and Van Steenkiste and Leander (2018), the position of *Parapharyngiella* as sister group to the other representatives of Trigonostominae is well supported in our current phylogeny. Three species of *Parapharyngiella* cluster in a

fully supported clade as well as cluster three specimens of *P. caribbaea*.

Trigonostomum

Willems et al. (2004b) revised the genus *Trigonostomum*, which they subdivided into three groups (1A, 1B, and 2) based on the morphology of both the stylet and bursal appendage. Representatives of all three group were included in our phylogenetic analyses. For group 1A, this is *T. venenosum*, for 1B these are *T. penicillatum*, *T. watsoni*, *T. vanmecheleni*, *T. tillicum*, and *T. sinensis*, and for group 2, these are *T. armatum*, *T. franki*, *T. setigerum*, and *T. tori*. Also one species with an aberrant morphology was included: *T. denhartogi*. More recently, Hu et al. (2019) reviewed the grouping system for *Trigonostomum* and proposed its differentiation in four groups (type 1 to type 4). Our phylogenetic analysis largely corresponds with the analysis of Hu et al. (2019); however, we were more conservative proposing species groups.

In the newly presented phylogeny, three clades of *Trigonostomum* are recovered (Fig. 23), whereas *T. penicillatum* is the sister species to a monophyletic clade formed by these three clades. Only group 2 of Willems et al. (2004b) forms a monophyletic clade in our analysis (see clade '*armatum*' in Fig. 23). All these species are characterised by a stylet showing a number of spirals (½ in *T. franki* to 5 ½ in *T. tori*) and the mantle following the course of the stylet. In this group, the bursal appendage consists of two tubules attached by a ring to the bursa, with both tubes coiled over 360° (for more details see Willems et al., 2004b). Although we named the species groups supported by our phylogenetic analysis, we are not proposing a new classification system for *Trigonostomum* due to the similarity of our results with those of Hu et al. (2019). Particularly, we refrain to propose a species group to *T. penicillatum* because it is the only species of the group type 1 of Hu et al. (2019) included in phylogenetic analyses.

Trigonostomum armatum is one of several known rhabdocoel species with an apparently worldwide distribution (see Willems et al., 2004b and references therein). However, our results suggest that *T. armatum* may in fact be a species complex. The two specimens included in the analysis do not constitute a monophyletic group, as the population from France is recovered as the sister species to the rest of clade 2, including a population of *T. armatum* from the Caribbean. Some marked morphological differences do exist between specimens from different populations of *T. armatum* (summarised in Willems et al., 2004b). In specimens from the northern Atlantic (France), eastern Australia, and New Caledonia, pigmentation is lacking, whereas anterior dark spots are found in specimens from Cuba, Curaçao, and the southern Atlantic. The stylet of the Cuban specimens (333–369 µm) is more similar in length to that of the specimens from Curaçao (274–378 µm) and New Caledonia (386 µm). It is larger than specimens from France (158–196 µm) and Eastern Australia (183 µm long). The largest stylet is recorded for one specimen from the Southern Atlantic (434 µm). Similarly, the bursal appendage varies in length: 84–100 µm in the specimens from Cuba, 100–108 µm in the specimens from Curaçao, 127 µm in the specimen from New Caledonia, and 149 µm in the specimen from the southern Atlantic. However, it is necessary to include more populations in the phylogenetic analysis and perhaps additional, fast-evolving markers to elaborate the taxonomy of this species complex.

Clade 3 includes three recently described species of *Trigonostomum* which are very similar to each other. *Trigonostomum tillicum* is inferred as the sister to the clade containing *T. vanmecheleni* and *T. sinensis*. Until now, *T. vanmecheleni* was only known from channels of Venice (Italy), but it is now recorded for the first time from the Caribbean coast of Cuba. The morphology of individuals from both populations is indistinguishable. *Trigonostomum sinensis*, described from China, is very similar to *T. vanmecheleni*. Measures of the male hard structures of *T. sinensis* are within the range of these structures in *T. vanmecheleni*. Also the bursal appendage is very similar in both species, albeit slightly smaller in *T. sinensis*. The only discernible morphological difference that can be used to differentiate between both species is the angle of the proximal curvature of the stylet (120° in *T. sinensis* vs 90° in *T. vanmecheleni*) (for details see Hu et al., 2019). However, we consider the taxonomic value of this trait questionable and subject to the interpretation of authors when measuring the structures. In fact, both stylets appear almost identical when comparing their outline shape. Moreover, when considering the genetic distance, *T. sinensis* and *T. vanmecheleni* exhibit the smallest disparity among all species of *Trigonostomum* (ML distance 0.001). This is nearly ten times smaller than the closest lower distance observed between *T. tillicum* and *T. sinensis*/*T. vanmecheleni* (ML distance 0.010). Based on the morphological and genetic distance data, we propose the synonymisation of *T. sinensis* with *T. vanmecheleni*.

All the species in clade 3 are characterised by the sclerotised parts of the copulatory organ consisting of two mantle plates that run parallel to each other and differ in width—the thinner plate located in between the wider plate and the tubiform stylet. Moreover, all species have a bursal organ that consists of a heavily coiled tube that distally splits into a number of finer tubes. Both features could be morphological apomorphies for this clade.

Because of lack of material, *T. yoandrisi* **sp. n.** could not be included in the phylogenetic analyses. The morphology of the atrial organs of this species is similar to those of the species included in group 1B of Willems et al. (2004b), but these species are now spread out over our clades 1 and 3. *Trigonostomum yoandrisi* **sp. n.** shows the two typical

features (apomorphies?) mentioned above for clade 3, and therefore, we provisionally consider it to belong to that clade. In what follows, we will compare the new species with the species of group 1B of Willems et al. (2004b).

Trigonostomum yoandrisi **sp. n.** differs from all other species in group 1B in the shape of its stylet, which is proximally funnel-shaped and does not bend. Moreover, the stylet of *T. yoandrisi* **sp. n.** (~24 µm) is considerably shorter than that of all other species of the group, and the mantle of *T. yoandrisi* **sp. n.** forms two plates, an organisation only found in *T. mirabile* and *T. nataschae* (Willems et al., 2004b). However, in *T. yoandrisi* **sp. n.**, one of the plates is X-shaped and forms two distal sharp projections, whereas, in the other two species both triangular plates form a single distal projection.

The bursal appendage of all species of group 1B of Willems et al. (2004b) shows an obvious striation, which is not the case in *T. yoandrisi* **sp. n**. The bursal appendage of *T. yoandrisi* **sp. n.** consists of a proximal part and two distally-coiled tubes (~360°) of ~48 µm long, which is comparable to the situation in *T. watsoni*. However, in *T. watsoni*, the bursal appendage is ~70 µm long and the tubes are coiled more than 360°. The other species of this group also possess a bursal appendage larger than that of *T. yoandrisi* **sp. n.** and with a different number of tubes. The bursal appendage in *T. breitfussi* is 24 µm long and branches distally in 9 or 10 tubes; in *T. coronatum*, it is 78 µm long with a proximal, crown-like part and one terminally-bent, striated tube; in *T. lilliei*, it is ~97 µm long, heavily coiled, distally split into five or six tubes; in *T. vanmecheleni*, it is ~115 µm long, and distally split into six finer tubes; in *T. mirabile*, it is 66 µm long, proximally with a barrel-like casing and approximately ten distal tubules; in *T. nataschae*, it is ~65 µm long, with proximal barrel-like part and very narrow tubules, forming two bundles of curved tubules distally; and it is ~65 µm long, with a barrel-like casing and ~12 distal tubules in *T. penicillatum* (see Willems et al., 2004b). The unique morphology of the stylet (funnel-shaped, lacking the proximal bend) and mantle plates (one of which is X shaped with two distal tips) warrants the description as a new species for *T. yoandrisi* **sp. n.**

Adenorhynchidae Ax & Heller, 1970 status novus

Updated diagnosis (after Ax & Heller, 1970). Representatives of Thalassotyphloplanida lacking eyes; female genital canal simple, an unpaired seminal receptaculum is present (except in *Tvaerminnea direceptacula* Ehlers et al., 1994 where there is a pair, and *Listea simplex* Ax & Heller, 1970 where there is none), a bursa may or may not be present, paired ovaries lying caudal; testes anterior to the pharynx (except in *Litucivis*) and male copulatory organ with a funnel-shaped stylet.

Type genus. *Adenorhynchus* Luther, 1948, designated by Ax and Heller (1970).

Contained taxa. *Cilionema*, *Coronhelmis*, *Tvaerminnea*, *Adenorhynchus* Meixner, 1938, *Listea* Ax & Heller, 1970, *Litucivis* Ax & Heller, 1970, and *Scoliopharyngia* Ehlers et al., 1994.

Considering the fact that we suppressed Brinkmanniellinae and that other taxa previously included in this subfamily, except *Gaziella*, cluster in a fully supported clade in our phylogenetic analysis together with *Litucivis serpens*, we raise Adenorhynchinae to family rank (Adenorhynchidae **status novus**). We also include in the new family all other members of Adenorhynchinae (*Adenorhynchus*, *Listea*, and *Scoliopharyngia*). The only representative of Adenorhynchinae included in the phylogenetic analyses was *L. serpens*. However, Adenorhynchinae is a morphologically homogeneous group (Ax & Heller, 1970). These characteristics are also present in the brinkmanniellinids transferred to Adenorhynchidae **status novus.** Furthermore, all representatives of Adenorhynchidae **status novus** possess the testes anterior to the pharynx (except in *Litucivis*, where the testes are caudally located to the pharynx, a plesiomorphic condition).

Other representatives of the suppressed Brinkmanniellinae also share most features of Adenorhynchidae **status novus.** However, considering the diversity of the group, they are retained within Promesostomidae until new molecular information is available.

Supplementary Information The online version contains supplementary material available at https://doi.org/10.1007/s13127-023-00623-w.

Acknowledgements Mrs. Natascha Steffanie is thanked for making the histological sections, and Mrs. Ria Vanderspikken is thanked for her invaluable administrative support in the lab and for her help in organising the collecting campaigns. Wolfgang Sterrer kindly supported the collecting in Ciénaga de Zapata. We thank Prof. Dr María Teresa Aguado from Georg-August-Universität Göttingen for sending the holotype of *Neokytorhynchus pacificus* for our study.

Author contribution All authors contributed to the study conception and design. Material preparation, data collection, and analysis were performed by Yander L. Diez, Marlies Monnens, Arlien Wuyts, Patrick Reygel, and Tom Artois. The first draft of the manuscript was written by Yander L. Diez, and all authors commented on previous versions of the manuscript. All authors read and approved the final manuscript.

Funding Open Access funding enabled and organized by Projekt DEAL. This work was partially supported by VLIR-UOS, Belgium, under the project 'Risk mitigation plan for biodiversity and food production to face climatic change in the eastern region of Cuba'. YLD was supported by BOF-Hasselt University, Belgium, under grant BOF15BL09, and currently by a Georg Forster Research Fellowship (Alexander von Humboldt Foundation, Germany, grant number 3.2 — CUB — 1226121 — GF-P). MM was supported by a PhD fellowship from the Research Foundation Flanders, Belgium (FWO, grant number 1141817N). The research leading to results presented in this publication was carried out with infrastructure funded by EMBRC Belgium — FWO project GOH3817N.

Data availability All new sequences generated during this study are available in GenBank. Supplementary Information is provided in the online version of this paper in Supplementary Table 1.

Declarations

Ethics approval No approval or research ethics commithees was required to accomplish the goals of this study since experimental work was conducted on unregulated invertebrate species.

Conflict of interest The authors declare no competing interests.

References

Altschul, S. F., Gish, W., Miller, W., Myers, E. W., & Lipman, D. J. (1990). Basic local alignment search tool. *Journal of Molecular Biology, 215*, 403–410. https://doi.org/10.1016/S0022-2836(05)80360-2

Armonies, W., & Hellwig, M. (1987). Neue Plathelminthes aus dem Brackwasser der Insel Sylt (Nordsee). *Microfauna Marina, 3*, 249–260.

Armonies, W. (2017). Long-term change of meiofaunal species composition in a sandy beach, with description of 7 new species of Platyhelminthes. *Helgoland Marine Research, 71*, 12. https://doi.org/10.1186/s10152-017-0492-0

Armonies, W. (2018). Uncharted biodiversity in the marine benthos: The void of the smallish with description of ten new Platyhelminth taxa from the well-studied North Sea. *Helgoland Marine Research, 72*(18), 1–29. https://doi.org/10.1186/s10152-018-0520-8

Armonies, W. (2023). Platyhelminth fauna of the Island of Sylt: A meta-analysis of distributional patterns and description of 19 new species. *Marine Biodiversity, 53*, 17. https://doi.org/10.1007/s12526-022-01309-w

Artois, T., Schockaert, E., Beenaerts, N., & Reygel, P. (2013) *Trigonostomum vanmecheleni* sp. nov., a new species of Trigonostomidae (Rhabdocoela: Dalytyphloplanida) from the channels of Venice (Italy), with discussion on the *T. lilliei* species group. *Italian Journal of Zoology*, *80*(1), 46–51. https://doi.org/10.1080/11250003.2012.754058

Attems, C. G. (1896). Beitrag zur kenntnis der rhabdocoelen turbellarien Helgolands. *Wissenschaftliche Meeresuntersuchungen Der Kommission Abteilung Kiel, 2*(1), 219–232.

Attems, C. G. (1897). Beitrag zur Meeresfauna von Helgoland. VI. Beitrag zur Kenntnis der rhabdocoelen Turbellarien Helgolands. *Wissenschaftliche Meeresüntersüchungen, Neue Folge, 2*, 219–232.

Ax, P., & Armoines, W. (1987). Amphiatlantic identities in the composition of the boreal brackish water community of Plathelminthes. A comparison between the Canadian and European Atlantic coast. *Microfauna Marina, 3*, 7–80.

Ax, P., & Armonies, W. (1990). Brackish water plathelminthes from Alaska as evidence for the existence of a boreal brackish water community with circumpolar distribution. *Microfauna Marina, 6*, 7–109.

Ax, P., & Ehlers, U. (1973). Interstitielle fauna von Galapagos - 3. Promesostominae (Turbellaria, Typhloplanoida). *Mikrofauna Des Meeresbodens, 23*, 203–216.

Ax, P., & Heller, R. (1970). Neue Neorhabdocoela (Turbellaria) vom sandstrand der Nordsee-inseln sylt. *Mikrofauna Des Meeresbodens, 2*, 55–98.

Ax, P. (1951). Die Turbellarien des Eulitorals der Kieler Bucht. *Zoologische Jahrbücher. Abteilung Für Systematik, Ökologie Und Geographie Der Tiere, 80*, 277–378.

Ax, P. (1952). Turbellarien der Gattung *Promesostoma* von den deutschen Küsten. *Kieler Meeresforschungen, 8*(2), 218–226.

Ax, P. (1956). Turbellarien der Gattung *Promesostoma* von der französischen Atlantikküste. *Kieler Meeresforschungen, 12*(1), 110–113.

Ax, P. (1992). *Promesostoma teshirogii* n. sp. (Plathelminthes, Rhabdocoela) aus Brackgewässern von Japan. *Microfauna Marina, 7*, 159–165.

Ax, P. (1993). *Promesostoma*-Arten (Plathelminthes, Rhabdocoela) von Grönland. *Microfauna Marina, 8*, 153–162.

Ax, P. (1995). New *Promesostoma*-species (Rhabdocoela, plathelminthes) from the north inlet salt marsh of Hobcaw Barony, South Carolina, USA. *Microfauna Marina, 10*, 313–318.

Ax, P. (2008). *Plathelminthes aus Brackgewässern der Nordhalbkugel. Abhandlungen der Mathematisch-naturwissenschaftlichen Klasse, Jahrgang 2008, 1*. Mainz, *696*.

Benson, D. A., Karsch-Mizrachi, I., Clark, K., Lipman, D. J., Ostell, J., & Sayers, E. W. (2012). GenBank. *Nucleic Acids Research, 40*, D48–D53. https://doi.org/10.1093/nar/gkr1202

Boyko, C. B. (1996). Catalog of recent type specimens in the Department of Invertebrates, American Museum of Natural History. III. "Parasitica" (Phyla Platyhelminthes, Rhombozoa, and Pentastomida) and Gastrotricha (Supplement). *American Museum Novitates, 3174*, 1–59.

Brusa, F., Ponce de Leon, R., & Damboranea, C. (2006). A new *Paravortex* (Platyhelminthes, Dalyellioida) endoparasite of *Mesodesma mactroides* (Bivalvia, Mesodesmatidae) from Uruguay. *Parasitology Research, 99*(5), 566–571. https://doi.org/10.1007/s00436-006-0193-0

Brusa, F., Vázquez, N., & Cremonte, F. (2011). Paravortex panopea n. sp. (Platyhelminthes: Rhabdocoela) on clams from the northern Patagonian coast, Argentina: Pathogeny and specificity. Helminthologia, 48 (2), 94–100. https://doi.org/10.2478/s11687-011-0016-4

Cannon, L. R. G. (1981). Endosymbiotic Umagillids (Turbellaria) from Holothurians of the Great Barrier Reef. *Zoologica Scripta, 11*(3), 173–188.

Cannon, L. R. G., & Lester, R. J. G. (1988). Two turbellarians parasitic in fish. *Diseases of Aquatic Organisms, 5*, 15–22.

Castresana, J. (2000). Selection of conserved blocks from multiple alignments for their use in phylogenetic analysis. *Molecular Biology and Evolution, 17*, 540–552. https://doi.org/10.1093/oxfordjournals.molbev.a026334

De Clerck, G. G., & Schockaert, E. R. (1995). Two peculiar new genera of Typhloplanoida from the Western Indian Ocean. *Hydrobiologia, 305*, 3–9.

Den Hartog, C. (1964). A preliminary revision of the Proxenetes group (Trigonostomidae, Turbellaria) 1–3. *Koninklijke Nederlandse Akademie Van Wetenschappen - Amsterdam Proceedings Series C, 67*(5), 371–407.

Diez, Y. L., Reygel, P., & Artois, T. (2018). *Parapharyngiella caribbaea* n. sp., a new species of Trigonostomidae (Rhabdocoela; Platyhelminthes) from Cuba, with a taxonomical reassessment of the genus. *Tropical Zoology*, *31*(1), 34–43. https://doi.org/10.1080/03946975.2017.1395258

Diez, Y. L., Sanjuan, C., Bosch, C., Catalá, A., Monnens, M., Curini-Galletti, M., & Artois, T. (2023). Diversity of free-living flatworms (Platyhelminthes) in Cuba. *Biological Journal of the Linnean Society*. https://doi.org/10.1093/biolinnean/blad041

Edgar, R. C. (2004). MUSCLE: Multiple sequence alignment with high accuracy and high throughput. *Nucleic Acids Research, 32*, 1792–1797. https://doi.org/10.1093/nar/gkh340

Ehlers, U., & Ax, P. (1974). Interstitielle fauna von Galapagos - 8. Trigonostominae (Turbellaria, Typhloplanoida). *Mikrofauna Des Meeresbodens, 30*, 641–671.

Ehlers, U., & Ehlers, B. (1981). Interstitielle Fauna von Galapagos XXVII. Byrsophlebidae, Promesostomidae Brinkmanniellinae, Kytorhynchidae (Turbellaria, Typhloplanoida). *Mikrofauna Des Meeresbodens, 83*, 83–113.

Ehlers, U., & Sopott-Ehlers, B. (1989). Drei neue interstitielle Rhabdocoela (Plathelminthes) von der französischen Atlantikküste. *Microfauna Marina, 5*, 207–218.

Ehlers, U. (1972). Systematisch-phylogenetische untersuchungen an der familie Solenopharyngidae (Turbellaria, Neorhabdocoela). *Mikrofauna Des Meeresbodens, 11*, 3–78.

Ehlers, U. (1974). Interstitielle Typhloplanoida (Turbellaria) aus dem litoral der nordseeinsel sylt. *Mikrofauna Des Meeresbodens, 49*, 427–526.

Ehlers, U., Müller, B., & Franke, M. (1994). Three new species of the Typhloplanoida (Plathelminthes, Rhabdocoela) from the Island of Sylt (North Sea). *Microfauna Marina, 9*, 313–332.

Fernández, F. A, Corrada, R. I., & Armenteros, M. (2015). Variaciones de la infracomunidad parásita durante la ontogenia de *Chromis cyanea* (Perciformes: Pomacentridae) en la costa norte de La Habana, Cuba. *Revista de Biología Tropical*, *63*(3), 717–726. https://doi.org/10.15517/rbt.v63i3.15583

Findenegg, I. (1924). Beiträge zur Kenntnis der Familie Typhloplanidae. *Zoologischen Anzeiger, 61*, 19–30.

Gamble, F. W. (1893). Contributions to a knowledge of British marine Turbellaria. *Microscopical Science, 34*, 433–528.

Gamble, F. W. (1900). Report on the Turbellaria of Valencia Harbour. *Proceedings of the Royal Irish Academy, 5*, 812.

Gobert, S., Armonies, W., Diez, Y. L., Jouk, P., Monnens, M., Revis, N., Reygel, P., Smith J. III, Van Steenkiste, V., & Artois, T. (2022). *Orostylis* gen. nov., a new genus of Dalytyphloplanida with seven new species (Platyhelminthes: Rhabdocoela). *Zootaxa*, *5115*(1), 29–46. https://doi.org/10.11646/zootaxa.5115.1.2

Guindon, S., Dufayard, J. -F., Lefort, V., Anisimova, M., Hordijk, W., & Gascuel, O. (2010). New algorithms and methods to estimate maximum-likelihood phylogenies: Assessing the performance of PhyML 3.0. *Systematic Biology*, *59*(3), 307–321. https://doi.org/10.1093/sysbio/syq010

Hertel, L. A., Duszynski, D. W., & Ubelaker, J. E. (1990). Turbellarians (Umagillidae) from Caribbean Urchins with a description of *Syndisyrinx collongistyla* n. sp. *Transactions of the American Microscopic Society*, *109*(3), 273–281. https://doi.org/10.2307/3226798

Hoang, D. T., Chernomor, O., Von Haeseler, A., Minh, B. Q., & Vinh, L. S. (2017). UFBoot2: Improving the ultrafast bootstrap approximation. *Molecular Biology and Evolution, 35*(2), 518–522. https://doi.org/10.1093/molbev/msx281

Hu, X. -Z., Chen, Y. -S., Zhong, L. -H., Xie, Y. -H., Feng, W. -T., Zhang, Y., & Wang, A. -T. (2019). Two new species of Rhabdocoela (Polycystididae and Trigonostomidae) from China. *Zootaxa*, *4695*(4), 351–366. https://doi.org/10.11646/zootaxa.4695.4.3

Jensen, O. S. (1878). *Turbellaria ad litora Norvegiae occidentalia. Turbellaria ved Norges vestkyst*. JW Eided Bogtrykkeri, Bergen, 97 pp.

Jondelius, U. (1996). Three Echinoderm inhabiting flatworms (Platylminthes, Rhabdocoela) from Western Australia. *Belgian Journal of Zoology, 126*(1), 37–48.

Jones, E. R. (1938). Observations on some lower Turbellaria of the United States. *The Collecting Net, 13*(114), 109–110.

Kalyaanamoorthy, S., Minh, B. Q., Wong, T. K. F., von Haeseler, A., & Jermiin, L. S. (2017). ModelFinder: Fast model selection for accurate phylogenetic estimates. *Nature Methods, 14*(6), 587–589. https://doi.org/10.1038/nmeth.4285

Karling, T. G. (1931). Untersuchungen über Kalyptorhynchia (Turbellaria Rhabdocoela) aus dem brackwasser des finnischen meerbusens. *Acta Zoologica Fennica, 11*, 1–67.

Karling, T. G. (1935). Mitteilungen über Turbellarien aus dem Finnischen Meerbusen 1. *Dalyellia nigrifrons* n. sp. 2. *Promesostoma cochlearis* n. sp. *Memoranda Societatis pro Fauna Et Flora Fennica, 10*, 289–395.

Karling, T. G. (1957). Drei neue Turbellaria Neorhabdocoela aus dem Grundwasser der schwedischen Ostseeküste. *Kungl Fysiograf Saellskap Lund Foerh, 27*(3), 25–33.

Karling, T. G. (1967). On the genus *Promeosostoma* (Turbellaria), with descriptions of four new species from Scandinavia and California. *Sarsia, 29*, 257–268.

Karling, T. G. (1978). Anatomy and systematics of marine turbellaria from Bermuda. *Zoologica Scripta, 7*, 225–248. https://doi.org/10.1111/j.1463-6409.1978.tb00605.x

Karling, T. G. (1985). Revision of Byrsophlebidae (Turbellaria Typhloplanoida). *Annales Zoologici Fennici, 22*, 105–116.

Karling, T. G. (1986). Free-living marine Rhabdocoela (Platyhelminthes) from the N. American Pacific coast. With remarks on species from other areas. *Zoologica Scripta*, *15*(4), 201–219. https://doi.org/10.1111/j.1463-6409.1986.tb00223.x

Karling, T. G., Mack-Fira, V., & Dörjes, J. (1972). First report on marine microturbellarians from Hawaii. *Zoologica Scripta, 1*(5), 251–269. https://doi.org/10.1111/j.1463-6409.1972.tb00575.x

Katoh, K., & Standley, D. M. (2013). MAFFT Multiple Sequence Alignment Software Version 7: Improvements in performance and usability. *Molecular Biology and Evolution, 30*(4), 772–780. https://doi.org/10.1093/molbev/mst010

Katoh, K., Rozewicki, J., & Yamada, K. D. (2017). MAFFT online service: Multiple sequence alignment, interactive sequence choice and visualization. *Briefings in Bioinformatics, 20*(4), 1160–1166. https://doi.org/10.1093/bib/bbx108

Kearse, M., Moir, R., Wilson, A., Stones-Havas, S., Cheung, M., Sturrock, S., Buxton, S., Cooper, A., Markowitz, S., Duran, C., Thierer, T., Ashton, B., Meintjes, P., & Drummond, A. A. (2012). Geneious Basic: An integrated and extendable desktop software platform for the organization and analysis of sequence data. *Bioinformatics, 28*(12), 1647–2164. https://doi.org/10.1093/bioinformatics/bts199

Lanfear, R., Calcott, B., Ho, S. Y. W., & Guindon, S. (2012). Partition Finder: Combined selection of partitioning schemes and substitution models for phylogenetic analyses. *Molecular Biology and Evolution, 29*, 1695–1701. https://doi.org/10.1093/molbev/mss020

Levinsen, G. M. R. (1879). Bidrag til kundskap om Grönlands Turbellaria-Fauna. *Videnskabelige Meddelelser Naturhistorisk Forening i København, 3*, 165–204.

Luther, A. (1918). Vorlaufiges verzeichnis der rhabdocolen und alloeocolen turbellarien Finnlands. *Meddelelanden Af Societas pro Fauna Et Flora Fennica, 44*, 47–52.

Luther, A. (1943). Untersuchungen an rhabdocoelen turbellarian - 4 - ber einige repräsentanten der familie Proxenetidae. *Acta Zoologica Fennica, 35*, 3–95.

Luther, A. (1946). Untersuchungen an rhabdocoelen turbellarien 5. *Ueber Einige Typhloplaniden. Acta Zoologica Fennica, 46*, 1–54.

Luther, A. (1948). Untersuchungen an rhabdocoelen turbellarien -7 - Uber einige marine Dalyellioida - 8 - Beitrage zur kenntnis der Typloplanoida. *Acta Zoologica Fennica, 55*, 3–122.

Luther, A. (1962). Die turbellarien ostfennoskandiens 3 Neorhabdocoela 1. Dalyellioida, Typhloplanoida: Byrsophlebidae und Trigonostomidae. *Fauna Fennica, 12*, 1–71.

Luther, A. (1963). Die turbellarien ostfennoskandiens 4 Neorhabdocoela 2. Typhloplanoida: Typhloplanidae. *Solenopharyngidae Und Carcharodopharyngidae. Fauna Fennica, 16*, 5–163.

Marcus, E. (1948). Turbellaria do Brasil. *Boletins Da Faculdade De Filosofia Cienciase Letras, Universidade De Sao Paulo Zoologia, 13*, 111–243.

Marcus, E. (1951). Turbellaria Brasileiros (9). *Boletins Da Faculdade De Filosofia Ciencias e Letras, Universidade De Sao Paulo Zoologia, 16*, 1–215.

Marcus, E. (1952). Turbellaria Brasileiros (10). *Boletins Da Faculdade De Filosofia Cienciase Letras, Universidade De Sao Paulo, 17*, 5–188.

Marcus, E. (1954). Turbellaria Brasileiros (11). *Papeis Avulsos Do Departamento De Zoologia Secretaria Da Agricultura Sao Paulo, 11*, 419–489.

Marcus, E. (1968). A new *Syndesmis* from Saint-Barthélemy, Lesser Antilles (Neorhabdocoela). *Studies on the Fauna of Curacao and Other Caribbean Islands, 25*, 134–139.

Meixner, J. (1924). Studien zu einer Monographie der Kalyptorhynchia und zum System der Turbellaria-Rhabdocoela. *Zoologischer Anzeiger, 60*, 89–105.

Meixner, J. (1925). Beitrag zur morphologie und zum system der Turbellaria-Rhabdocoela: 1. Die Kalyptorhynchia. *Zeitschrift Für Morphologie Und Ökologie Der Tiere, 3*, 255–343.

Meixner, J. (1938). 4. Turbellaria (Strudelwürmer). *Die Tierewelt Der Nord- Und Ostsee, 33*, 1–146.

Micoletzky, H. (1910). Die Turbellarienfauna des Golfes von Triest. *Zoologischen Institut Der Universität Wien, 18*, 167–182.

Miller, M. A., Pfeiffer, W., & Schwartz, T. (2010). Creating the CIPRES Science Gateway for inference of large phylogenetic trees. *Proceedings of the Gateway Computing Environments Workshop*, 1–8. https://doi.org/10.1109/GCE.2010.5676129

Nguyen, L.-T., Schmidt, H. A., von Haeseler, A., & Minh, B. Q. (2015). IQ-TREE: A fast and effective stochastic algorithm for estimating maximum-likelihood phylogenies. *Molecular Biology and Evolution, 32*(1), 268–274. https://doi.org/10.1093/molbev/msu300

Pereyaslawzewa, S. (1892). Monographie des Turbellaries de la Mer Noire. *Memoires De La Societe Des Naturalistes De La Nouvelle-Russie, 17*, 1–303.

Ponce de León, R., & Mañé-Garzón, F. (1979). *Collastoma wahli* n. sp. (Turbellaria, Rhabdocoela) simbionte del intestino de un sipúncula del Atlántico Sur. *Revista de Biologia del Uruguay*, *7*(2), 89–99.

Powers, P. B. A. (1936). Studies on the ciliates of sea urchins. A general survey occuring in Tortugas echinoids. *Papers from the Tortugas Laboratory of the Carnegie Institution of Washington, 29*, 205–326.

Purasjoki, K. J. (1945). Quantative untersuchungen uber die mikrofauna des meeresbodens in der umgebung der zoologischen station Tvarminne an der sudkuste Finnlands. *Societas Scientiarum Fennica, Commentationes Biologicae, 9*(14), 1–14.

Rambaut, A. (2006–2019). FigTree: Tree Figure Drawing Tool. Retrieved August 14, 2020, from http://tree.bio.ed.ac.uk/software/figtree/

Reisinger, E. (1929). Zum ductus genito-intestinalis-problem - 1. Uber primare geschlechtstrakt-darmverbindungen bei rahbdocoelen turbellarien. *Zeitschrift Fur Morphologie Und Okologie Der Tiere, 16*, 49–73.

Riedl, R. (1954). Neue turbellarien aus dem mediterranen Felslitoral Ergebnisse der Unterwasser-expedition AUSTRIA 1948–1949. *Zoologische Jahrbücher. Abteilung Für Systematik, Ökologie Und Geographie Der Tiere, 82*, 157–244.

Rieger, M. R. (1974). A new group of Turbellaria–Typhloplanoida with a proboscis and its relationship to Kalyptorhynchia. *In*: Riser, N.W., Morse, M.P. (Eds.), *Biology of the Turbellaria. Libbie H Hyman Memorial Volume* (pp. 23–62). Mc-Graw-Hill Company, New York.

Ronquist, F., Teslenko, M., Van Der Mark, P., Ayres, D. L., Darling, A., Höhna, S., ... & Huelsenbeck, J. P. (2012). MrBayes 3.2 efficient Bayesian phylogenetic inference and model choice across a large model space. *Systematic Biology*, *61*(3), 539–542. https://doi.org/10.1093/sysbio/sys029

Schmidt, O. (1852). Neue Rhabdocoelen aus dem nordischen und dem Adriatischen Meere. *Sitzungsberichte der Mathematisch-Naturwissenschaftlichen Classe der Kaiserlichen Akademie der Wissenschaften*, *9*, 490–505.

Schmidt, O. (1857). Zur Kenntnis der Turbellaria rhabdocoela und einiger anderer Wuermer des Mittelmeeres. *Sitzungsberichte der Kaiserliche Akademie der Wissenschaften, Wien, Mathematisch-Naturwissenschaftliche Klasse*, *23*(2), 347–366.

Schockaert, E. R., & Martens, P. M. (1985). Turbellaria from Somalia 3. *Lecithoepitheliata and Typhloplanoida. Monitore Zoologico Italiano, 20*(3), 27–41.

Schockaert, E. R. (1996). Turbellarians. In G. S. Hall (Ed.), *Methods for the examination of organismal diversity in soils and sediments* (pp. 211–225). CAB International.

Schultze, M. S. (1851). *Beiträge zur Naturgeschichte der Turbellarien*. Greifswald, 78 pp.

Southern, R. (1912). Clare Island Survey, Part 56 Platyhelmia. *Proceedings of the Royal Irish Academy, 31*, 18.

Southern, R. (1915). Turbellaria. In G. P. Farran (Ed.), *Results of a biological survey of Blacksod Bay, Co. Mayo* (pp. 33–35). HM Stationery Office.

Southern, R. (1936). Turbellaria of Ireland. *Proceedings of the Royal Irish Academy, 43*, 43–72.

Steinböck, O. (1931). *Marine Turbellaria. Zoology of the Faroes, 8*, 1–26.

Steinböck, O. (1938). *Marine Turbellaria. Zoology of Iceland, 2*, 1–26.

Stephenson, I., Van Steenkiste, N. W. L., & Leander, B. S. (2019). Molecular phylogeny of neodalyellid flatworms (Rhabdocoela), including three new species from British Columbia. *Journal of Zoological Systematics and Evolutionary Research, 57*(1), 41–56.

Strand, E. (1928). Miscellanea nomenclatorica zoologica et palaeontologica I-II. *Archiv Für Naturgeschichte, 92*(A8), 30–75.

Stunkard, H. W., & Corliss, J. O. (1951). New species of *Syndesmis* and a revision of the family Umagillidae Wahl, 1910 (Turbellaria: Rhabdocoela). *Biological Bulletin, 101*, 319–334.

Swofford, D. L. (2003). PAUP*. Phylogenetic analysis using parsimony (*and other methods). Version 4. Sinauer Associates, Sunderland.

Tessens, B., Janssen, T., & Artois, T. (2014). Molecular phylogeny of Kalyptorhynchia (Rhabdocoela, Platyhelminthes) inferred from ribosomal sequence data. *Zoologica Scripta, 43*(5), 519–530. https://doi.org/10.1111/zsc.12066

Trifinopoulos, J., Nguyen, L.-T., von Haeseler, A., & Minh, B. Q. (2016). W-IQ-TREE: A fast online phylogenetic tool for maximum likelihood analysis. *Nucleic Acids Research, 44*, W232–W235. https://doi.org/10.1093/molbev/msu300

Uljanin, W. (1870). Die Turbellarien der Bucht von Sebastopol. *Berichte Des Vereins Der Freunde Der Naturwissenschaften Zu Moskou, 4*, 1–96.

Van Steenkiste, N., Volonterio, O., Schockaert, E., & Artois, T. (2008). Marine Rhabdocoela (Platyhelminthes, Rhabditophora) from Uruguay, with the description of eight new species and two new genera. *Zootaxa*, *1914*, 1–33. https://doi.org/10.11646/zootaxa.1914.1.1

Van Steenkiste, N. W. L., & Leader, B. S. (2017). Molecular phylogeny of trigonostomine turbellarians (Platyhelminthes: Rhabdocoela: Trigonostomidae), including four new species from the Northeast Pacific Ocean. *Zoological Journal of the Linnean Society, 20*, 1–21. https://doi.org/10.1093/zoolinnean/zlx046

Van Steenkiste, N. W. L., & Leander, B. S. (2018). Species diversity of eukalyptorhynch flatworms (Platyhelminthes, Rhabdocoela) from the coastal margin of British Columbia: Polycystididae, Koinocystididae and Gnathorhynchidae. *Marine Biology Research, 14*(9–10), 899–923. https://doi.org/10.1080/17451000.2019.1575514

Van Steenkiste, N. W. L., & Leader, B. S. (2022). The molecular phylogenetic position of *Mariplanella piscadera* sp. nov. reveals a new major group of rhabdocoel flatworms: Mariplanellida status novus (Platyhelminthes: Rhabdocoela). *Organisms Diversity & Evolution*, *22*(3), 577–584. https://doi.org/10.1007/s13127-022-00542-2

Van Steenkiste, N. W. L., Herbert, E. R., & Leander, B. S. (2018). Species diversity in the marine microturbellarian *Astrotorhynchus bifidus* sensu lato (Platyhelminthes: Rhabdocoela) from the Northeast Pacific Ocean. *Molecular Phylogenetics and Evolution, 120*, 259–273. https://doi.org/10.1016/j.ympev.2017.12.012

Van Steenkiste, N. W. L., Tessens, B., Willems, W., Backeljau, T., Jondelius, U., & Artois, T. (2013). A comprehensive molecular phylogeny of Dalytyphloplanida (Platyhelminthes: Rhabdocoela) reveals multiple escapes from the marine environment and origins of symbiotic relationships. *PLoS ONE*, *8*(3), e59917. https://doi.org/10.1371/journal.pone.0059917

von Graff, L. (1882). *Monographie der Turbellarien I* (p. 442). Rhabdocoelida.

von Graff, L. (1905). Marine Turbellarien Orotavas und der Küsten Europas. Ergebnisse einiger, mit Unterstützung der Kaiserlichen Akademie der Wissenschaften in Wien (aus dem Legate Wedl) in den Jahren 1902 und 1903 unternommen Studienreise. *II. Rhabdocoela. Zeitschrift Fur Wissenschaftlige Zoologie, 83*, 68–148.

von Graff, L. (1911). Acoela, Rhabdocoela und Alloeocoela des Ostens de Vereinigden Staaten. Mit nachträgen zu den "Marinen turbellarien Orotavas und der küste europas. *Zeitschrift Für Wissenschaftliche Zoologie, 99*, 1–108.

von Graff, L. (1913). *Das Tierreich: Turbellaria II* (p. 484). Rhabdocoelida.

Wahl, B. (1906). Untersuchungen über den Bau der parasitischen Turbellarien aus der Familie der Dalyelliiden (Vorticiden). 1. Die Genera *Anoplodium*, *Graffilla* und *Paravortex*. *Sitzungsberichte Der Kaiserlichen Akademie Der Wissenschaften in Wien, 115*, 417–471.

Westblad, E. (1954). Some hydroidea and turbellaria from western Norway with description of three new species of turbellaria. *Publications from the Biological Station Bergen, 11*, 1–24.

Willems, W. R., Artois, T., Vermin, W., Backeljau, T., & Schockaert, E. (2004a). Reports on the free-living Platyhelminthes from Australia: Typhloplanoida, with the description of three new taxa. *Zoological Science, 21*(3), 333–341. https://doi.org/10.2108/zsj.21.333

Willems, W. R., Artois, T. J., Vermin, W. A., & Schockaert, E. R. (2004b). Revision of *Trigonostomum* Schmidt, 1852 (Platyhelminthes, Typhloplanoida, Trigonostomidae) with the description of seven new species. *Zoological Journal of the Linnean Society*, *141*(2), 271–296. https://doi.org/10.1111/j.1096-3642.2004.00124.x

Willems, W. R., Artois, T. J., Vermin, W., Backeljau, T., & Schockaert, E. R. (2005a). Reports on the free-living platyhelminthes from Australia: Typhloplanoida with the description of three new taxa. *Zoological Science, 21*(3), 333–341. https://doi.org/10.2108/zsj.21.333

Willems, W. R., Artois, T. J., Backeljau, T., & Schockaert, E. R. (2005b). Typhloplanoida (Platyhelminthes, Rhabdocoela) from New Caledonia and eastern Australia, with the description of six new taxa. *New Zealand Journal of Zoology, 32*, 79–98. https://doi.org/10.1080/03014223.2005.9518400

Willems, W. R., Wallberg, A., Jondelius, U., Littlewood, D. T. J., Backeljau, T., Schockaert, E. R., & Artois, T. (2006). Filling a gap in the phylogeny of flatworms: Relationships within the Rhabdocoela (Platyhelminthes), inferred from 18S ribosomal DNA sequences. *Zoologica Scripta, 35*(1), 1–17. https://doi.org/10.1111/j.1463-6409.2005.00216.x

WoRMS. (2023). World List of turbellarian worms: Acoelomorpha, Catenulida, Rhabditophora. *Promesostoma* Graff, 1882. Retreived March 12, 2023, from https://www.marinespecies.org/aphia.php?p=taxdetails&id=142412